

The Mechanism of the Regulation
of Energy Distribution
Between Photosystems 1 and 2 in the Cyanobacterium
Synechococcus sp. Strain PCC 7002

By
Randy Koop

A thesis submitted to the Department of Biological Sciences
in partial fulfillment of the requirements for the degree of
Master of Science.

Brock University,
St. Catharines, Ontario

© Randy Koop, 1997

Table of Contents

Table of Contents	1
Table of Figures and Tables	2
Acknowledgements	3
List of Abbreviations	4
Abstract	5
Introduction	6
Literature Review	10
i) Cyanobacteria	10
ii) Oxygenic Photosynthesis	12
iii) Respiration	14
iv) Photosystem 2 Organization	16
v) Photosystem 1 Organization	18
vi) Phycobilisomes	21
vii) Fluorescence Measurements	25
viii) State Transitions	26
a. Spillover	29
b. Phycobilisome Dissociation	31
c. Mobile Phycobilisome	32
ix) Connectivity in PS2	34
Materials and Methods	39
i) Cell Cultures	39
ii) PAM Measurements	40
iii) 77K Fluorescence Measurements	41
iv) Optical Cross-section Measurements	41
v) Connectivity Measurements	45
vi) Flow Through vs. Stirred Sample System	46
Results	48
i) 77K Fluorescence	48
ii) Room Temperature Fluorescence	54
iii) The <i>psaL</i> Mutant	61
iv) Cross-sections	68
v) PS2 Cross-Section Correction Using Connectivity Calibration Curves	79
vi) <i>PsaL</i> - State 2 F_o Correction	81
Discussion	89
i) Redox State of the Electron Transport Chain	89
ii) <i>Psa L</i> - F_o level	93
iii) State transitions	94
a. Chlorophyll Absorbed Light	94
b. Phycobilisome Absorbed Light	97
c. State Transition Model	99
iv) Connectivity	101
Conclusions	107
References	108
Appendix A: Liquid A+ Growth Medium	115
Appendix B: Connectivity Correction	116
Appendix C: Computer Simulated Connectivity	120

Table of Figures and Tables

Figures

1. Cyanobacterial cell structure.....	11
2. Z-scheme of photosynthesis.....	13
3. Photosynthetic and respiratory electron transport.....	17
4. PS1 structure	19
5. Phycobilisome structure.....	22
6. Three models of the state transition	28
7. Absorption cross-section apparatus	43
8. 77K fluorescence emission spectrum of 7002 wt cells	50
9. 77K fluorescence emission spectrum of 7002 apcD- cells	51
10. 77K fluorescence emission spectrum of 7002 psaL- cells	52
11. Room temperature fluorescence trace from 7002 wt cells.....	58
12. Room temperature fluorescence trace from 7002 apcD- cells	59
13. Room temperature fluorescence trace from 7002 psaL- cells.....	60
14. Room temperature fluorescence traces comparing 7002 wt and 7002 psaL- cells	64
15. Addition of far red light to psaL- cells.....	65
16. Benzoquinone addition to 7002 wt, psaL- (non-starved) and psaL- (starved) cells	66
17. Fructose addition to psaL- (starved) cells.....	67
18. PS2 flash saturation curve of 7002 wt cells in state 1 and 2 with 630nm excitation.....	70
19. PS2 flash saturation curve of 7002 wt cells in state 1 and 2 with 674nm excitation.....	71
20. PS2 flash saturation curve of 7002 apcD- cells in state 1 and 2 with 630nm excitation	72
21. PS2 flash saturation curve of 7002 apcD- cells in state 1 and 2 with 674nm excitation	73
22. PS2 flash saturation curve of 7002 psaL- cells in state 1 and 2 with 630nm excitation.....	74
23. PS2 flash saturation curve of 7002 psaL- cells in state 1 and 2 with 674nm excitation.....	75
24. PS1 flash saturation curve of 7002 wt cells in state 1 and 2 with 630nm excitation.....	76
25. Elevation of Fo level with red and far red illumination.....	82
26. Sample flash saturation curve with various elevations of Fo.....	83
27. Connectivity calibration curve for state 1 with 630nm excitation	84
28. Connectivity calibration curve for state 2 with 630nm excitation	85
29. Connectivity calibration curve for state 1 with 674nm excitation	86
30. Connectivity calibration curve for state 2 with 674nm excitation	87
31. Redox model.....	90
32. State transition model	100
33. Connectivity model.....	105

Tables

1. Summary of PS2:PS1 peak ratios from 77K fluorescence emission spectra	53
2. Summary of PS2 cross-section changes.....	77
3. Summary of Fo and Fm changes for cross-section measurements	78
4. Summary of cross-section changes after connectivity correction	88

Acknowledgements

Doug, I would first like to thank you for your coaching and friendship throughout my three years in your lab. I have appreciated your encouragement with my project and our discussions about the interpretation of my data. I'm thankful for your technical help when I was about ready to throw the delta absorbance amplifier (or some other uncooperative piece of equipment) out the window (if we had one!). I suppose I have also picked up a few extra-curricular pointers as well; haying, shallot and garlic harvesting, and general farm animal maintenance. Thanks for everything.

I would also like to thank the lab gang: Scott for his helpful thoughts on my project and for the Nerf baseball games, Aziz for his friendship and Serge for his time and expertise with computer simulations interspersed with games of magnet toss and frisbee.

Thank you, Rebecca, for your patience when I was working late in the lab or was preoccupied in my thoughts about the finer points of measuring cross-sections. I always appreciated the late night snacks and meals you joyfully brought. Thanks for your many encouragements, especially when things weren't going quite as expected.

I am so thankful for the help that I received over and over again from the guys in the electronics shop; John, Gary, Tom and Bob. I was particularly thankful for your willingness to help as soon as possible and for letting me get my own soldering gun going up there in your shop.

List of Abbreviations

ATP: adenosine triphosphate

DCMU: 3-(3',4'-dichlorophenyl)-1,1-dimethylurea

F_o: minimum fluorescence

F_m: maximum fluorescence

F_v: variable fluorescence (F_m-F_o)

FNR: ferredoxin NADPH oxidoreductase

NADP⁺: oxidised nicotinamide adenine dinucleotide phosphate

NADPH: reduced nicotinamide adenine dinucleotide phosphate

P680: Chlorophyll a pair in photosystem 2 reaction center

P700: Chlorophyll a pair in photosystem 1 reaction center

PAM Fluorometer: Pulse Amplitude Modulated Fluorometer

PBS: phycobilisome

PC: plastocyanin

PS1, PS2: photosystem 1, photosystem 2

PQ: plastoquinone

Q_A: Quinone A

Q_B: Quinone B

Abstract

Cyanobacteria are able to regulate the distribution of absorbed light energy between photosystems 1 and 2 in response to light conditions. The mechanism of this regulation (the state transition) was investigated in the marine cyanobacterium *Synechococcus* sp. strain PCC 7002. Three cell types were used: the wild type, *psaL* mutant (deletion of a photosystem 1 subunit thought to be involved in photosystem 1 trimerization) and the *apcD* mutant (a deletion of a phycobilisome subunit thought to be responsible for energy transfer to photosystem 1).

Evidence from 77K fluorescence emission spectroscopy, room temperature fluorescence and absorption cross-section measurements were used to determine a model of energy distribution from the phycobilisome and chlorophyll antennas in state 1 and state 2. The data confirm that in state 1 the phycobilisome is primarily attached to PS2. In state 2, a portion of the phycobilisome absorbed light energy is redistributed to photosystem 1. This energy is directly transferred to photosystem 1 by one of the phycobilisome terminal emitters, the product of the *apcD* gene, rather than via the photosystem 2 chlorophyll antenna by spillover (energy transfer between the photosystem 2 and photosystem 1 chlorophyll antenna). The data also show that energy absorbed by the photosystem 2 chlorophyll antenna is redistributed to photosystem 1 in state 2. This could occur in one of two ways; by spillover or in a way analogous to higher plants where a segment of the chlorophyll antenna is dissociated from photosystem 2 and becomes part of the photosystem 1 antenna.

The presence of energy transfer between neighbouring photosystem 2 antennae was determined at both the phycobilisome and chlorophyll level, in states 1 and 2. Increases in antenna absorption cross-section with increasing reaction center closure showed that there is energy transfer (connectivity) between photosystem 2 antennas. No significant difference was shown in the amount of connectivity under these four conditions.

Introduction

At its most basic level, photosynthesis is the conversion of light energy into stored chemical energy. The first step in this process is the absorption and conservation of light energy in the excited states of pigment molecules. In cyanobacteria, this is done by two photosystems linked in series, photosystem 2 (PS2) and photosystem 1 (PS1).

In order to increase light capture, both PS2 and PS1 have antennas of light absorbing pigments. The core antenna of PS2 consists of 35 (Manodori et al, 1984) to 50 (Myers et al, 1980) chlorophyll a molecules, and the core antenna of PS1, 120 (Myers et al, 1980) to 140 (Manodori et al, 1984). Therefore, red and blue light, which is absorbed by chlorophyll a, is primarily absorbed by photosystem 1. In addition to chlorophyll a, the cyanobacteria have accessory pigments, the phycobilisomes, which absorb yellow, orange and green light. These are primarily associated with PS2 (Manodori, 1984). As the total number of pigments increases, the photon absorbing area or optical absorption cross-section increases. The addition of different kinds of pigments, such as the phycobilisomes, broadens the range of absorbed light.

Light absorbed by PS2 causes a charge separation at the reaction center (P680). The reaction center is then able to reduce a quinone pool and, by a series of redox reactions, can ultimately reduce the PS1 reaction center. Here, light energy absorbed by the PS1 antenna causes charge separation at the PS1 reaction center (P700) which subsequently reduces NADP⁺. Since the two photosystems are linked in series, their relative rates are dependent on each other. The efficiency with which PS2 can utilize absorbed light energy for these photochemical reactions depends on how fast the electrons can be removed from Q_A, the first quinone acceptor, a process which ultimately depends on PS1 activity. PS1's efficiency depends on how fast electrons can be supplied from PS2 and, therefore, depends on PS2 activity. If light energy which is absorbed by

the phycobilisome is supplied, a higher rate of PS2 activity will occur because the majority of the energy absorbed by the phycobilisome is transferred to PS2. This will cause a backup of electrons between PS2 and PS1, slowing down Q_A oxidation and, therefore, decreasing PS2 efficiency. If, however, light which is absorbed by chlorophyll and is therefore mainly transferred to PS1 is supplied, oxidation of the electron transport chain will occur. This will cause a decrease in PS1 activity due to shortage of electron supply. In order for photosynthesis to operate optimally, a balance between these processes must be made.

As cyanobacteria are primarily aquatic organisms, there are constant changes in light quality and quantity caused by such things as the depth in the water column that the organism is found, cloud cover, waves and the density and species of organisms nearby. If the antenna systems were static, that is, the number and type of pigments associated with each reaction center were fixed, an imbalance in the distribution of light energy between the photosystems would occur frequently. If the light supplied to the organisms was primarily absorbed by either PS2 or PS1, photosynthesis would occur at a rate lower than its optimum.

In order to overcome this problem, cyanobacteria have a flexible antenna system. They are able to redistribute energy between the photosystems in response to light quality and quantity. This has been termed the light state transition. Light preferentially absorbed by PS2 causes an increase in PS1 antenna size at the expense of the PS2 antenna and light absorbed by PS1 causes the reverse change (Murata, 1969). These changes, which occur within seconds to minutes, are able to compensate for unbalanced light.

Three main models of how the state transition occurs have been suggested since 1969 when the phenomenon was first discovered by Murata: the spillover model, the mobile phycobilisome model and the phycobilisome dissociation model (Salehian and Bruce, 1992).

These models and the evidences for them are outlined in the literature review. No model has conclusively been shown to be the true mechanism of the state transition.

The focus of my project was to clarify the mechanism of the state transition in the cyanobacterium *Synechococcus* sp. strain PCC 7002. Using genetically manipulated cyanobacteria in conjunction with a number of spectroscopic techniques, a revised model has been formed. Don Bryant from Pennsylvania State University generously supplied two mutants which were thought to be impaired in some way with respect to the state transition. The *apcD* mutant was missing the allophycocyanin B subunit in the phycobilisome core (Maxson et al, 1989). It has been shown that this is likely the phycobilisome terminal emitter which transfers energy absorbed by the phycobilisome directly to PS1 in state 2 (Zhao et al, 1992). The *psaL* mutant lacked a subunit of PS1 which is thought to be responsible for the trimerization of PS1 reaction centers (Schluchter et al, 1996). A recent model suggests the necessity of PS1 trimerization for binding of the phycobilisome to PS1 (Bald et al, 1996).

Three spectroscopic methods were used in order to understand this mechanism: 77K fluorescence emission which measures the relative amount of fluorescence from PS1, PS2 and the phycobilisomes at 77 degrees K; absorption cross-section measurements which determine the optical cross-section of the antenna that is functionally linked to either PS1 or PS2; and room temperature fluorescence which is able to continuously measure fluorescence from PS2 under physiological conditions.

From the data, a new model for the state transition was developed which incorporated components from a number of the previously suggested models. Energy transfer occurs directly from the phycobilisome to PS2 in state 1 and to both PS2 and PS1 in state 2. In addition, there is an increase in energy absorbed by the chlorophyll antenna which is distributed to PS1 in state 2.

This likely occurs in a way analogous to that of higher plants where a segment of the chlorophyll antenna is energetically dissociated from PS2 and subsequently becomes associated with PS1.

It has been suggested that in higher plants there is energy transfer between neighbouring PS2 antennas in addition to transfer from PS2 to PS1. This process is called connectivity and can be observed as an increase in the cross-section of PS2 when some reaction centers are closed. Connectivity was measured in the wild type cells and it was shown that a limited number of PS2 centers are connected both in state 1 and state 2.

Literature Review

Cyanobacteria

Cyanobacteria have been termed “blue-green” algae. However, unlike other types of algae, they are procaryotic. Structurally and functionally they resemble bacteria in many ways (see figure 1). Being procaryotic, they have no membrane bound nucleus but rather a nucleoid. Cyanobacteria do, however, have three membrane structures. The outer membrane and the plasma membrane are separated by a cell wall which is made up of a thin peptidoglycan layer as in gram-negative bacteria. Inside the cell is found the third membrane, the thylakoid membrane, which, like eucaryotic algae, contains PS2, quinones, cytochrome b_6f and PS1. However, unlike eucaryotic algae, cyanobacteria have no chloroplast membrane surrounding the thylakoid. Also, cyanobacteria do not contain mitochondria in which all the respiratory processes are located.

The cyanobacteria resemble eucaryotic green algae and higher plants in that they carry out oxygenic photosynthesis. That is, in addition to PS1, they contain PS2, use water as the ultimate electron source for photosynthesis and therefore produce oxygen. Cyanobacteria contain chlorophyll a as well as the accessory phycobilisome pigment complexes which are attached externally to the stromal side of the thylakoid membrane (green algae and higher plants contain both chlorophyll a and b, but no phycobilisomes) (Prescott et al, 1990, Bold and La Claire, 1987).

Cyanobacteria have been widely used in the study of photosynthesis because of the many similarities they have to higher plants and algae in both the structure and function of the photosynthetic apparatus. One advantage that cyanobacteria offer is that they are easily genetically transformed. Therefore, by genetic manipulation the function of particular gene products can more readily be determined.

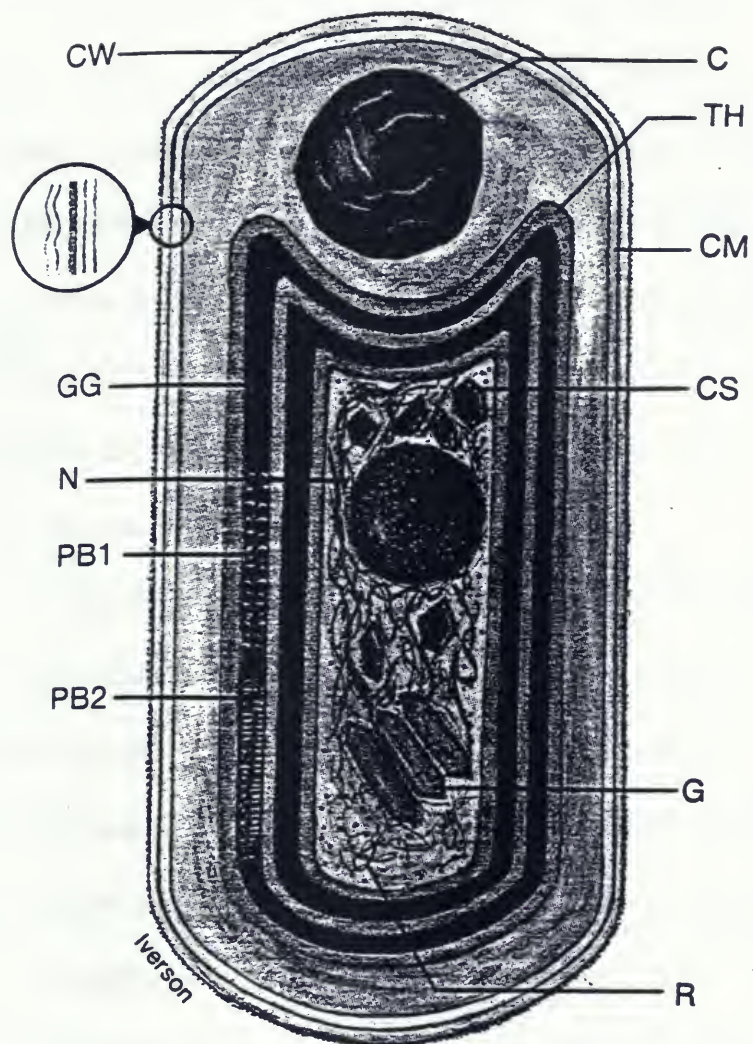


Figure 1. Cyanobacterial cell structure (Prescott et al, 1990). Schematic diagram of a vegetative cell with the following structures; CM, cell membrane; CW, cell wall; TH, thylakoid; PB1 and PB2, front and side views of phycobilisome rows; GG, glycogen granule; R, ribosomes; CS, carboxysome; N, nucleoid or nucleoplasm; G, gas vesicle. The insert shows an enlarged view of the envelope with its outer membrane and peptidoglycan.

Oxygenic Photosynthesis

Photosynthesis is the most basic process necessary for sustaining life on Earth. It is a series of reactions which converts the energy of light into stored chemical energy. Photosynthesis has been divided into two main categories of reactions: the light reactions and the dark reactions. In the light reactions, the reductant NADPH and the high energy molecule ATP are produced using the energy of absorbed light. In the dark reactions the products of the light reactions, NADPH and ATP, are used to reduce CO_2 , producing carbohydrates. This second set of reactions which does not directly require the input of light may occur in the presence or the absence of light as long as ATP and NADPH are available.

A summary of the light reactions as they occur in the thylakoid membrane is found in figure 2 (Zubay, 1995). This Z-scheme of photosynthesis can be viewed as two light harvesting photosystems linked in series by a number of electron carriers. Linear electron flow through this system requires an electron donor at the beginning and an electron acceptor at the end. The splitting of water produces oxygen, protons and electrons, and serves as the electron donor to the PS2 reaction center. NADP^+ serves as the ultimate electron sink after PS1.

The overall movement of electrons is from water to NADP^+ . However, water has a much higher redox potential (+0.8V) than NADP^+ (-0.4V) and therefore the spontaneous reduction of NADP^+ by water is energetically very unfavourable. Light energy trapped by the photosystems provides the driving force for this uphill reaction (Fork, 1989).

Light energy used by PS2 is first absorbed by its antenna complex. Photons incident on the antenna which have an energy equal to one of the excited electronic states of a pigment molecule in the antenna are absorbed. By resonance energy transfer, this excited state or exciton is transferred to a special pair of chlorophyll molecules called the PS2 reaction center or P680.

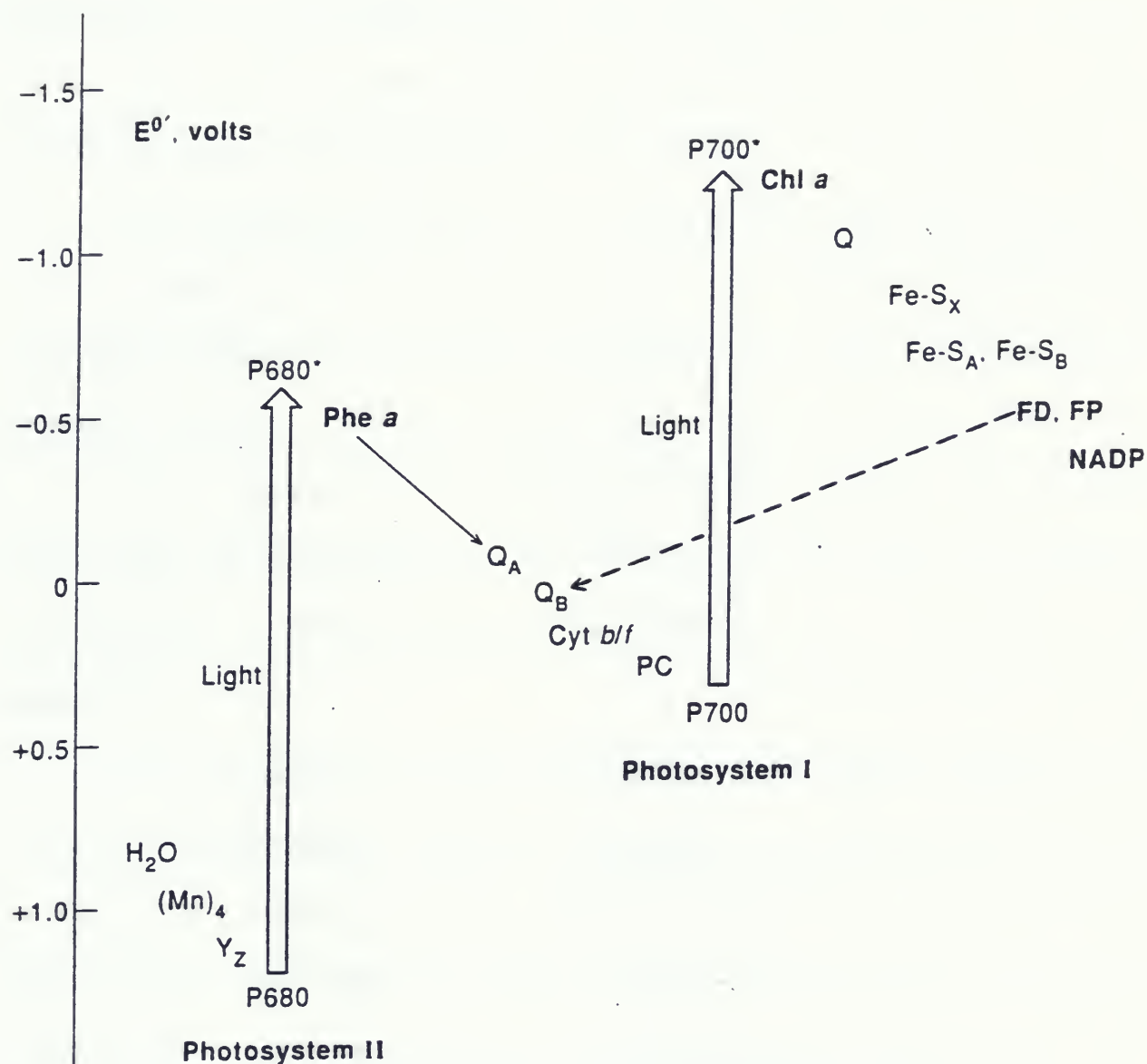


Figure 2. Z-scheme of photosynthesis (Zubay, 1995). Mn, Manganese water splitting complex; Yz, tyrosine residue; P680, reaction center of PS2; Phe a, pheophytin; Q, quinone; Cyt, cytochrome; PC, plastocyanin; P700, reaction center of PS1; FD, ferredoxin; FP, flavoprotein.

P680 is promoted to an excited state, P680*, by this exciton. The redox potential of P680* is much lower than that of P680 and allows the reaction center to reduce pheophytin, the primary electron acceptor of PS2, resulting in charge separation. Oxidized P680 (P680+) is a strong oxidant and is spontaneously re-reduced by the splitting of water.

Reduced pheophytin also has a low redox potential, and is able to reduce the primary quinone acceptor Q_A, followed by the secondary quinone acceptor Q_B, cytochrome b/f, plastocyanin or cytochrome c₅₅₃ and finally the PS1 reaction center, P700. The electron carriers between PS2 and PS1 are collectively called the photosynthetic electron transport chain.

Light energy absorbed by the antenna pigments of PS1 is transferred to its reaction center, P700, where charge separation again occurs. The redox potential of P700* is high enough to allow reduction of NADP⁺ via ferredoxin, producing NADPH.

Respiration

Since cyanobacteria do not contain mitochondria, their respiratory processes are not located in a separate organelle. Rather, the constituents of the respiratory electron chain are located in both the thylakoid and plasma membranes. Not only are some of the respiratory electron carriers located in the same membrane as the photosynthetic apparatus, but there is also evidence that some of the components of these two systems are shared (Scherer, 1990).

Aoki and Katoh (1982) using *Synechococcus* sp. showed that it was possible to monitor changes in the PQ redox state using PS2 fluorescence induction kinetics. They found that PQ was reduced by respiratory substrates in the dark and was oxidized by a KCN-sensitive oxidase. Decreasing the concentration of respiratory substrates by incubating the cells in the dark caused a decrease in PQ reduction which could be brought back by addition of fructose. Evidence from this report strongly suggested that PQ was involved in respiratory electron transport. Mi et al

(1994) confirmed the findings that dark starvation of cells caused a decrease in the reduction of the photosynthetic electron transport chain.

Mi et al (1992a) came to similar conclusions by measuring ease of P700 oxidation with low intensity far red light under various conditions in *Synechococcus* sp. strain 7002. They showed that, compared to spinach and *Anabaena*, P700 of *Synechococcus* was considerably more reduced in the dark and that this was the result of reduction by respiratory substrates. Using the electron inhibitors DCMU and DBMIB which inhibit the oxidation of Q_A and PQ respectively they showed that electrons were donated to the photosynthetic electron transport chain at PQ. They showed that in the dark, the majority of the reducing potential came from respiratory substrates but that after a brief illumination (during which the photoreductants of PS1 were produced), P700+ was reduced more quickly. This was a result of donation of electrons to PQ from these photoreductants, a process which was able to occur at a faster rate than the reduction by respiratory substrates. This showed that reduction of PQ was rate limited at the generation of NAD(P)H from the respiratory substrates.

Mi et al (1992b) showed that the donation of electrons to PQ was inhibited by mercury, which is a known inhibitor of mitochondrial NAD(P)H dehydrogenase (NDH). In addition, NDH mutants which were constructed had a much lower level of P700 reduction in the dark. Therefore, a mercury sensitive dehydrogenase was responsible for donation of electrons to PQ from either the photoreductant of PS1 or from stored respiratory substrates.

A number of experiments have recently shown that this NAD(P)H dehydrogenase may be associated with both PS1 and the phycobilisome. Scherer et al (1988) and Guedeney (1996) concluded that NAD(P)H dehydrogenase was either identical to or was complexed with ferredoxin-NADP-oxidoreductase (FNR) in *Anabaena variabilis* and *Solanum tuberosum* L.

respectively. Schluchter and Bryant (1992) while characterizing FNR from *Synechococcus* sp. strain 7002 found that it had an N-terminal sequence which was 78% similar to a linker protein in the phycobilisome. Correspondingly, they found that FNR is copurified with the phycobilisome. This strongly suggests that the N-terminal region serves as a binding region to the phycobilisome. On the PS1 side, Andersen et al (1992) found with cross-linking experiments that FNR was associated with the psa-E subunit of PS1 in barley. Summarizing all of these findings, Bald et al (1996) has suggested that FNR may be a bridge which joins phycobilisomes and PS1. It should be remembered, however, that since these studies were done on such a variety of organisms (from cyanobacteria to higher plants) this model is only speculative at present. To date, no phycobilisome/PS1 complex has been isolated. This may be due to the loose linkage between these two complexes.

Scherer (1990) outlined a tentative map of the overlap between respiratory and photosynthetic electron transport chains (shown in figure 3). He reviews data which showed that in addition to plastoquinone, cytochrome b_6/f and cytochrome c_{553} or plastocyanin are also involved in respiration.

Photosystem 2 Organization

It has been shown using electron microscopy that rows of dimeric PS2 particles are found in thylakoid membranes (Morschel and Schatz, 1987, Dekker et al, 1988). Morschel and Schatz (1987) suggest a model where each phycobilisome is attached to two PS2 particles. Each phycobilisome has two basal core complexes (discussed in more detail under phycobilisomes), each of which could attach to a separate PS2 complex. Manodori and Melis (1985) using fluorescence induction experiments have also suggested that two PS2 complexes are functionally

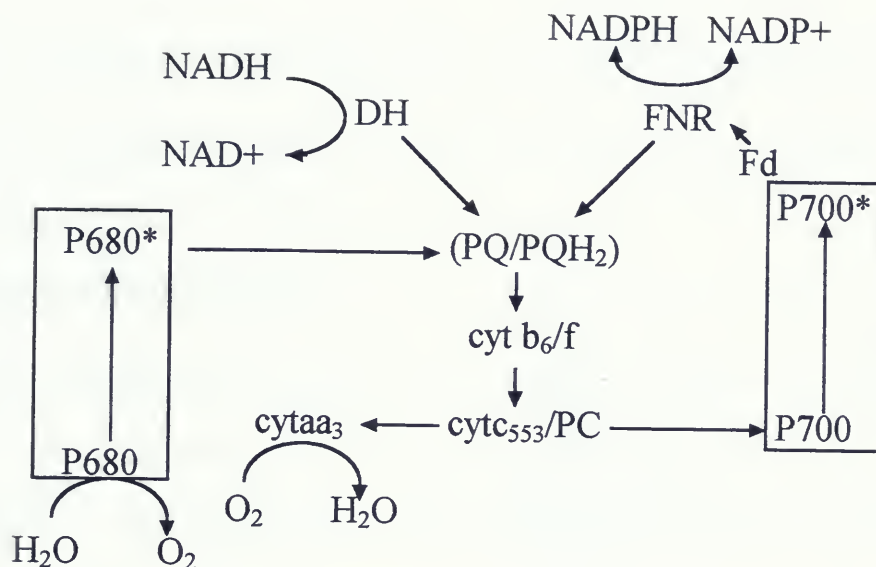


Figure 3. Interaction of respiratory and photosynthetic electron transport chains in *Anabaena variabilis*. P680, reaction center of PS2; P700, reaction center of PS1; PQ/PQH₂, oxidized and reduced plastoquinone; cyt, cytochrome; PC, plastocyanin; DH, dehydrogenase; Fd, ferredoxin; FNR, ferredoxin NADP oxidoreductase.

linked to one phycobilisome complex. Morschel and Schatz suggest that rows of PS2 particles with phycobilisomes attached facilitates energy transfer between neighbouring PS2/phycobilisome complexes.

The binding of phycobilisomes to PS2 complexes has been shown *in vitro* by Cheriskin et al (1985) and Kirilovsky and Ohad (1986). This supports the *in vivo* evidence that there is direct contact between these two complexes.

Photosystem 1 Organization

PS1 is a multisubunit complex which consists of 11 polypeptides as shown in figure 4 (Golbeck, 1994). Of special note are the *psaE* and *psaL* subunits. The *psaE* subunit which binds FNR (as discussed under respiration) is located on the stromal side of the thylakoid membrane. The *psaL* mutant used in this study was deficient in the peripherally located, transmembrane *psaL* subunit.

Whether the PS1 complex exists as a monomer or a trimer *in vivo* has been a subject of some controversy. Boekma et al (1987) isolated PS1 complexes from *Synechococcus* sp. and, using electron microscopy, detected trimers of PS1. Rogner et al (1990) isolated PS1 complexes from the same species using a different isolation technique which yielded three sizes of pigment-protein complexes with a ratio of molecular weights of 1:1.8:2.5. They suggested that these were mono, di and trimeric PS1 complexes. They were of the opinion that the trimeric PS1 complex existed *in vivo*. This was supported by its stability during experiments. Interestingly, they saw no evidence that extracted PS1 monomers could form trimers.

Foord and Holzenburg (1988) opposed the view that PS1 exists *in vivo* as trimers. They suggested that the formation of trimers during isolation was an artifact caused by the detergents used. Electron micrograph images of the thylakoid membrane showed little evidence for trimers

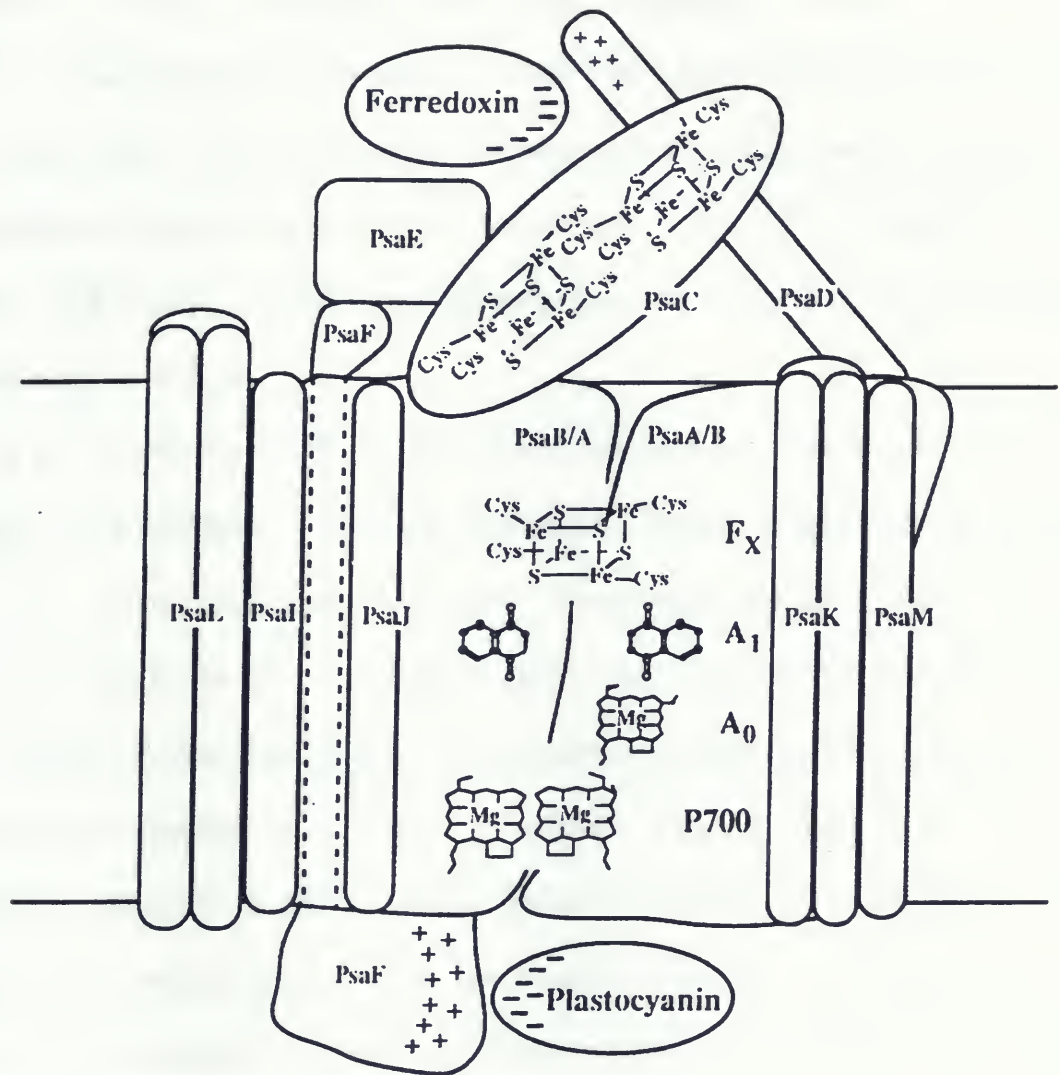


Figure 4. PS1 structure (Golbeck, 1994). Subunits PsaC, PsaD and PsaE as well as ferredoxin are located on the stromal side of the thylakoid membrane. Plastocyanin is on the lumenal side.

and possibly some evidence for monomers in *Phormidium laminosum*. However, the resolution of these images was admittedly poor.

Hladik and Sofrova (1991) discuss several lines of evidence that suggest PS1 exists *in vivo* as trimers. They show that the stronger the solubilizing techniques, the higher the isolated monomer concentration. They say that under various conditions which might be experienced during solubilization, trimers are not formed from monomers, but rather monomers are formed from trimers. And finally, cross-linking experiments have substantiated the claim that native PS1 probably exists as a trimer.

Kruip et al (1994) showed that the isolation of monomers or trimers depends on the ion concentration during isolation. A high salt concentration during isolation favours monomer formation and low salt concentration the trimer. Interestingly, they have shown that after isolation, an increase in the ionic concentration (even 2 to 3 times greater than that used in isolation) is not able to dissociate trimers. After isolation, the trimers or monomers seem to be locked in their conformation. A mechanism is suggested where, at high ionic concentration during isolation, while PS1 is still within the thylakoid membrane, ions are able to screen electrostatic surface charges which hold the trimers together, thereby causing monomerization. They further suggest that *in vivo*, a dynamic equilibrium of monomers and trimers exists which is regulated by a process which mimics the effect of the ion concentration changes (e.g. phosphorylation).

Some of the most convincing evidence for PS1 trimerization has come from a PS1 mutant lacking one of its subunits. Chitnis et al (1993), Chitnis and Chitnis (1993) and Schluchter et al (1996) have constructed *psaL* mutants in *Synechocystis* sp. strain PCC 6803 and *Synechococcus* sp. strain PCC 7002 respectively. Both have shown that whereas in the wild type a portion of the

isolated PS1 complexes are trimers, none of the complexes isolated from *psaL* mutant cells are trimers.

None of the procedures outlined above have clearly demonstrated that PS1 exists as trimers *in vivo*. Electron freeze fracture experiments may be able to determine this if the resolution can be increased. Alternatively, exciton annihilation experiments may be able to determine this *in vivo*. Two excitons which meet each other in the antenna quench each other. With a larger antenna (the trimer rather than the monomer), there is a greater chance of absorbing more than one exciton and therefore an increase in the probability of exciton annihilation.

Phycobilisomes

Analogous to the light harvesting complexes in higher plants, cyanobacteria have accessory pigments called phycobilisomes which are bound to the cytoplasmic side of the thylakoid membrane (Morschel and Schatz, 1987). As shown in figure 5, which depicts the phycobilisome structure in *Synechococcus* sp. PCC 7002 used in this study, phycobilisomes have two distinct regions, the peripheral rods and the central core (Maxson et al, 1989).

The primary subunits of the phycobilisome rods are the phycobiliproteins which contain chromophores called phycobilins. Each phycobiliprotein is made up of two different subunits, α and β . Phycobiliproteins occur in either single trimer complexes or in complexes with two trimers joined together to form hexamers (Zilinskas and Greenwald, 1986). These hexamers are joined by non-chromophore containing linker proteins which were discovered by Tandeau de Marsac and Cohen-Bazire (1977). The rods of all species of cyanobacteria contain at least one type of phycobiliprotein, phycocyanin (absorbance maximum at 625-630nm) but may also

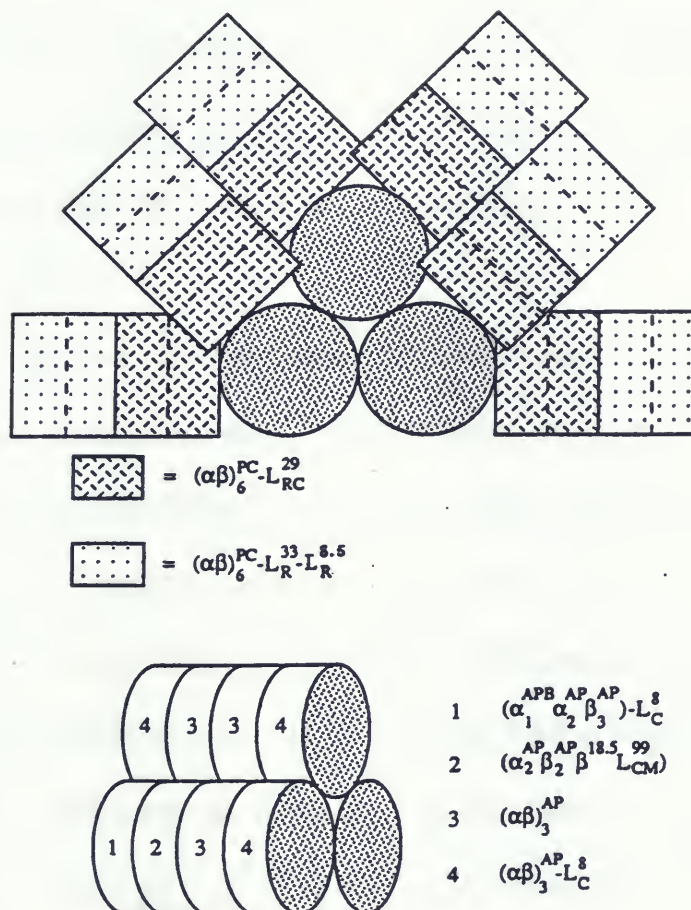


Figure 5. Phycobilisome structure of *Synechococcus* sp. PCC 7002 (Maxson et al, 1989). The abbreviations AP, APB and PC are used for the biliproteins allophycocyanin, allophycocyanin B and phycocyanin, and α and β for the α and β subunits of these proteins. Linker polypeptides are abbreviated L, with the superscript denoting the size in kDa, and a subscript that specifies the location of the polypeptide: R, rod substructure; RC, rod-core junction; C, core; CM, core-membrane junction.

contain phycoerythrin (absorbance maximum at 560nm) or phycoerythrocyanin (absorbance maximum at 570nm). Phycobiliproteins are always organized with the higher energy photon absorbing units to the periphery and the low energy photon absorbing units towards the core (Bryant et al, 1990). This facilitates a directional flow of energy toward the core as was shown by Yamazaki et al (1984) using time-resolved fluorescence decay spectra. The rods of *Synechococcus* sp. PCC 7002, which was used in this study, only contain phycocyanin (Bryant et al, 1990).

In most species, as is the case with *Synechococcus* sp. PCC 7002, there are three cylindrical core complexes which are primarily composed of allophycocyanin trimers (absorbance maximum at 650nm) (Maxson et al, 1989). Each core complex is composed of 4 trimer subunits. The upper core complex contains two of each of two types of allophycocyanin trimers. These two types differ in that one has an 8kDa linker polypeptide attached. The bottom two core complexes each contain 1 of each of the 2 types of trimers in the upper core complex. In addition they contain a trimer which has a unique α subunit, allophycocyanin B (encoded by the *apcD* gene), which gives this trimer a longer wavelength emission compared to normal allophycocyanin trimers. The fourth trimer has a unique high molecular weight polypeptide (99kDa for *Synechococcus* sp. PCC 7002) encoded by the *apcE* gene which gives this trimer a longer wavelength emission. Due to the longer wavelength emission of these two unique core trimers (680nm maximum fluorescence emission), they have been suggested to be the terminal excitation energy acceptors of the phycobilisomes. That is, energy absorbed by the phycobilisome is funneled down to these two trimers.

The *apcE* gene was mapped and the role of the gene product which is termed the linker core membrane protein was studied by Capuano et al (1991). It contains a loop domain which is

thought to be responsible for binding of the phycobilisome to PS2. As has been suggested by others (Lundell et al, 1981), this protein is thought to be the terminal phycobilin energy emitter which transfers energy from the phycobilisome to the chlorophyll antenna of PS2. The role of the linker core membrane protein not only in energy transfer to PS2 but also as a phycobilisome anchor was shown by Redlinger and Gantt (1982). They showed that the same high molecular weight protein was not only located in the phycobilisome, but also with thylakoids from which the phycobilisomes had been removed. The thylakoid attached proteins contained a chlorophyll chromophore and the phycobilisome attached proteins contained both a chlorophyll and a phycobilin chromophore. It is thought that *in vivo* these two chromophores are energetically coupled allowing energy transfer from the phycobilisome to the chlorophyll antenna.

In 1989 Maxson et al first published data on a mutant lacking the *apcD* gene which caused the elimination of allophycocyanin B from the core. The mutation caused no change in the structure of the rest of the phycobilisome, the allophycocyanin B probably being replaced by a normal allophycocyanin polypeptide. The mutant grew with a similar rate to the wild type in both high and low white light, and isolated phycobilisomes had similar fluorescence properties to those of the wild type (blue shifted by 12-15nm). No significant phenotype was originally assigned to the polypeptide. Later however, the same group showed with 77K fluorescence emission and room temperature fluorescence induction measurements that this mutant was not able to do the state transition. In addition, a greater doubling time of mutant cells under light preferentially absorbed by the phycobilisome suggested that allophycocyanin B was responsible for direct energy transfer from the phycobilisome to PS1 in state 2 (Zhao et al, 1992).

Fluorescence Measurements

Most of the spectroscopic techniques used in this study involved the measurement of fluorescence from PS2. Room temperature variable fluorescence originates only from PS2 since P700 and P700+ are equally efficient quenchers (Owens et al, 1988). The importance of fluorescence measurements in the diagnosis of what is occurring in photosynthesis is briefly outlined here (Schreiber et al, 1994, Krause, 1991).

Light energy absorbed by the antenna of PS2 should optimally all be transferred to the reaction center and used for photochemistry. Within this perfectly efficient system, no energy absorbed by the antenna would fail to be dispensed of usefully. This system assumes two things; first, that all energy absorbed by the antenna is efficiently transferred to the reaction center and second, that the rate limiting step is not at the use of excitation energy by the reaction center, but rather at the level of absorbing enough energy by the antenna. These assumptions however, are incorrect.

First, there is a measure of inefficiency associated with the antenna collection system. Some of the energy absorbed by the antenna is emitted as fluorescence before it even reaches the reaction center. This base amount of fluorescence is termed the F_0 level of fluorescence.

Second, under conditions where the primary electron acceptor of PS2, Q_A , is reduced, more energy is lost as fluorescence. Excitation energy which does reach the PS2 reaction center under these conditions may cause charge separation to occur. However, since Q_A is already reduced and can not accept another electron, charge recombination occurs causing an excited state in the chlorophyll antenna. The energy is emitted from the antenna as fluorescence. PS2 is said to be closed under these conditions. Fluorescence from a population of cells increases as more and more reaction centers are closed. When all centers are closed, the maximum level of

fluorescence F_m is reached. Variable fluorescence is considered to be the difference between F_m and F_o .

Looking at this from the opposite side, we can say that any process that causes a decrease in the fluorescence from the maximum level F_m is called quenching. Photochemistry is a quencher of fluorescence because it utilizes absorbed energy and therefore decreases the amount of fluorescence.

Other than photochemistry, there are some factors which can affect the amount of fluorescence. These fall into the broad category termed non-photochemical quenchers of fluorescence. These processes also cause a decrease in the F_m level. One type of non-photochemical quenching is called energy quenching and is caused by the build up of a pH gradient across the thylakoid membrane. It ultimately causes an increase in the amount of energy which is lost as heat.

The state transition is also a type of non-photochemical quenching. A decrease in the number of pigments functionally associated with PS2 will cause a decrease in both F_m and F_o . Fewer pigments absorb less energy and so these fluorescent parameters decrease.

Utilizing fluorescence, such parameters as the amount of energy distributed to either photosystem, the antenna size of PS2, the redox state of the electron transport chain and the rate of exciton migration in the antenna can be determined. Some of these applications will be discussed in more detail in the Materials and Methods.

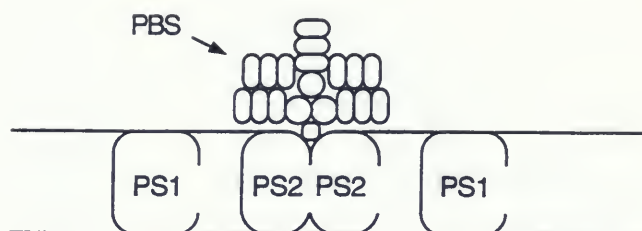
State Transitions

In 1969, Murata first discussed a possible mechanism to explain changes in the amplitude of fluorescence emission from PS2 that occurred when light preferentially absorbed by either photosystem was used to illuminate the phycobilisome containing organism *Porphyridium*

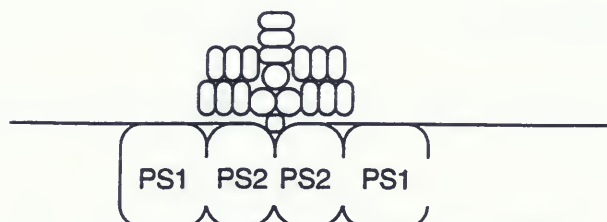
cruetum. Murata and others before him had seen changes in chlorophyll fluorescence that appeared to be a result of two kinetics: photochemistry and another unknown process. In order to separate these two, he froze samples which had been illuminated by light either preferentially absorbed by PS1 or PS2 in liquid nitrogen (77K). Continuous photochemical reactions were not able to take place at this low temperature, allowing undisturbed observation of the second process.

Results showed that the amplitude of the fluorescence from the PS2 peaks (at 684 and 695nm) decreased compared to that from the PS1 peak (at 715-740nm) when cells had been preilluminated with light absorbed by PS2. This was termed state 2. The opposite occurred when cells were preilluminated with light absorbed by PS1 and this was termed state 1. These results were interpreted to mean that there was a redistribution of excitation energy between the photosystems that was induced by preillumination.

Murata described two models which could explain these changes in distribution that occurred when cells went from state 1 to state 2. First, there could be a decrease in the amount of energy transferred from the collecting pigments to the PS2 reaction center. The excess energy could be directed instead to PS1; this is called the mobile phycobilisome model (outlined clearly in Allen and Holmes, 1986). Second, energy which is collected and directed to PS2 could have an increased rate of transfer directly to PS1 from the PS2 core antenna; the spillover model. A third model, has since been suggested (Mullineaux and Allen, 1988) in which the phycobilisome simply detaches from PS2 allowing a closer association between PS2 and PS1 so that spillover may occur between these two; the phycobilisome dissociation model. Each of these models is shown schematically in figure 6.

STATE 1**STATE 2**

Spillover



Mobile PBS

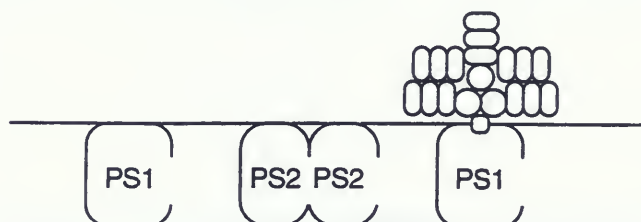
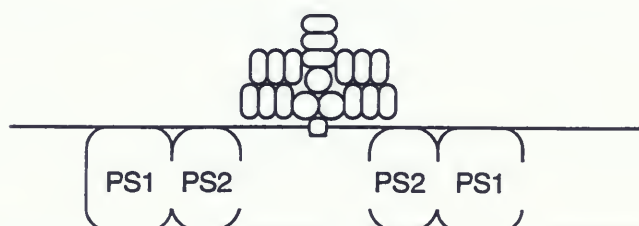
PBS
Dissociation

Figure 6. Three models of the state transition (Salehian and Bruce, 1992). State 1 is shown with the accessory phycobilisome (PBS) pigment attached to PS2. State 2 is shown in three possible configurations: spillover, where PS2 and PS1 are in close enough proximity that there is transfer of energy between them; mobile PBS, where the phycobilisome is detached from PS2 and subsequently attached to PS1; and PBS dissociation, where the phycobilisome pigment is simply detached from PS2 and there is spillover between the chlorophyll antennas.

Each model makes a prediction about how light energy is distributed. The spillover model predicts that in state 2 there will be a decrease in the amount of both phycobilisome and chlorophyll absorbed light energy that is transferred to PS2 with an equal but opposite increase in the amount of energy transferred to PS1. The mobile phycobilisome model predicts that the amount of energy absorbed by the phycobilisome which is transferred to PS2 will decrease in state 2 with an increase in transfer to PS1. However, there will be no change in the distribution of chlorophyll absorbed energy. The phycobilisome dissociation model predicts that the amount of energy transferred from the phycobilisome to PS2 will decrease in state 2 with no increase in transfer to PS1 and that there will be an increase in spillover from the chlorophyll antenna of PS2 to PS1.

Spillover

One of the most important contributions to the spillover model is that the changes in 77K fluorescence emission, which were first shown by Murata (1969), occur with either chlorophyll excitation or phycobilisome excitation (Salehian and Bruce, 1992). If changes in the PS2/PS1 fluorescence peak ratio occurred with phycobilisome excitation but not with chlorophyll excitation, it would be easy to envisage that the energy absorbed by the phycobilisome was transferred directly to PS1 instead of PS2 in state 2. However, changes in PS2/PS1 fluorescence peak ratio do occur with chlorophyll excitation showing that energy is redistributed between the chlorophyll antennas. The changes in phycobilisome energy distribution could therefore be brought about by changes in the rate of energy transfer between the chlorophyll antennas if the phycobilisomes always transferred their energy to PS2. This model was particularly supported by the finding that a phycobilisome-less mutant was able to do state transitions (Bruce et al, 1989). It showed that direct energy transfer from the phycobilisomes to the PS1 chlorophyll

antenna was not necessary for a state transition. Although data from 77K fluorescence showed that this was not necessary, it did not prove that it did not occur.

Work by Ley and Butler (1980) supported the spillover model. Calculations from millisecond fluorescence rise kinetics suggested that there was an increase in the rate of spillover in state 2. They suggested that PS2 and PS1 had a closer physical contact in state 2 allowing this to occur.

Vernotte et al (1990) strongly supported the spillover model. Using fluorescence induction for cyanobacteria they attempted to measure whether all PS2 reaction centers were functionally linked to phycobilisomes. According to their theory, if all PS2 reaction centers were attached to phycobilisomes, excitation with phycobilisome absorbed light would close all PS2 reaction centers and further illumination with chlorophyll absorbed light would fail to close anymore. They did observe this. However, their results mean little because they only measured this in state 1; it is in state 2 that phycobilisome dissociation from PS2 has been postulated.

Early picosecond fluorescence emission measurements at 77K by Bruce et al (1985) showed that chlorophyll associated with PS2 had an increased fluorescence lifetime in state 1. This was interpreted as uncoupling of PS2 and PS1 chlorophyll antenna in state 1. That is, when energy is transferred to PS2 in state 2, some of the energy will be transferred to PS1 which will decrease the fluorescence lifetime of the PS2 chlorophyll antenna. In state 1, decreased energy transfer to PS1 will mean that the energy transferred to PS2 will be utilized slower with a concomitant increase in fluorescence.

In the spillover model, the difference between state 1 and state 2 is a change in the rate of energy transfer between the chlorophyll antenna of PS2 and PS1 (Biggins et al, 1989). This could be caused by a large change in the orientation of PS2 and PS1 but need not be; a small

change in the distance between them would be sufficient to substantially change the rate of energy transfer (Bruce et al, 1985). Olive et al (1986) have shown with electron micrographs that in state 1 there is a greater alignment of exoplasmic freeze fracture particles (probably PS2) in rows. In state 2, their orientation is more random. They suggest that this shows that in state 1 PS2 complexes are closely associated and therefore not accessible to PS1. Randomization of PS2 particles in state 2 allows for greater contact with PS1.

Phycobilisome Dissociation

A second model to explain the state transition was described by Mullineaux and Allen (1988). This model was supported by experiments measuring fluorescence induction transients at room temperature in *Synechococcus* cells as they moved from state 1 to state 2. They discuss how if a change in cross-section occurs, both the F_0 and F_m levels will change proportionately. However, if spillover occurs, F_m will change to a greater degree than F_0 because there will be increased spillover as more of the reaction centers are closed. This group observed that for the phycobilisome absorbed light, F_0 and F_m changed proportionately indicating a changed cross-section due to phycobilisome dissociation. However, F_0 and F_m changed disproportionately for chlorophyll absorbed light indicating spillover. This research suggested a model where in state 1 the phycobilisomes are associated with PS2. In this state steric hindrance caused by the large phycobilisome complex limits spillover between PS1 and PS2 chlorophyll antenna. In state 2, the phycobilisome becomes detached from PS2, allowing closer association of the PS1 and PS2 chlorophyll antenna and therefore spillover. In this model, Mullineaux and Allen do not show the detached phycobilisomes associating with PS1. Instead, they suggest that the fluorescence from these detached phycobilisomes is quenched and the energy dissipated as heat.

Mullineaux et al (1990), using picosecond time-resolved fluorescence emission spectra of *Synechococcus* 6301 found that the phycobilisome became detached from PS2 in state 2. They observed that the amplitude of the PS2 fluorescence lifetime decreased but that there was no change in its lifetime. A change in amplitude supports a decrease in cross-section due to decreased energy transfer from the phycobilisomes. If fewer phycobilisomes are functionally attached to PS2, less energy will be transferred resulting in a decrease in amplitude. If, however, there is a change in the rate of spillover between the photosystems, a change in the lifetime of the decay would be expected.

By measuring fluorescence induction transients Mullineaux and Holzwarth (1990). found that in state 2 a portion of the PS2 centers remained detached from the phycobilisomes but that on transition to state 1 the amount of PS2 centers which remained detached decreased.

Mobile Phycobilisome

A mobile phycobilisome model, analogous to the mobile light harvesting complex in higher plants, was suggested by Allen and Holmes (1986). In this model, the phycobilisome is detached from PS2 and attached to PS1 in state 2. It differs from the spillover model in that the energy is directly transferred from the phycobilisome to PS1 rather than via spillover between the chlorophyll antenna. No energy transfer between chlorophyll antenna occurs.

Tsinoremas et al (1989) measured the absorption cross-section of PS1 in state 1 and 2 and found that the phycobilisome antenna size increased in state 2. However, they were not able to determine whether the chlorophyll antenna size changed. These measurements are consistent with the mobile phycobilisome model, but because of their incompleteness they do not prove that it occurs.

Mullineaux (1992) also measured the relative absorption cross-section of PS1 in state 2 and state 1 conditions. He observed no change in the chlorophyll antenna cross-section but a 30% increase in the phycobilisome cross-section in state 2. The increase in the PS1 phycobilisome cross-section indicates that the phycobilisome becomes attached to PS1 in state 2. The lack of change in the chlorophyll cross-section suggested that there was no spillover between PS2 and PS1 in state 2. However, the change in the PS1 chlorophyll cross-section was likely very difficult to observe. There are usually two or three times more PS1 complexes than PS2 complexes and the chlorophyll antenna size of PS1 is approximately three times larger than that of PS2. Therefore, an increase in spillover from smaller and fewer PS2 complexes to larger and more PS1 complexes would be very difficult to observe.

The data of Mullineaux et al (1990) and Mullineaux and Holzwarth (1990) which were presented in favour of the phycobilisome dissociation model could also be interpreted in terms of the mobile phycobilisome model (they have outlined this as an alternative model). If phycobilisomes would become detached from PS2 and remain detached from PS1 the energy they absorb would need to be released either as fluorescence or as heat. As no increased fluorescence was seen from the phycobilisomes when they were detached from PS2 (Mullineaux et al, 1990), light energy which was absorbed was supposed to have been dissipated as heat. In this case, a decrease in energy storage as seen by an increase in heat loss should have been evident in state 2. However, using photoacoustic measurements which determine the amount of heat loss from the primary photosynthetic processes, it was shown by Mullineaux et al (1991) and Bruce and Salehian (1992) that energy absorbed by the phycobilisome is stored equally well in state 1 and state 2. Mullineaux actually observed that energy was stored more efficiently in

state 2 than state 1 for phycobilisome absorbed light. These measurements strongly suggest that phycobilisomes which are functionally detached from PS2 become attached to PS1.

Since spillover had not been completely ruled out, it was difficult to say with certainty that energy was directly transferred from the phycobilisome to PS1 and not via the PS2 chlorophyll antenna. However, in 1994 Mullineaux showed using a mutant which lacked PS2 and therefore was incapable of spillover from the PS2 chlorophyll antenna to PS1, that energy transfer occurred from the phycobilisome directly to PS1 under state 1 conditions and that the extent of this transfer doubled under state 2 conditions. These results showed that energy transfer from the phycobilisome to PS1 was not dependent on the spillover mechanism.

Glazer et al (1994) showed that energy transfer could be disrupted between the phycobilisome and PS1 without decreasing energy transfer from the phycobilisome to PS2. This result is incompatible with a model where energy transfer from the phycobilisome to PS1 occurs via the PS2 chlorophyll antenna. This disruption of energy transfer was done using N-ethylmaleimide (NEM), a compound which reacts with sulfhydryl groups. It was shown that NEM decreases the amount of FNR associated with the phycobilisomes. If FNR is involved in linking the phycobilisome and PS1 (Schluchter and Bryant, 1992), then this decrease in FNR binding may be the cause of the decreased energy transfer from the phycobilisome to PS1.

Connectivity Between PS2 Complexes

Morschel and Schatz (1987) presented a model for the arrangement of PS2 and phycobilisome complexes (discussed earlier under photosystem 2). They proposed that rows of these PS2/phycobilisome complexes were often seen *in vivo* and suggested that in this conformation there would likely be a high degree of energy transfer between PS2 chlorophyll

antenna and/or between the associated phycobilisomes. That is, PS2 complexes would be highly connected.

To understand the implications of this connectivity model on antenna cross-sections a theoretical model where only two complexes are connected will be discussed. If both complexes have open reaction centers, then an exciton in the antenna will have equal probability of being trapped by either center. The size of the antenna associated with each individual reaction center will be equal to half the total cross-section of both antennas. However, if one reaction center is closed and is therefore not able to trap an exciton from the antenna, then the probability of the exciton being trapped by the remaining open reaction center will be doubled. This is assuming that no quenching by the closed reaction center occurs and that the rate of exciton migration between antenna is equal to that within the antenna. The functional size of the antenna associated with the one open reaction center will be equal to the total cross-section of both antenna. In a theoretical system containing two PS2 complexes or in one which includes many more, if there is perfect connectivity between all complexes, then closing half the reaction centers should cause a doubling of the cross-sections of the remaining open reaction centers.

Connectivity has been measured in two ways in the past. The first method makes use of fluorescence induction curves. It was observed that when samples which had been dark adapted were illuminated with a bright light, the fluorescence increased from the initial F_0 level to the F_m level over a period of milliseconds. Strasser et al (1995) have shown that the fluorescence induction curve is multiphasic. The first phase shows a typical rise time of 2ms, the second 20ms and the third 200ms. They suggest that the initial rise is photochemical in nature and represents the reduction of the primary quinone acceptor Q_A to Q_A^- . The second two phases are non-photochemical in nature and are probably related to the filling up of the PQ pool.

Interpretation of the complex multi-phase rise in fluorescence during illumination in terms of connectivity is complicated by these different phases. In order to avoid these problems DCMU, which blocks the reoxidation of Q_A by Q_B , has been used.

Assuming that all PS2 centers were disconnected, it was expected that the increase from F_0 to F_m would be exponential when DCMU was present. However, a sigmoidal increase has been observed (Renger and Schulze, 1985 and Valkunas et al, 1991). The rise in fluorescence was too slow near F_0 and too fast near F_m to fit an exponential curve. This was interpreted to mean that PS2 centers were energetically connected. That is, as more and more centers became closed during illumination, the cross-section of the remaining centers increased, leading to an increasing rate of trap closure. This would give rise to the sigmoidal induction curve.

However, even under these conditions with DCMU one major assumption was still made; that a photosystem's history has no effect on it. At the beginning of the induction curve, photosystems have only been hit once. However, as the illumination time increases, additional hits are received by many of the photosystems. It was assumed that there is no significant effect of these multiple hits. France et al (1992) have shown that the presence of a sigmoidal induction curve is dependent on photosystems being hit two successive times with a time delay of $\sim 2\text{-}50\mu\text{s}$ between hits. This suggests that a photosystem's history does affect its fluorescence emission characteristics.

Picosecond fluorescence lifetimes have also been used in order to determine the presence of connectivity. Open reaction centers have specific fluorescence lifetime component(s) associated with them which are shorter than the component(s) associated with closed reaction centers. If there is no connectivity, each PS2 complex will be isolated from all others. In theory, open reaction centers will emit fluorescence at the shorter lifetimes and closed reaction centers

will emit fluorescence at the longer lifetimes. As more centers become closed, the amplitude of the short lifetime components will decrease and the amplitude of the long lifetime components will increase. If however, there is connectivity between a group of PS2 complexes, intermediate fluorescence lifetime components will be observed. These lifetimes will be an average of the lifetimes of all of the linked complexes. Therefore, as centers become closed, the fluorescence lifetime will gradually increase from the short to the long lifetime (Mullineaux and Holzwarth, 1993).

A number of groups have used this method to determine the presence of connectivity in *Chlorella*, *Chlamydomonas* and spinach (Haehnel et al, 1983, Moya et al, 1986, Hodges and Moya, 1987 and Keuper and Sauer, 1989). All groups saw complex changes in both fluorescence lifetimes and yields and interpreted these in terms of various connectivity models. In more recent work on cyanobacteria, Mullineaux and Holzwarth (1993) observed changes in the amplitudes of the lifetimes for closed and open centers, but saw only small changes in lifetimes. They interpreted this to mean that there was no connectivity in cyanobacteria.

In all of these cases with picosecond fluorescence decay, it is likely that what was interpreted as a single component was a function of more than one overlapping components. To interpret the changes in both yield and lifetime of these mixed components is difficult at best. One would expect to see complicated changes in yields and lifetimes which were not necessarily caused by connectivity.

In addition, multiple turnover light was used to close reaction centers prior to measurements. All of the groups doing picosecond measurements used a constant preillumination that varied in duration from 200 μ s to 5s. As was stated previously, multiple hits

on a photosystem do have an effect on the fluorescence characteristics of the cells. This then is another factor which complicates the interpretation of the picosecond measurements.

Materials and Methods

Cell Cultures

The marine cyanobacterium *Synechococcus* sp. strain PCC 7002 was obtained from D. Bryant at the Pennsylvania State University. In addition to the wild type of this strain, two mutant strains (psaL- and apcD-) constructed in Bryants lab, were also used. The psaL and apcD genes were insertionally inactivated by homologous recombination with inactivated genes carrying a cartridge for kanamycin resistance. Growth on solid A+ medium containing kanamycin allowed for selection of transformants (Schluchter et al, 1996 and Maxson et al, 1989).

The psaL gene codes for the PS1 reaction center psaL subunit which is likely responsible for PS1 trimerization. The apcD gene codes for the allophycocyanin B subunit which is one of the terminal energy emitters in the phycobilisome core. A detailed description of both mutants is included in the literature review.

Stock cultures of all cell types were grown in liquid A+ medium on a shaker under low light conditions ($10\mu\text{mol photons m}^{-2} \text{ s}^{-1}$ of white fluorescent light) at 32 degrees C. Prior to use in experiments, cells were grown under higher light ($100\mu\text{mol photons m}^{-2} \text{ s}^{-1}$) conditions with air bubbling for at least 2 or 3 days. During this time, cultures were diluted daily in order to keep cells in a rapid growth phase. Approximately 24 hours before an experiment, a fresh culture of cells was started using the actively growing high light cells as seed culture.

Cells were removed from the growth chamber prior to an experiment and the chlorophyll a concentration determined (Mackinney, 1941). The chlorophyll a concentration at the time of harvesting was usually between 3 and 7 $\mu\text{g chlorophyll a/ml}$. For most experiments,

the cell culture was diluted with A+ medium to a final chlorophyll a concentration of 2.5 μg chlorophyll a/mL. This low concentration was used in order to avoid self shading and self absorption artifacts. Wild type and *apcD*- cells were used directly after their removal from the growth chamber. *PsaL*- cells were used either directly after removal from the growth chamber (non-starved) or after they had been dark adapted for at least 12 hours at 32 degrees C (starved).

PAM measurements

Room temperature fluorescence measurements were done using a Pulse Amplitude Modulated (PAM) fluorometer (Model PAM 101 Chlorophyll Fluorometer; H. Walz, Effeltrich, Germany). A detailed description of the theory and uses of the PAM is given by Schreiber et al (1986). Briefly, a light emitting diode (LED; 650nm peak emission) provides a pulsed beam of light (pulsed at either 100 or 1.6 KHz) which illuminates the sample cuvette and is absorbed by both phycobilisomes and chlorophyll. A synchronized detector measures fluorescence which is emitted from the sample on the same frequency as the emitting diode. Therefore, only fluorescence which is a result of the pulsed emitting diode is detected. As a result, samples can be illuminated by other non-pulsed light sources which are in excess of 1000 times more intense than the pulsed emitter, but because they are not pulsed, the fluorescence which is a result of these external light sources is not detected. Rather, the effects of this light, such as reduced Q_A , are detected by changes in the yield of fluorescence from the LED. In addition, because the integrated light intensity of the emitter is so low (around 3-6 $\mu\text{mol photons m}^{-2} \text{ s}^{-1}$ at 100 KHz and $\ll 1$ $\mu\text{mol photons m}^{-2} \text{ s}^{-1}$ at 1.6 KHz), fluorescence parameters of samples can be measured while samples are effectively in the dark.

77K Fluorescence measurements

A spectrofluorometer which is described by Bruce et al (1989) was used to measure fluorescence emission from samples frozen in liquid nitrogen (77 degrees K). Two excitation wavelengths, 435nm, which is absorbed by chlorophyll and 590nm, which is absorbed by the phycobilisomes, were used to illuminate samples for measurements. Prior to freezing, samples were either dark adapted (state 2) or illuminated with red light for at least 2 minutes (state 1) in Pasteur pipettes sealed on one end. Fluorescence emission spectra were obtained by averaging 12 scans of seven second duration (435nm excitation) or 5 scans of five second duration (590nm excitation).

Optical Cross Section Measurements

When determining the cross-section of a photosynthetic antenna, it is not the physical cross-section of the complex that is being measured but rather the area that a group of pigments has that absorbs light at a specific wavelength (Mauzerall and Greenbaum, 1989). In much the same way that the physical cross-sectional area determines how easy it is to hit a target with a physical projectile, the optical or absorption cross-section determines how easy a complex of pigments is to hit with a photon of light. The greater the number of pigments associated with a particular reaction center that absorb a particular wavelength of light (i.e. the greater the optical cross-section), the easier it is to hit that photosystem with that wavelength of light. In the present case, where there is a large population of photosystems in the sample, the greater the cross-section of individual photosystem antenna complexes, the lower the flux of photons that will be needed to hit a certain percentage of the photosystems.

Absorption cross-sections were measured using a pump-probe system as shown in figure 7. The pump (laser pulse) hits a percentage of the photosystems and the probe (xenon/fluorescence for PS2 and delta absorbance for PS1) determines what percentage were hit. Photons of a particular wavelength are supplied by a pulse from a Phase-R flash lamp pumped dye laser (time constant 200ns). The intensity of the laser flash is controlled using various neutral density filters. Part of the laser beam is reflected by a glass slide and the intensity measured with a pyrometer (Molelectron Pyroelectric Joulemeter which has an output of 2.58V/mJ, calibrated at 633nm). The other part of the beam passes through the glass slide and is directed via one arm of a trifurcated fibre optic light guide to the bottom surface of the sample cuvette where the cyanobacteria sample is located.

For PS2 absorption cross-sections a weak xenon flash, triggered by the laser pulse, is flashed 100 μ s after the laser flash and is directed to the bottom of the sample cuvette via the remaining two arms of the trifurcated fibre optic. Fluorescence emitted as a result of the xenon flash is detected by a photomultiplier tube from the side of the sample cuvette 1cm from the bottom via a fibre optic. Previously the xenon flash was only 50 μ s after the laser. However, I found that at high laser flash intensities, the baseline against which the fluorescence is measured had not fully recovered from the laser flash. At 100 μ s not only was the baseline flat but there was also an increase in the amount of signal.

When cells are left in the dark, the Q_A site at PS2 becomes oxidized (open reaction center). When photosystem 2 absorbs a photon from the laser flash, Q_A becomes transiently reduced (closed reaction center). The xenon flash 100 μ s after the laser flash is used to probe for a reduced Q_A (and therefore a hit photosystem). When a PS2 center which has a reduced Q_A is

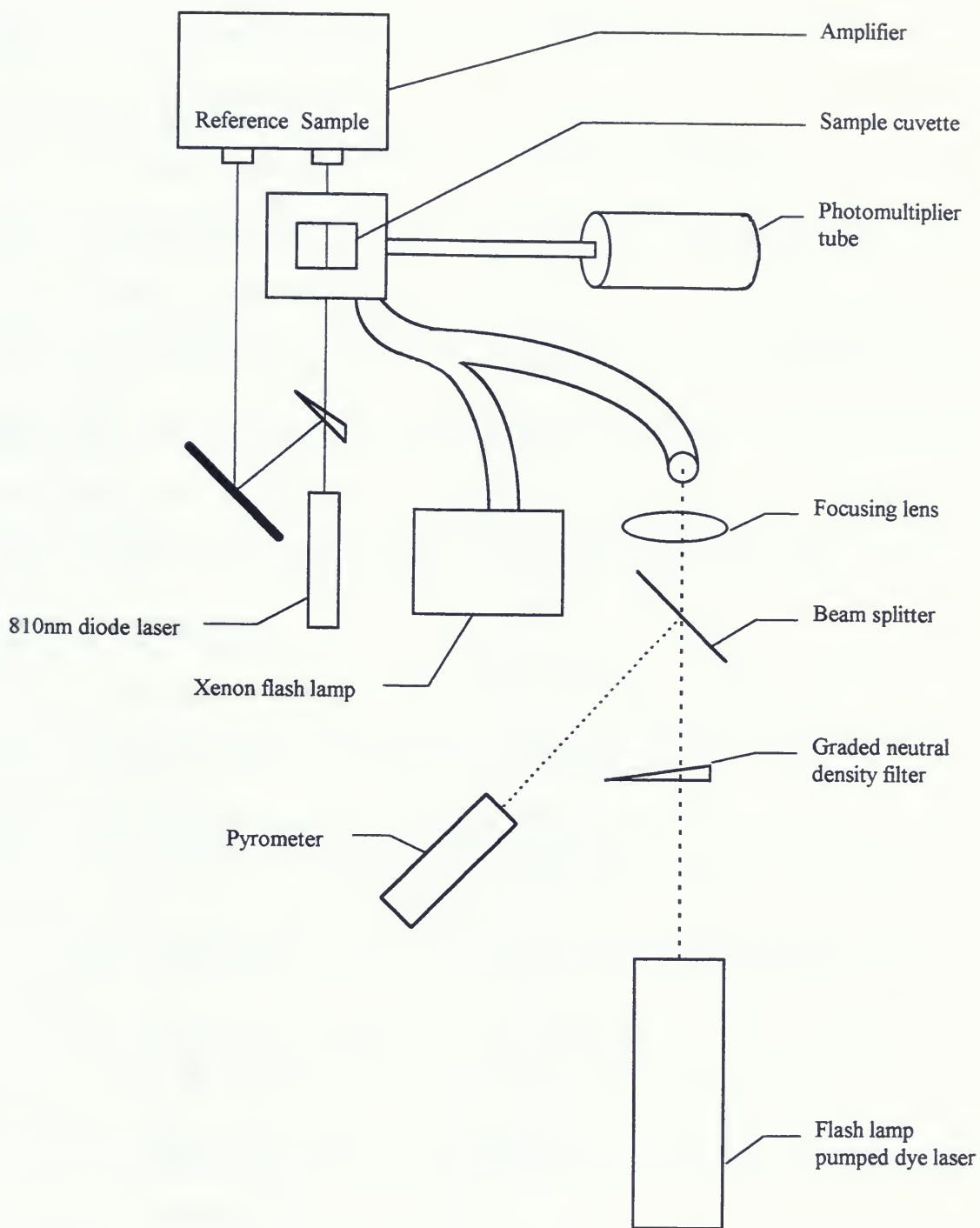


Figure 7. Absorption cross-section apparatus. Outputs from the pyrometer, photomultiplier tube and delta absorbance amplifier are stored first by a digital scope and then loaded into an IBM computer. Details of the theory and operation are found in the accompanying text.

hit by a photon from the xenon flash, there is no photochemical quenching of fluorescence and therefore variable fluorescence is emitted.

At a laser flash intensity of zero, all photocenters will be open and, therefore, a minimum fluorescence, F_0 , will be emitted from the xenon flash. At some high laser flash intensity, all photocenters will be hit by the laser flash and therefore become closed. Maximum fluorescence (F_m) from the xenon flash will be attained under these conditions. When the laser intensity is at an intermediate level, only a percentage of the photocenters will be hit by the laser flash and, therefore, some intermediate level of fluorescence will be emitted when probed with the xenon flash. A flash saturation curve for PS2 is obtained by varying the laser flash intensity from zero to some intensity above saturation.

Since there is no variable fluorescence from PS1 (Owens et al, 1988), a technique other than fluorescence has to be used to determine what percentage of PS1 centers are hit at a particular laser intensity (Mullineaux, 1992). When PS1 absorbs a photon, it becomes transiently oxidized ($P700^+$). The absorbance of 810nm light by P700 increases when it is oxidized to $P700^+$. Therefore, by monitoring the delta absorbance at 810nm after the laser flash, the percentage of hit PS1 centers can be determined. In a way analogous to PS2 fluorescence, when the laser intensity is zero, the delta absorbance will be zero showing that no centers were hit. As the laser intensity increases, more centers will be hit and the delta absorbance will increase until it reaches a maximum where all centers are being hit.

In order to determine absolute cross-section measurements, the actual intensity of light hitting the cells needed to be determined. During the experiment only the relative light intensity incident on the cell sample was measured by the pyrometer. A conversion factor, which accounted both for the optical density of the cell suspension and the distance from the light

source (the end of the fibre optic) to the cells where fluorescence and delta absorbance was measured, was used to determine the actual light intensity.

By fitting the curve with the single hit Poisson distribution, the absorption cross-section can be solved (Mauzerall and Greenbaum, 1989). For PS2:

$$\Phi_F(I) = F_0 + F_m(1 - e^{-I\sigma})$$

Where Φ_F is the fluorescence intensity, F_0 is the base level of fluorescence, F_m is the maximum fluorescence, I is the laser flash intensity (photons/Å²) and σ is the optical cross-section in Å². For PS1, delta absorbance is substituted for fluorescence. Cross-sections were fit using Sigma Plot.

Connectivity Measurements

To measure cross-sections in state 1, cells were illuminated with red light. In addition to driving the state transition this light had a secondary effect; it caused a partial reduction of Q_A . As outlined in the literature review, closing some reaction centers will increase the size of the PS2 cross-section if there is connectivity between PS2 centers. In order to separate these two effects, connectivity needed to be measured independently from the state transition.

In order to measure the changes in cross-section due to connectivity, the apparent F_0 level needed to be raised without driving the state transition. As outlined in the literature review, this has been done by a number of researchers in the past with a short period of illumination just prior to the measurement. This method, however, has inherent problems. Even if the illumination time is much shorter (milliseconds) than that needed to drive the state transition (seconds), other changes which are the result of multiple turnover illumination may be induced (outlined in the literature review).

To circumvent these problems I devised a method where cells were preflashed with a single turnover xenon flash 700 μ s before the laser flash. By doing this, I was able to close a percentage of the reaction centers just prior to measurement without causing a state transition or inducing the effects caused by multiple turnovers. By changing the intensity of the single turnover flash using neutral density filters I was able to vary the apparent F_0 level from zero elevation to F_m .

The computer which was triggering the laser did not have the capabilities to also trigger the first xenon flash closer than 22ms before the laser. This was too long as many of the reaction centers would reopen during this time. So, together with the assistance of the electronics shop, I built a trigger delay which enabled me to trigger the xenon flash 700 μ s before the laser. Briefly, the trigger pulse from the computer was split; the first half triggering the preflash xenon lamp and the second half triggering the laser after being delayed (delay could be varied between approximately 100 μ s and 3ms).

Flow Through vs. Stirred Sample System

For some experiments (especially PS2 cross-section measurements), the speed of the experiment increased and the quality of the data improved when cells were pumped through the sample cuvette. In the pumping system, 25ml of cells were circulated through a standard 3ml sample cuvette with the majority of the sample being held in a temperature regulated glass chamber. For state 2 experiments, the entire system was kept in the dark whereas for state 1 experiments, cells were preilluminated in the large glass chamber. There was a travel time of approximately 3 seconds in the dark between the preillumination and the cuvette.

Alternatively, in the non-circulating system, only 2.5 mls of sample, which remained in the cuvette, were used. Cells were either continuously stirred (PAM measurements) or stirred periodically (PS1 measurements) to avoid changes in cell concentration due to settling. Illumination of the sample was direct. In the case of state 1 PS1 cross-section measurements, where the sample needed to be illuminated in order to drive the state transition, a light dark regime was devised which mimicked the 3 second delay in the PS2 circulating measurements. That is, a cycle was used where cells were alternately illuminated for 10 seconds and then dark adapted for 4 seconds. The laser flash was triggered at the 3rd second of the 4 second dark time.

Results

77K Fluorescence

In order to determine if the state transition was occurring in the wild type and mutant cells, 77K fluorescence emission spectra were measured as shown in figures 8, 9 and 10. A signature of the state transition is a higher ratio of the PS2:PS1 fluorescence emission from their respective peaks in state 1 than state 2. These ratios are found in table 1. Panel A in each of the figures shows fluorescence from 435nm (chlorophyll) excitation and panel B shows fluorescence from 590nm (phycobilisome) excitation.

With 435nm excitation an increase in the amplitude of the PS2 peaks (685nm and 695nm) relative to the PS1 (715nm) peak was observed, from state 2 to 1 in the wild type (figure 8). This shows that there is a redistribution of energy from PS1 to PS2 at the chlorophyll level. With 590nm excitation, a similar trend occurred where the amplitude of the PS2 peaks increase relative to the PS1 peak from state 2 to 1. This shows that there is also a redistribution of phycobilisome absorbed light between states. Relatively more of the energy absorbed by the phycobilisome is directed towards PS2 in state 1 than in state 2. Energy absorbed by the phycobilisome in state 2 may either be directly transferred to the PS1 antenna or alternatively it is first transferred to the PS2 chlorophyll antenna and then to the PS1 antenna by spillover.

There was no increase in the ratio of the PS2:PS1 peaks in state 1 for the *apcD*- cells (figure 9). Rather, at both 435nm and 590nm excitation, a small but consistent trend in the opposite direction to that in the wild type was observed. A similar trend was observed in the PAM data (figure 12) when *apcD*- cells were illuminated with red light in order to induce the state transition. These data show that a state transition is not occurring in these cells. Instead, there is a small quenching of fluorescence in state 1.

The *psaL*⁻ cells showed the same trends as the wild type cells, an increase in the ratio of fluorescence emission from PS2:PS1 in state 1 at both 435nm and 590nm excitation (figure 10). This shows that the state transition does occur in this mutant. However, since the change in the ratio between states is approximately half that of the wild type, there is less of a redistribution between states compared to the wild type.

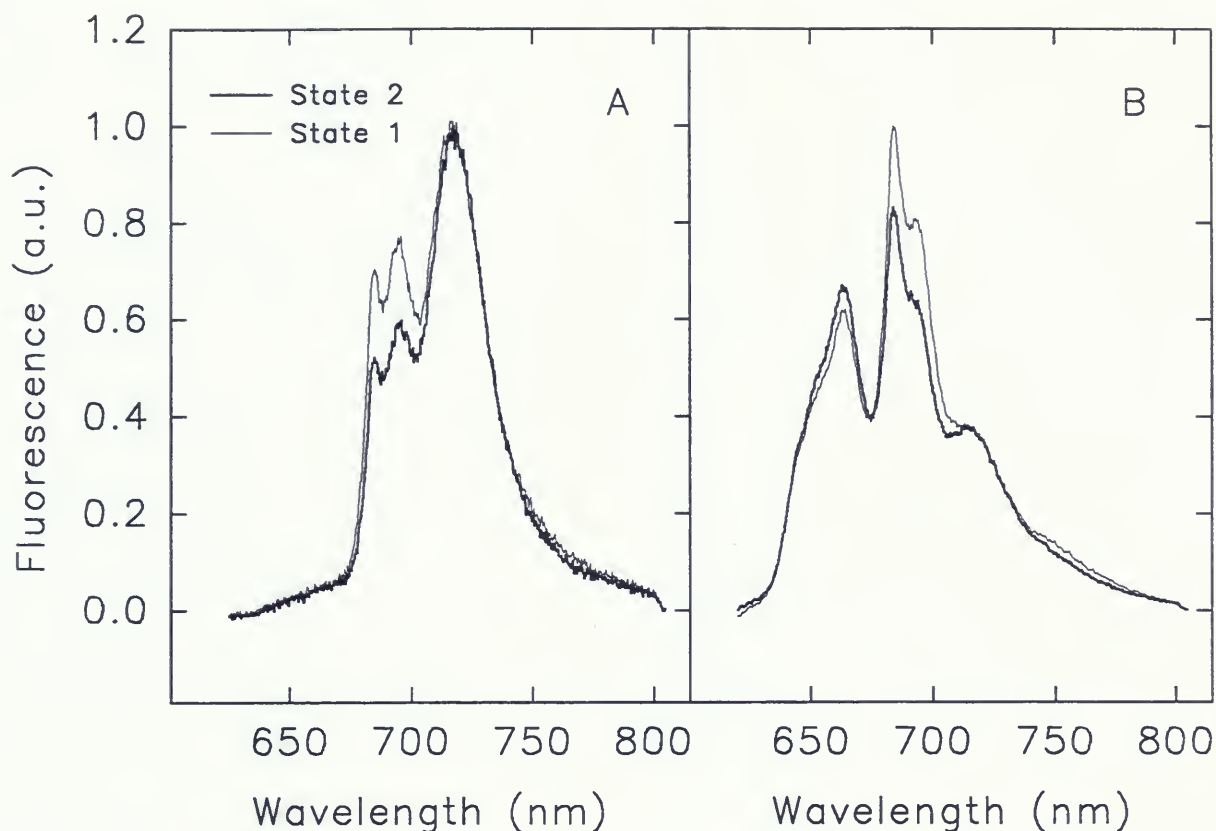


Figure 8. 77K fluorescence emission spectra of 7002 wild type cells (chl a concentration of $5\mu\text{g/ml}$) in state 2 and state 1. Panel A has spectra for 435nm excitation (chlorophyll absorbed) and panel B for 590nm excitation (phycobilisome absorbed). The fluorescence emission peaks at 665nm originate from the phycobilisomes, at 685nm and 695nm from PS2 and at 715nm from PS1. Spectra were normalized to the 715nm peak for both excitation wavelengths. Cells were frozen in liquid nitrogen immediately after being dark adapted for at least 5 minutes (state 2) or after red light illumination for at least 2 minutes (state 1).

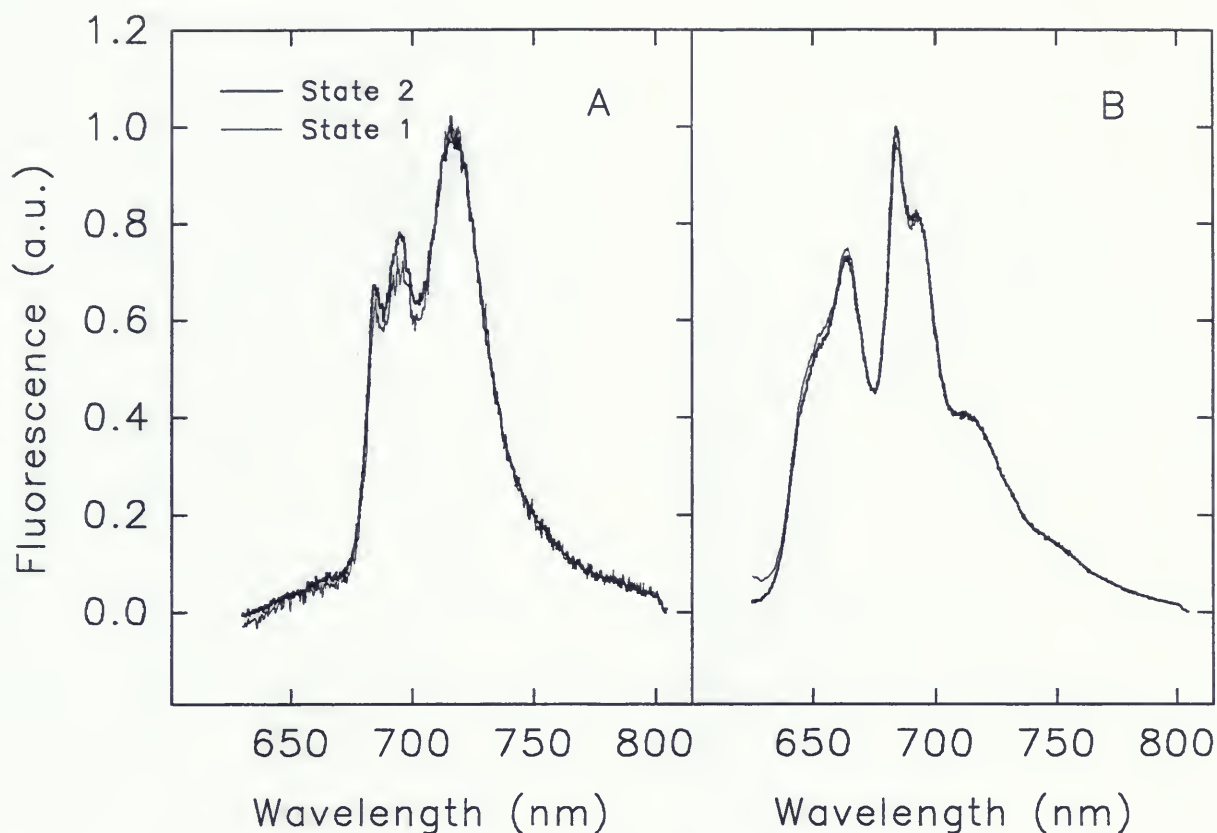


Figure 9. 77K fluorescence emission spectra of 7002 *apcD*⁻ cells. Panel A has spectra for 435nm excitation (chlorophyll absorbed) and panel B for 590nm excitation (phycobilisome absorbed). The fluorescence emission peaks at 665nm originate from the phycobilisomes, at 685nm and 695nm from PS2 and at 715nm from PS1. Spectra were normalized to the 715nm peak for both excitation wavelengths. All conditions for the experiment were the same as described in figure 8.

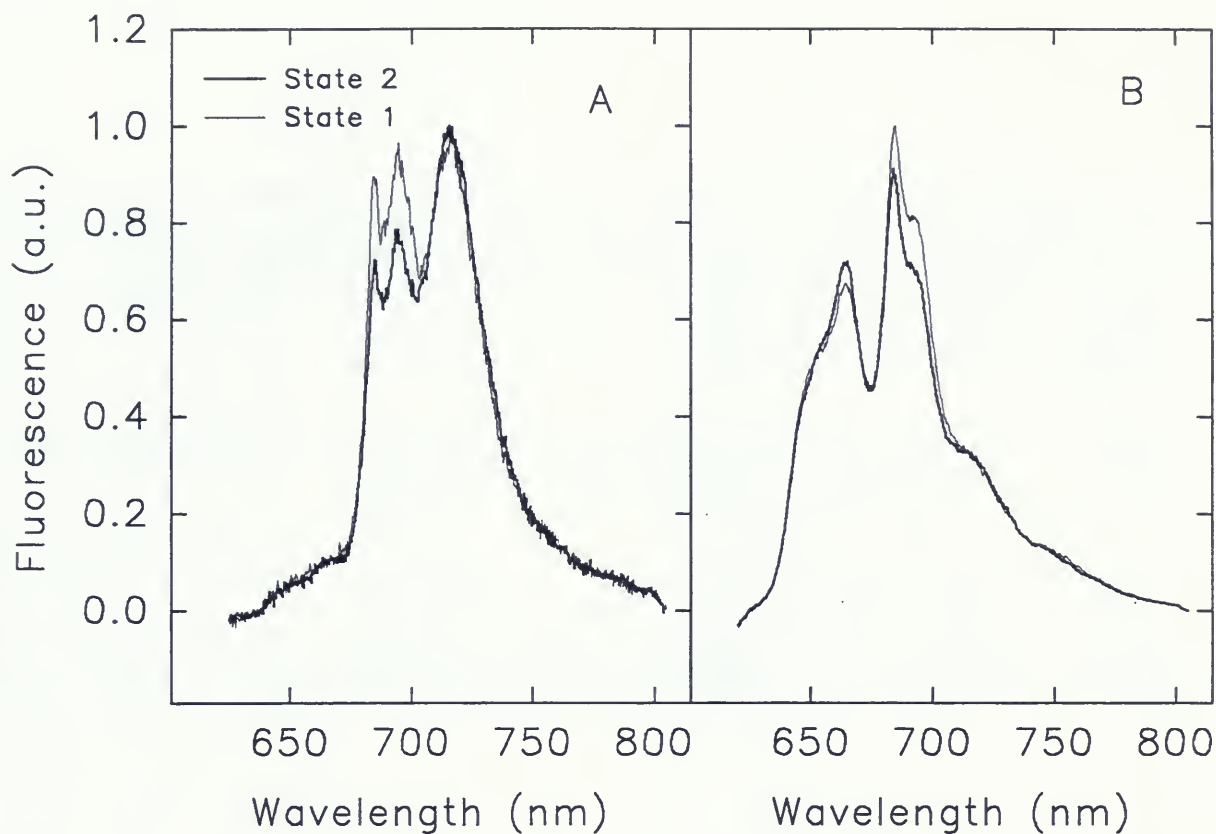


Figure 10. 77K fluorescence emission spectra of 7002 *psaL⁻* cells. Panel A has spectra for 435nm excitation (chlorophyll absorbed) and panel B for 590nm excitation (phycobilisome absorbed). The fluorescence emission peaks at 665nm originate from the phycobilisomes, 685nm and 695nm from PS2 and at 715nm from PS1. Spectra were normalized to the 715nm peak for both excitation wavelengths. All conditions for the experiment were the same as described in figure 8.

Cell type	Excitation λ	State 2	State 1	% increase
7002 wild type	435nm	0.54 ± 0.04	0.74 ± 0.04	37%
	590nm	2.16 ± 0.02	2.62 ± 0.01	21%
7002 apcD-	435nm	0.68 ± 0.01	0.64 ± 0.01	-6%
	590nm	2.49 ± 0.06	2.38 ± 0.01	-4%
7002 psaL-	435nm	0.72 ± 0.01	0.88 ± 0.04	22%
	590nm	2.75 ± 0.01	3.02 ± 0.01	10%

Table 1. Summary of the 685nm:715nm fluorescence emission peak ratios from 77K fluorescence emission data of 7002 wild type, apcD- and psaL- cells (sample spectra shown in figures 8, 9 and 10 respectively). 435nm excitation is absorbed by chlorophyll and 590nm excitation by the phycobilisomes. The fluorescence emission peak at 685nm is from PS2 and at 715nm from PS1. Experimental conditions are described in figure 8.

Room Temperature Fluorescence

Room temperature fluorescence as determined on the PAM fluorometer confirmed trends shown at low temperature. Panel A in figures 11, 12 and 13 shows PAM traces as observed in a non-circulating system (illumination directly on sample being measured), whereas panel B shows traces with a circulating system (preillumination in a 22ml chamber before cells are pumped through the sample cuvette; 3 second delay time between preillumination and fluorescence measurements). The measurements on the non-circulating system reveal characteristics of cells as they are being illuminated. However, since fluorescence measurements are made 3 seconds after illumination in the circulating system, use of this system monitors continuously what the cells are like in the dark (when red light is off) or 3 seconds after the light is turned off (when preillumination light is on). Since cross-section measurements were made using the circulating system, the panel B traces show characteristics of each cell type as they were while these measurements were being made.

For all experiments, cells were dark adapted prior to measurements with the PAM. This was done to insure that Q_A was oxidized and, therefore, that the cells were at F_o . At time 10 seconds on each trace, the pulsed light from the PAM was turned on, allowing a measurement of F_o . At 20 second intervals a 500ms saturating flash ($6000\mu\text{mol photons m}^{-2} \text{s}^{-1}$) illuminated the sample, transiently reducing all Q_A . As Q_A went from being oxidized to being fully reduced, fluorescence went from F_o to the maximum fluorescence F_m . Q_A quickly became reoxidized resulting in a return to F_o . Between the times indicated on the figures, cells were continuously illuminated with red light. The saturating flashes during this time gave a measurement of the F_m value under state 1 conditions.

Figure 11 shows PAM traces for wild type cells. Several trends are readily apparent. First, there is a large increase in F_m when cells are illuminated with red light and a decrease after the light is turned off. This is distinctive of the state transition. An increase in PS2 cross-section in state 1 causes an increase in the fluorescence emission from PS2. Second, the increase in F_m is similar when cells are either illuminated directly or when they are preilluminated. This is important as cross-section measurements were made with preilluminated cells. If there was a significant transition from state 1 back to state 2 in less than three seconds, the circulating system would not have allowed for a measure of the cross-section while cells were fully or almost fully in state 1. Third, in both panels, an increase in fluorescence is observed when the red light is on. Some of this increase may be due to a real change in F_o between states (as will be discussed later), but the majority of this increase is due to an apparent increase in F_o caused by reduction of Q_A as a result of illumination. The extent of the increase in fluorescence is less in the circulating system than in the direct illumination. In the circulating system, the 3 second delay between illumination and measurement allows for some oxidation of Q_A . For cross-section measurements it is important to have a minimum increase in continuous fluorescence and a maximum increase in F_m (this idea will be discussed in more detail together with the connectivity data). If there is too long of a delay between illumination and measurement, there will be a significant transition back to state 2. However, if there is an insufficient amount of time before measurement, Q_A will still be highly reduced. The three second delay struck a balance between these two extremes. The fourth trend (seen best in panel A) is that when the light is turned off there are three events which occur: a fast (1-2s) decrease in fluorescence, a slower increase in fluorescence (approx. 15s) and a slow decrease in fluorescence to the state 2 F_o level (approx. 200-250s). Since the fluorescence level is related to the redox state of the electron transport chain, these fluctuations

show that after the red light is turned off there is a fast oxidation, a slower reduction and finally a slow oxidation of Q_A .

Data from the *apcD*- cells appears in figure 12. The first obvious trend for this mutant is that there is no increase in F_m with red light illumination. Just the opposite occurs; there is a slight depression of F_m showing a quenching of fluorescence. This trend is more obvious with direct illumination than with preillumination, suggesting that the quenching of fluorescence is mostly relieved within 3 seconds. This quenching coincides with the decrease in PS2:PS1 ratio of fluorescence emission seen in the 77K measurements under state 1 conditions. The second trend is that there is an increase in fluorescence when the light is turned on similar to that observed in the wild type. Finally, changes in fluorescence similar to those in the wild type occur when the red light is turned off. However, the kinetics and amplitudes are different. The fast oxidation occurred in 1-2s, the slow reduction in approximately 50s and the slow oxidation in approximately 50s. It was not possible to tell if the first oxidation was faster than the wild type. However, the reduction was 4 times slower and the slow oxidation was 4 or 5 times faster. In addition, the extent of the reduction was considerably less than in the wild type.

Figure 13 shows traces from the *psaL*- cells. Panels A and B both show an increase in F_m with red light, showing that a state transition occurred. The elevation in F_m was smaller than that shown for the wild type, suggesting that there was somewhat less of a change in the distribution of energy between states. With direct illumination there was an increase in fluorescence similar to the wild type, but to a lesser degree. However, in contrast to the wild type, there was a decrease in fluorescence when cells were illuminated in the circulating system. That is, red light caused the fluorescence to drop below the level that was originally thought to be F_o . This suggested that when the cells were in the dark before illumination, a portion of Q_A

remained reduced, causing an elevation in the fluorescence above F_o . This phenomenon was masked in the non-circulating system by the large increase in Q_A reduction caused by the direct illumination. After the red light was turned off, the same trend seen in the wild type and *apcD*-cells was observed for the *psaL*- cells. The fast oxidation of Q_A occurred in 1-2s, the slow reduction in 10-20s and the slow oxidation in excess of 300s. Unlike the wild type or the *apcD*-cells, the increase of the fluorescence due to the reduction of Q_A is considerably higher than the F_v level while the light is on.

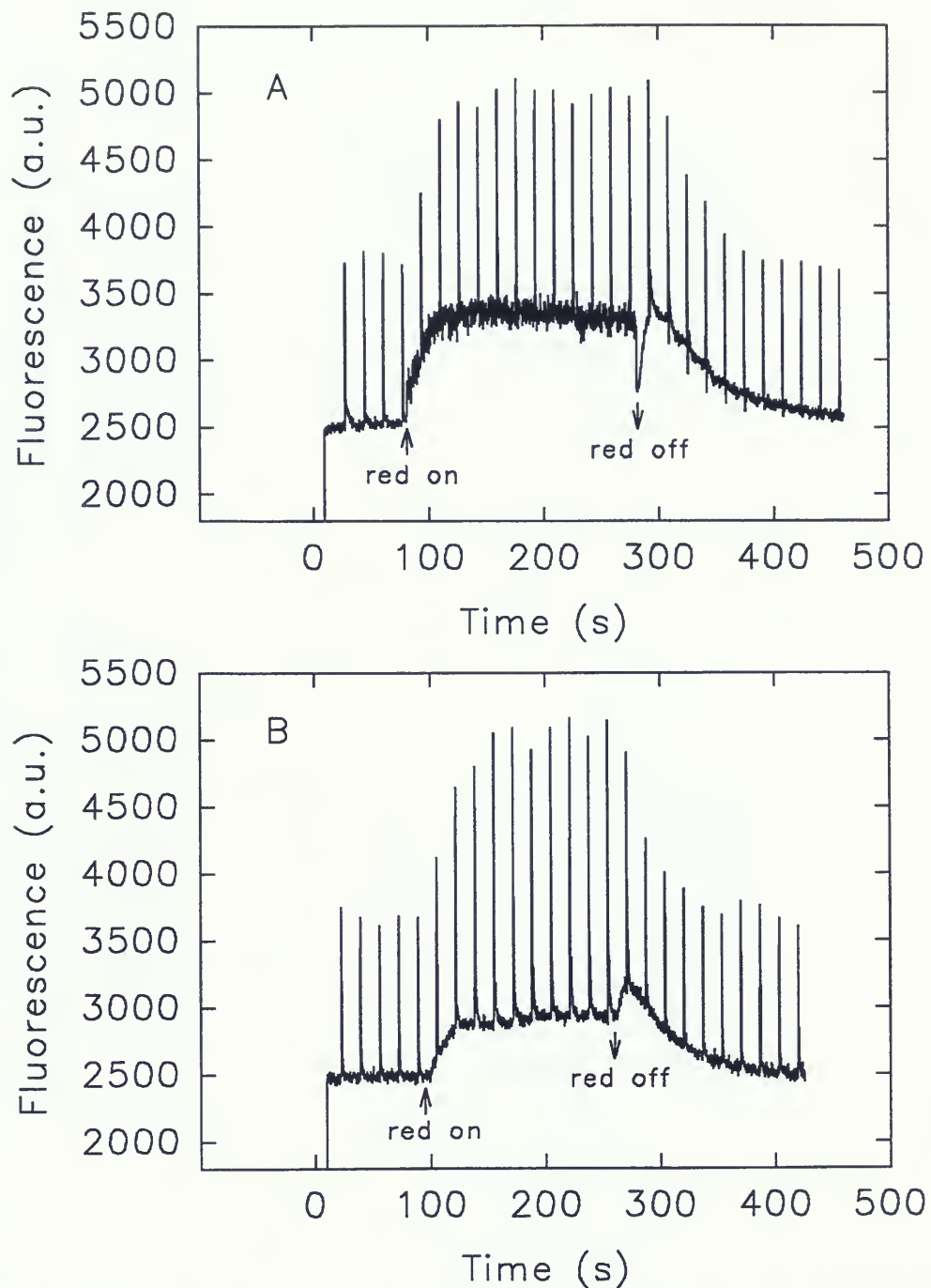


Figure 11. Room temperature fluorescence emission (on PAM) of 7002 wild type cells. Cells were harvested, diluted to $2.5\mu\text{g/ml}$ and dark adapted for at least 5 minutes before use in experiments. Panel A shows fluorescence emission from 3ml of cells which were continuously stirred in a cuvette. Red light illumination was directly on the cells being measured. Panel B shows fluorescence emission from cells which were preilluminated with red light and circulated through the cuvette. Every 20 seconds the F_m level was determined by illuminating the sample in the cuvette with a saturating flash of white light ($6000\mu\text{mol photons m}^{-2} \text{s}^{-1}$ for 500ms). The frequency of the pulsed light from the PAM was 1.6KHz.

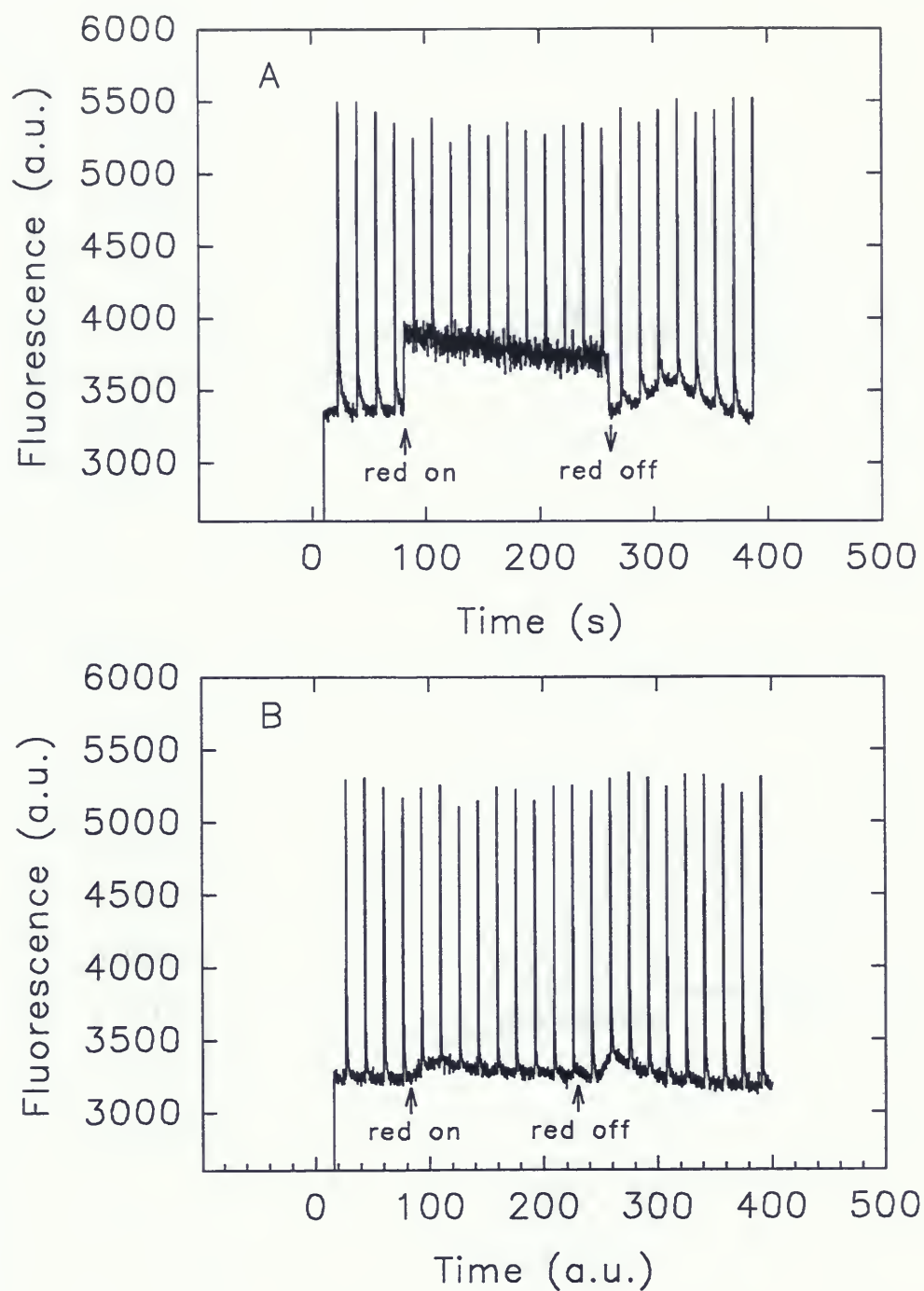


Figure 12. Room temperature fluorescence emission (on PAM) of 7002 *apcD⁻* cells. Experimental conditions were the same as those described in figure 11. Panel A shows the non-circulating data and panel B the circulating data.

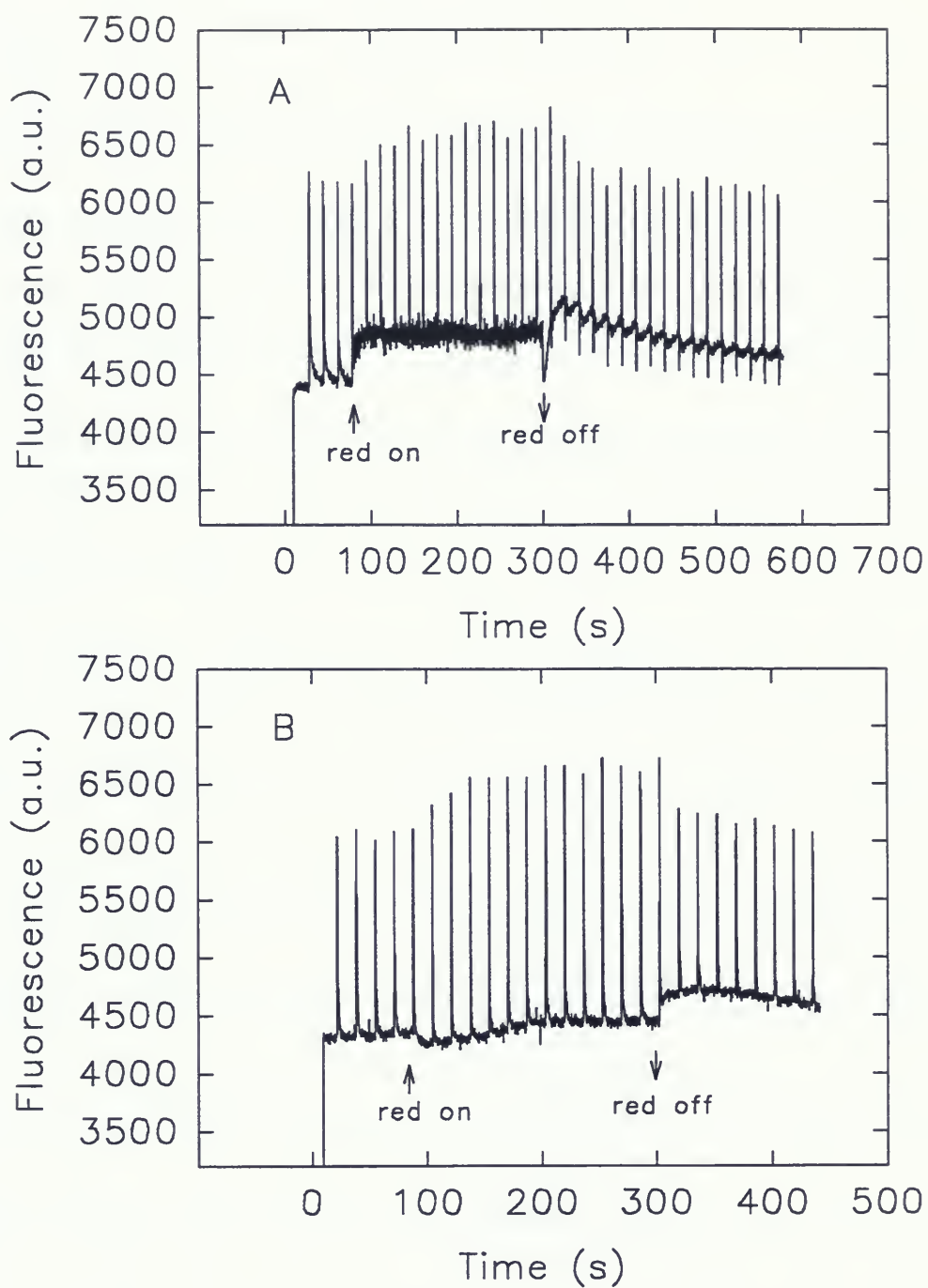


Figure 13. Room temperature fluorescence emission (on PAM) of 7002 *psaL-* cells. Experimental conditions were the same as those described in figure 11. Panel A shows the non-circulating data and panel B the circulating data.

The *psaL* mutant

Differences between the *psaL*- and the wild type cells were first discovered when cross-section measurements were being made. Wild type cells always showed some increase in the apparent F_o level in state 1 compared to state 2 (figure 11). The *psaL*- cells, however, showed the exact opposite: a decrease in apparent F_o in state 1 (data not shown). This was a puzzling observation and meant that either there was an actual decrease in the apparent F_o level in state 1 (no theoretical basis for this), or that when measurements were done in state 2 (dark adapted), the apparent F_o level was elevated.

Figure 14 shows PAM traces from the wild type and the *psaL*- cells. The wild type trace shows the same characteristics as those shown previously. The *psaL*- trace shows similar characteristics to the trace shown earlier; however they are more accentuated. In the previous PAM traces the LED from the PAM was pulsed at frequency of 1.6KHz. In this trace it was pulsed at 100KHz (meaning that the integrated light intensity of the pulsed beam was 62.5 times higher; still only a very low intensity of $3\text{-}6\mu\text{mol photons m}^{-2} \text{ s}^{-1}$). This slightly higher background light may have caused a small increase in Q_A reduction when the cells were to be in the dark and, therefore, probably accounts for the differences between these and earlier data.

One of the most noticeable differences between the wild type and the *psaL*- is that with the *psaL*- after a saturating flash of light the fluorescence not only returns to what it was prior to the flash, but goes below it. This evidence built on the idea that cells were not at F_o in the dark and suggested that there is a reduction of Q_A in the dark. It appeared that in the dark Q_A was partly reduced, and that a flash of light was able to first reduce all of Q_A and then cause it to become more oxidized than its resting level. In the previous experiments with the pulsed light at 1.6KHz, the saturating flash did not cause this extra oxidation after a saturating flash. However,

when the red light was turned on, the fluorescence level dropped below the apparent F_o level, showing that in this case too the F_o level was elevated. The effect of having the 100KHz pulsed light might have been that this elevated the fluorescence level slightly higher than it would have been in the dark or with the 1.6KHz pulse light. Even if this did occur, the phenomenon is still interesting because this same effect was not observed with the wild type cells. Therefore, it looks as though the apparent F_o level in the *psaL*- cells is elevated in the dark as shown with the 1.6KHz pulsed light, and that any extra PS2 absorbed light is able to cause further elevation.

These two traces again show the fast decrease, followed by a slower increase and finally a slow decrease in variable fluorescence when the red light is turned off. Similar trends were observed in the earlier PAM traces. These are indicative of a fast oxidation, slower reduction and slow oxidation of Q_A .

The complex changes in fluorescence that occur after a saturating flash, during illumination and after the red light is turned off are the result of a number of competing photosynthetic and respiratory processes. These will be discussed in detail in the context of a model for photosynthetic and respiratory electron transport in the discussion.

The original intent of the more intense experiments with the *psaL*- cells was to determine whether the apparent F_o level was elevated in the dark and, if it was, whether this elevation could be alleviated in order for cross-section measurements to be made. If the problem was that the PQ pool and, therefore, Q_A was reduced, it would seem reasonable that far red illumination, only hitting PS1, would oxidize the electron transport chain. Figure 15 shows that illumination with far red light was able to decrease the apparent F_o level. However, oxidized PQ causes a transition to state 1, as seen by the increase in F_m , which made state 2 measurements impossible by this method. The addition of p-benzoquinone, an electron acceptor of PQ also caused an

oxidation of Q_A and a transition to state 1. Neither of these methods allowed a measurement with oxidized Q_A while cells were in state 2.

Mimicking an experiment by Hualing et al (1994), in which cells were starved by placing them in the dark for an extended period of time, decreased the elevation of the apparent F_o to a level much closer to the real F_o . The dark adaptation caused a depletion of respiratory substrates and, therefore, a lack of substrate for the NAD(P)H dehydrogenase. Figure 16 shows the result of this experiment. Addition of p-benzoquinone, which oxidizes PQ should have little or no effect on the apparent F_o level if it is not elevated. This was shown with the wild type cells (figure 16A). In the case of *psaL*- cells which had not been dark starved, a large decrease in apparent F_o was observed upon addition of p-benzoquinone, showing that the apparent F_o level had been elevated. With the *psaL*- cells which had been starved for over 12 hours, a much smaller decrease in apparent F_o was observed. This showed that the source of the dark reduction of PQ was stored respiratory substrates.

A further experiment to show conclusively that this was the case is shown in figure 17. Dark starvation changed the extent of the reduction of Q_A after illumination with red light. After a brief time of illumination, there was no increase in reduction of Q_A as had been seen previously with non-starved cells. However, incubation with 80mM fructose for 1 hour (shown by Hualing et al, 1994 to replenish internal respiratory substrate stores) caused the starved cells to become reduced after the red light illumination (the same as non-starved cells).

A method for measuring cross-sections in the *psaL*- cells was developed where cells were grown as they had been before, but they were starved in the dark for at least 12 hours before measurements.

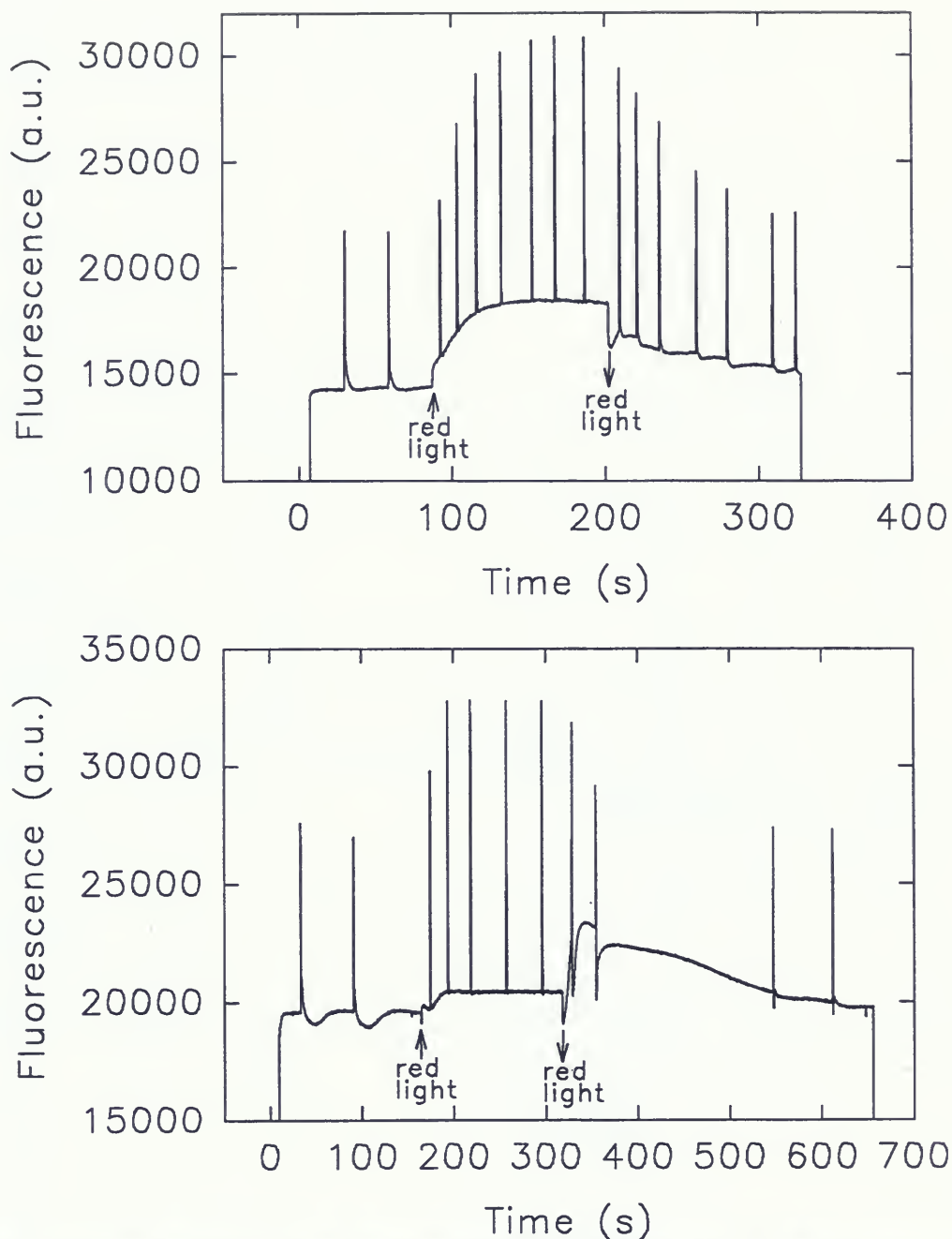


Figure 14. Room temperature fluorescence emission (on PAM) showing the differences between 7002 wild type cells (panel A) and 7002 *psaL*- cells (panel B). Cells were dark adapted for at least 5 minutes prior to measurements. Measurements were done in a non-circulating system with red light illumination directly on stirred cells in the cuvette. Periodically F_m was determined by illuminating the sample with a saturating flash of white light ($6000 \mu\text{mol photons m}^{-2} \text{s}^{-1}$ for 500ms). The frequency of the pulsed light from the PAM was 100KHz.

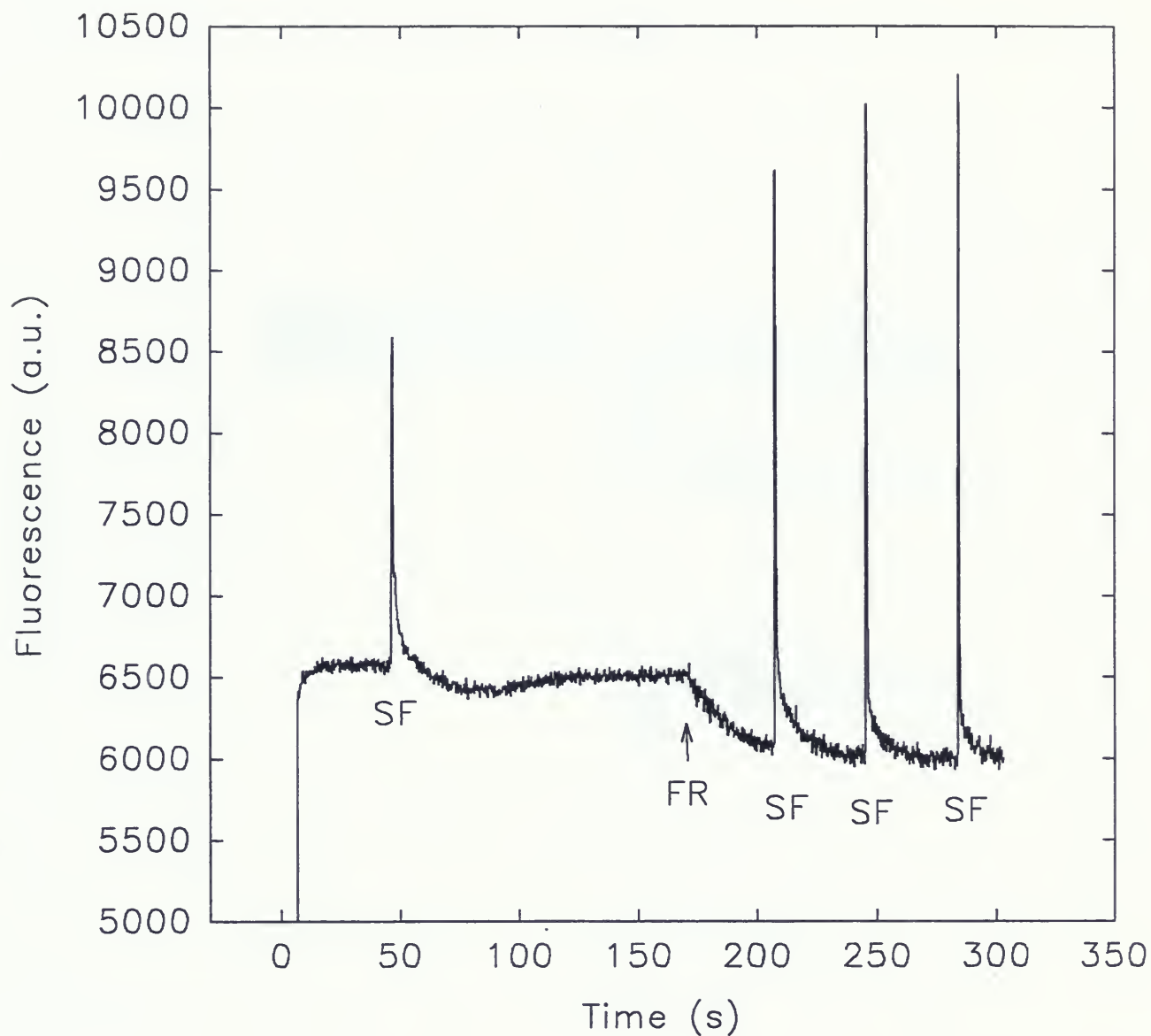


Figure 15. Room temperature fluorescence emission (on PAM) from 7002 psaL- cells. Cells harvested and dark adapted for at least 5 minutes before use in experiments. During the experiment, cells were in the dark until illumination by a far red light at time 172s; except for a saturating flash (SF, $6000\mu\text{mol photons m}^{-2} \text{s}^{-1}$ for 500ms).

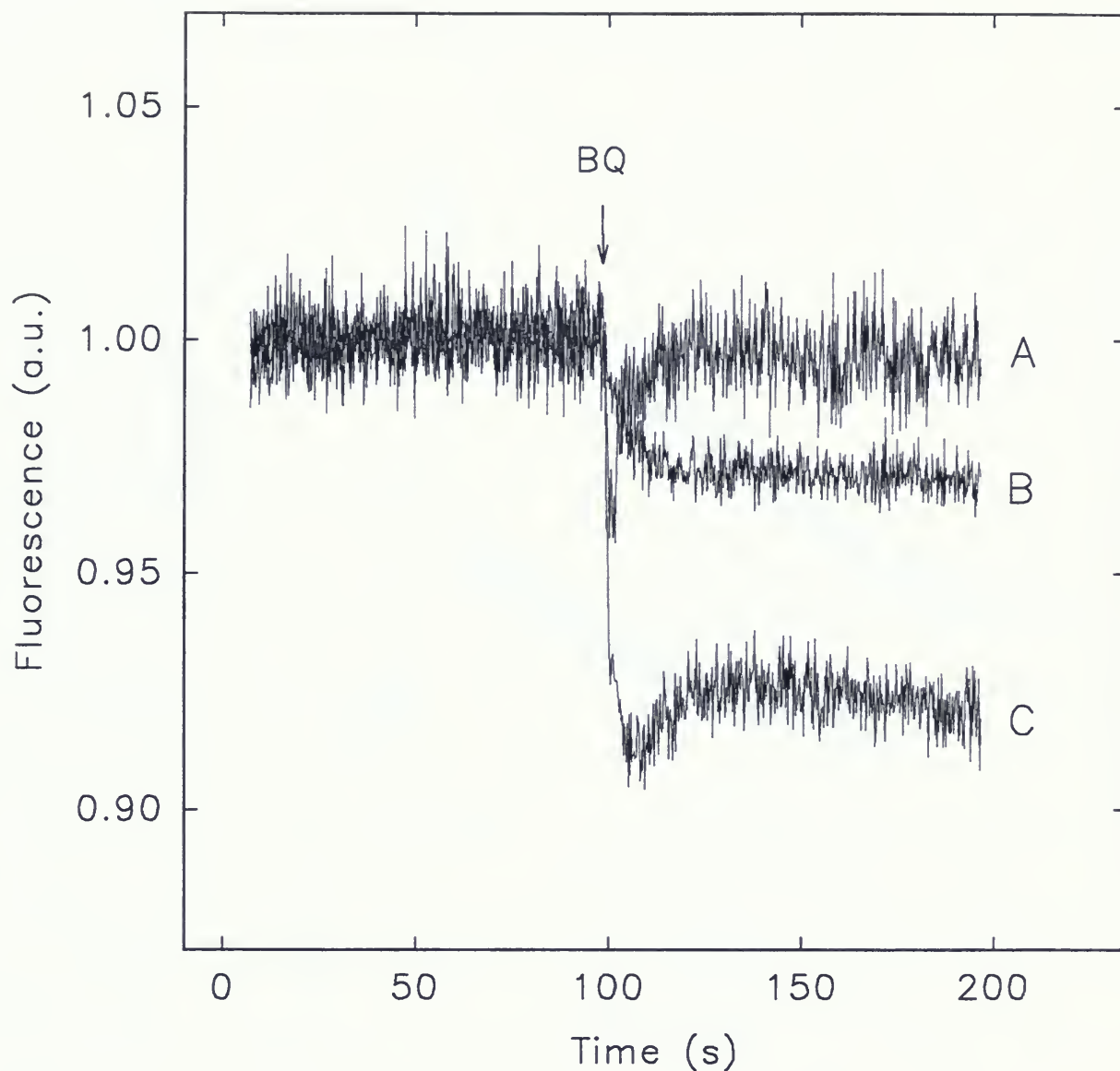


Figure 16. Room temperature fluorescence emission (on PAM) demonstrating differential effect of P-Benzoquinone on the fluorescence level of 7002 wild type cells dark adapted for 10min. (A), 7002 *psaL*⁻ cells dark adapted for over 12 hours (B) and 7002 *psaL*⁻ cells dark adapted for 10min. (C). Cells were in the dark throughout the experiment. 500 μ M P-Benzoquinone was added to cells in the dark at the time indicated.

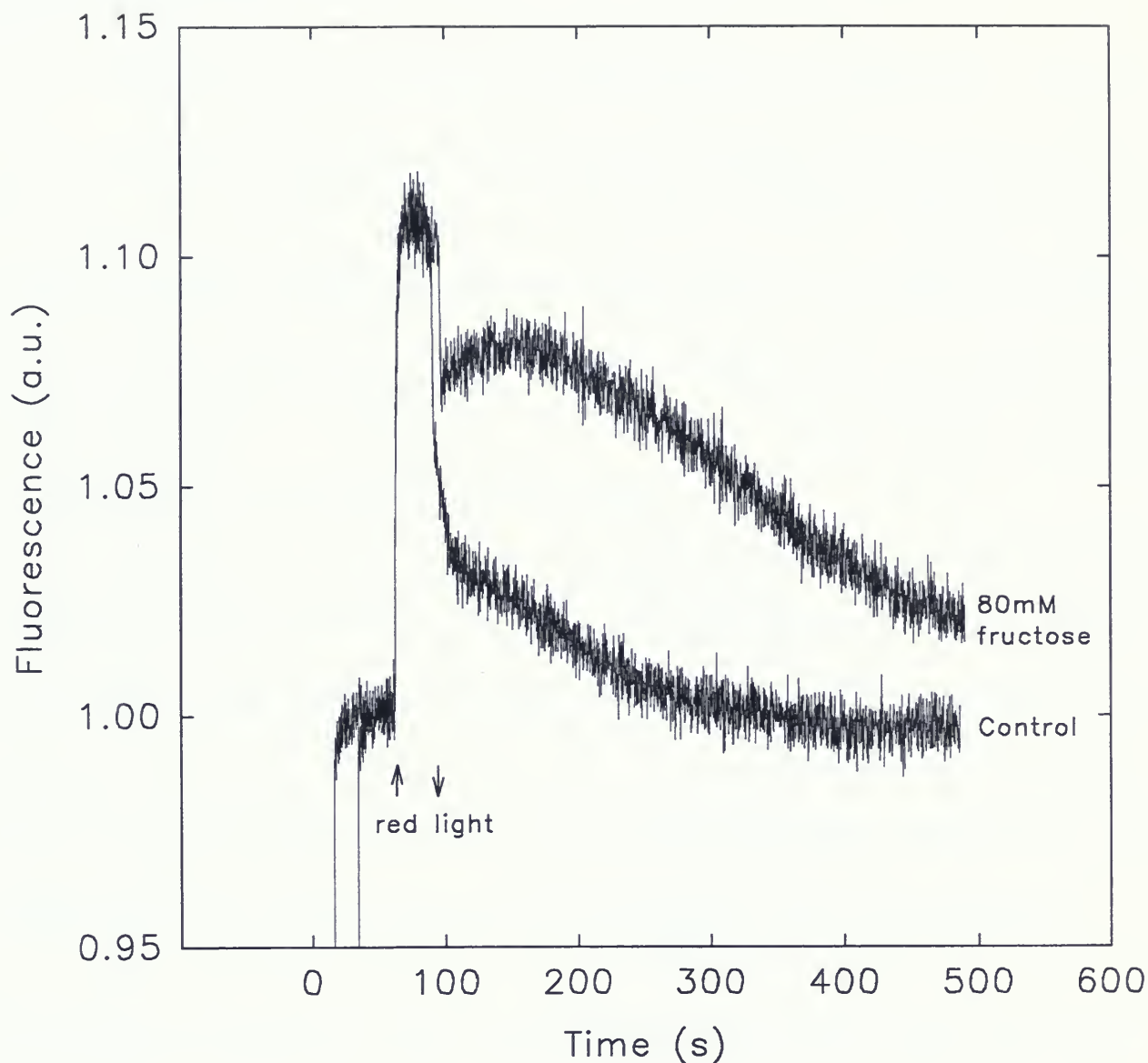


Figure 17. Room temperature fluorescence emission (on PAM) from 7002 *psaL*⁻ cells showing the effect of incubation with fructose on dark starved *psaL*⁻ cells (cells were dark adapted for approximately 12 hours at 32 °C). Control cells were taken straight from the dark adaptation for measurement and compared to cells which, in addition to dark adaptation, were incubated with 80mM fructose for 1 hour in the dark just prior to measurement. Measurements were done in the dark except for a 30 second period of illumination with red light in the non-circulating system.

Cross-section Data

Figures 18 to 23 show examples of PS2 flash saturation curves from states 1 and 2 for 630nm (phycobilisome absorbed) and 674nm (chlorophyll absorbed) light for wild type, *apcD*- and *psaL*- cells. All curves were fit with a single hit Poisson probability distribution, which is plotted with the data. A shift in the curve toward the left indicates an increase in cross-section size. That is, if the absorption cross-section is larger, a lower photon flux will be able to hit all photosystems. Table 2 summarizes the averaged cross-section changes for all these cell types, and table 3 lists the changes in F_o and F_m between states.

Wild type cells had an increase in the phycobilisome cross-section of 44% and of the chlorophyll cross-section of 17% in state 1. Curves for wild type cells all show the expected increase in F_m in state 1 due to a larger cross-section. They also show an increase in F_o . This increase may be caused by a real change in F_o , due to a larger cross-section, and/or an apparent increase due to some residually reduced Q_A , caused by the preillumination used for state 1. The relative contributions of these two factors are discussed together with the connectivity data.

ApcD- cells had no significant increase in phycobilisome cross-section. This was apparent from the sample curve where flash saturation curves under state 1 and state 2 conditions were overlapping. A 22% increase in chlorophyll cross-section was observed in state 1 with no increase in F_m . However, there was an increase in apparent F_o . Again, the contribution of this increase in apparent F_o will be discussed with the connectivity data.

The *psaL*- cells had a 27% increase in phycobilisome cross-section but no significant change in chlorophyll cross-section. The 630nm flash saturation curve had similar characteristics to the wild type, a large increase in F_m and a small increase in apparent F_o .

Limited data were available for the PS1 cross-section measurements. However, there were measurements for PS1 comparing the phycobilisome cross-section in states 1 and 2 (sample in figure 24). Only PS1 cross-sections which were accompanied by an increase in PS2 cross-section in state 1 were analyzed. In addition, only sets of data which had both a state 1 and state 2 measurement done with the same cells on the same day were used. Cross-sections increased by 19% in state 2, opposite to the trend seen with the PS2 measurements.

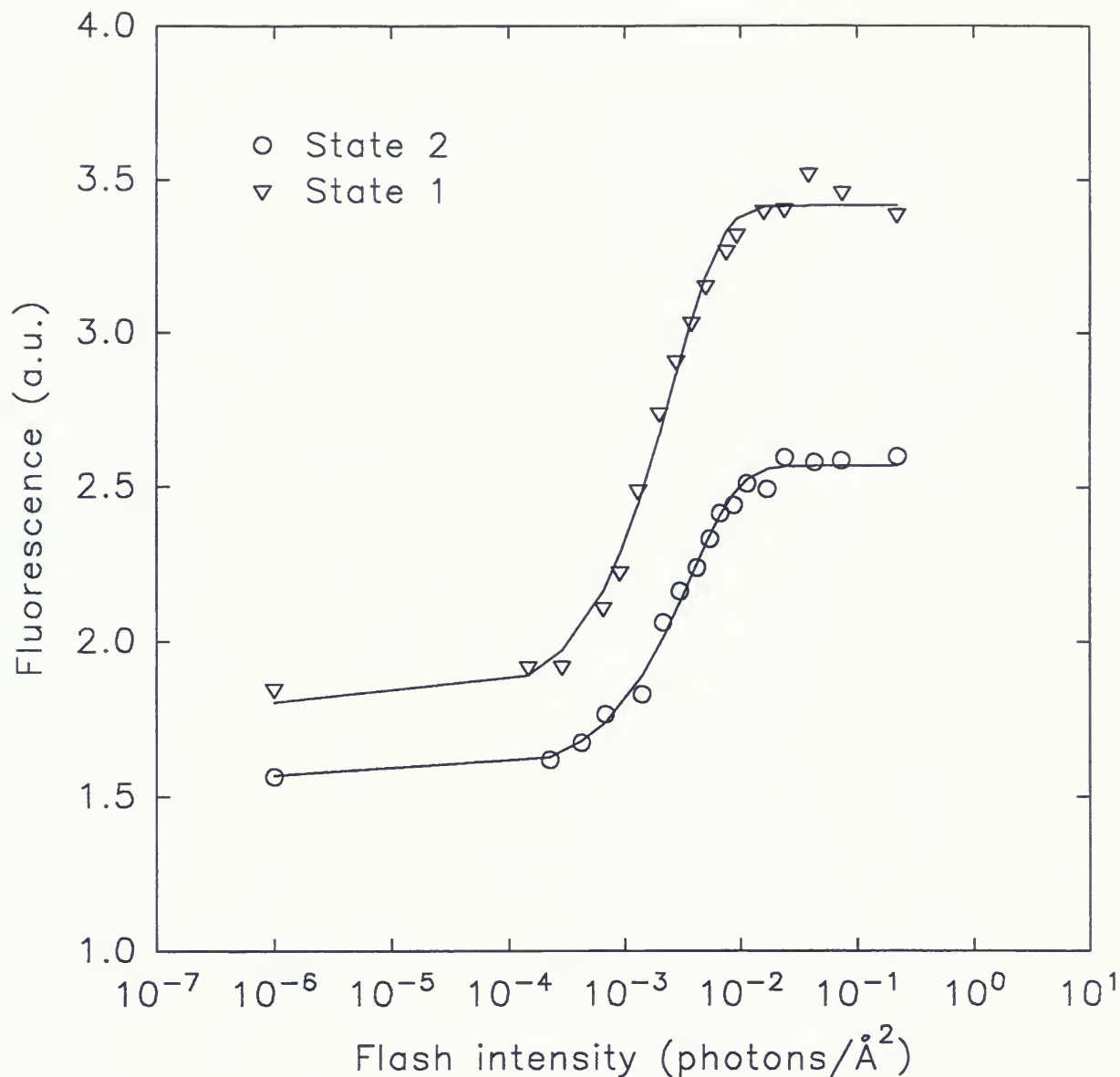


Figure 18. Sample PS2 flash saturation curves in both state 1 and state 2 for excitation wavelength 630nm (phycobilisome absorbed) for 7002 wild type cells. Cells were diluted to a chlorophyll concentration of 2.5µg/ml for experiments. Cells were circulated through the sample cuvette; state 2 being achieved by dark adaptation and state 1 by preillumination before the cuvette with red light. The data was fit with a single hit Poisson distribution (plotted with the raw data) in order to determine the absorption cross-section in both states.

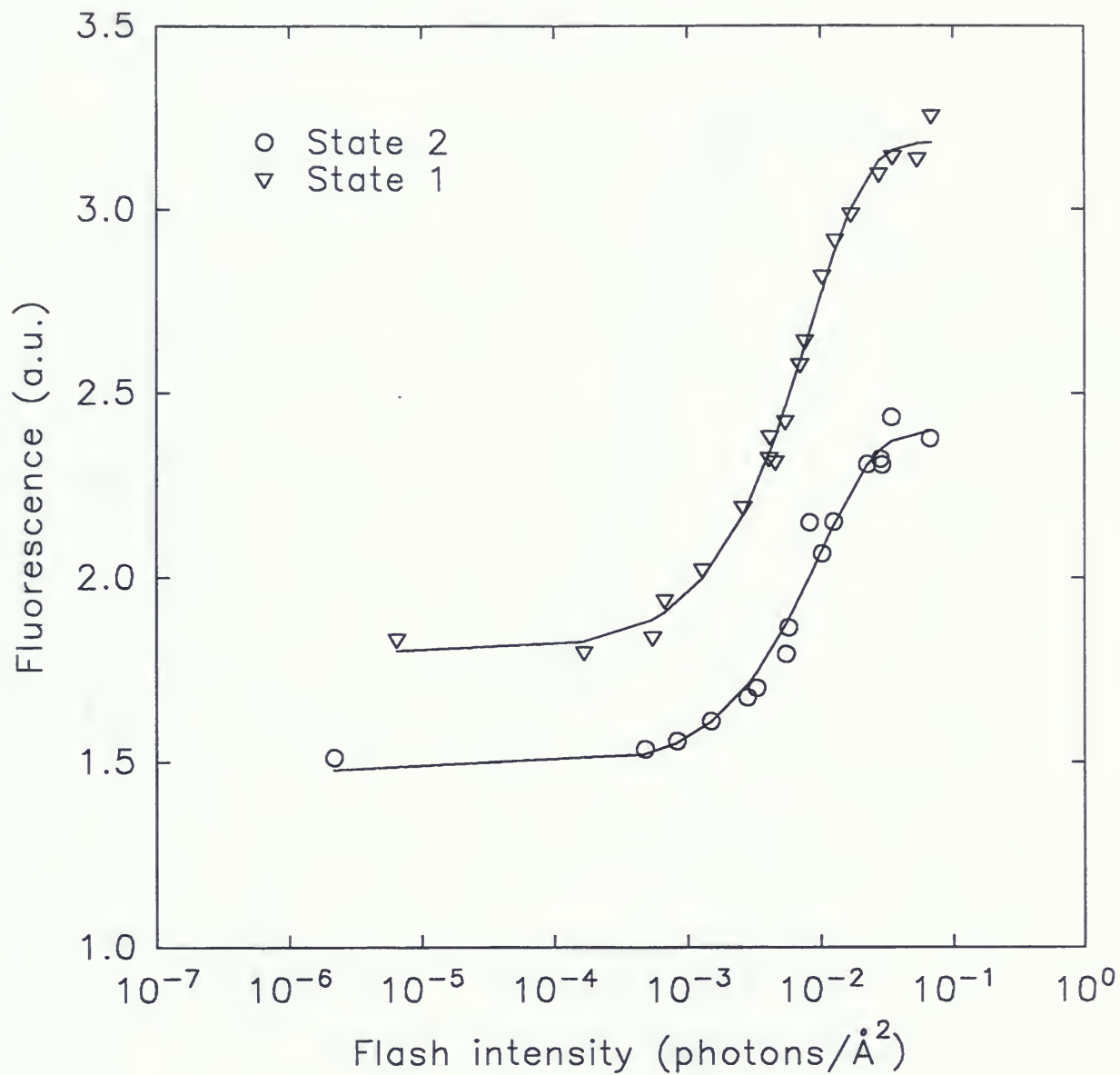


Figure 19. Sample PS2 flash saturation curve in both state 1 and state 2 for excitation wavelength 674nm (chlorophyll absorbed) for 7002 wild type cells. Experimental protocol was identical to that described in figure 18.



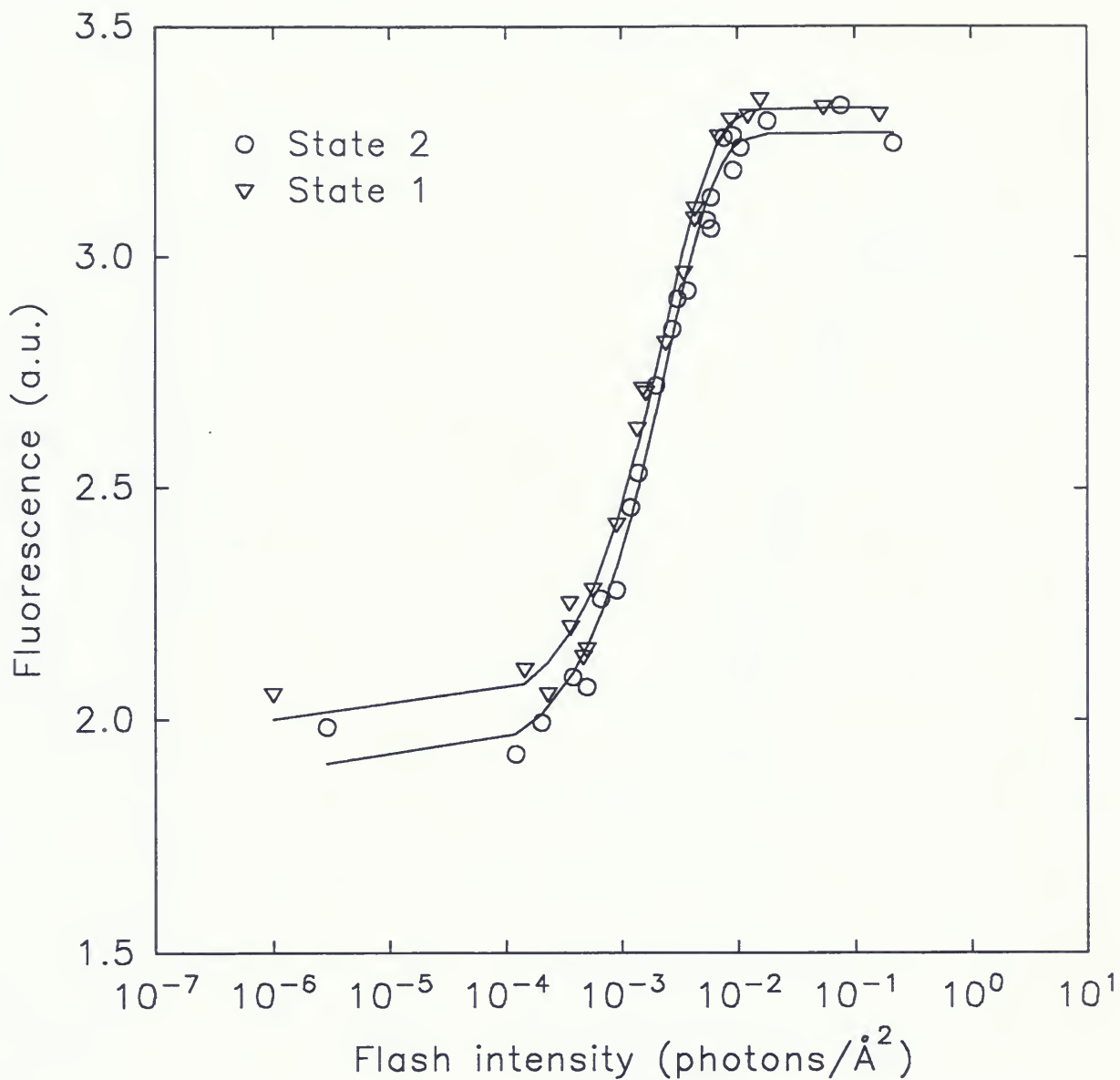


Figure 20. Sample PS2 flash saturation curve in both state 1 and state 2 for excitation wavelength 630nm (phycobilisome absorbed) for 7002 apcD- cells. Experimental protocol was the same as that described in figure 18.

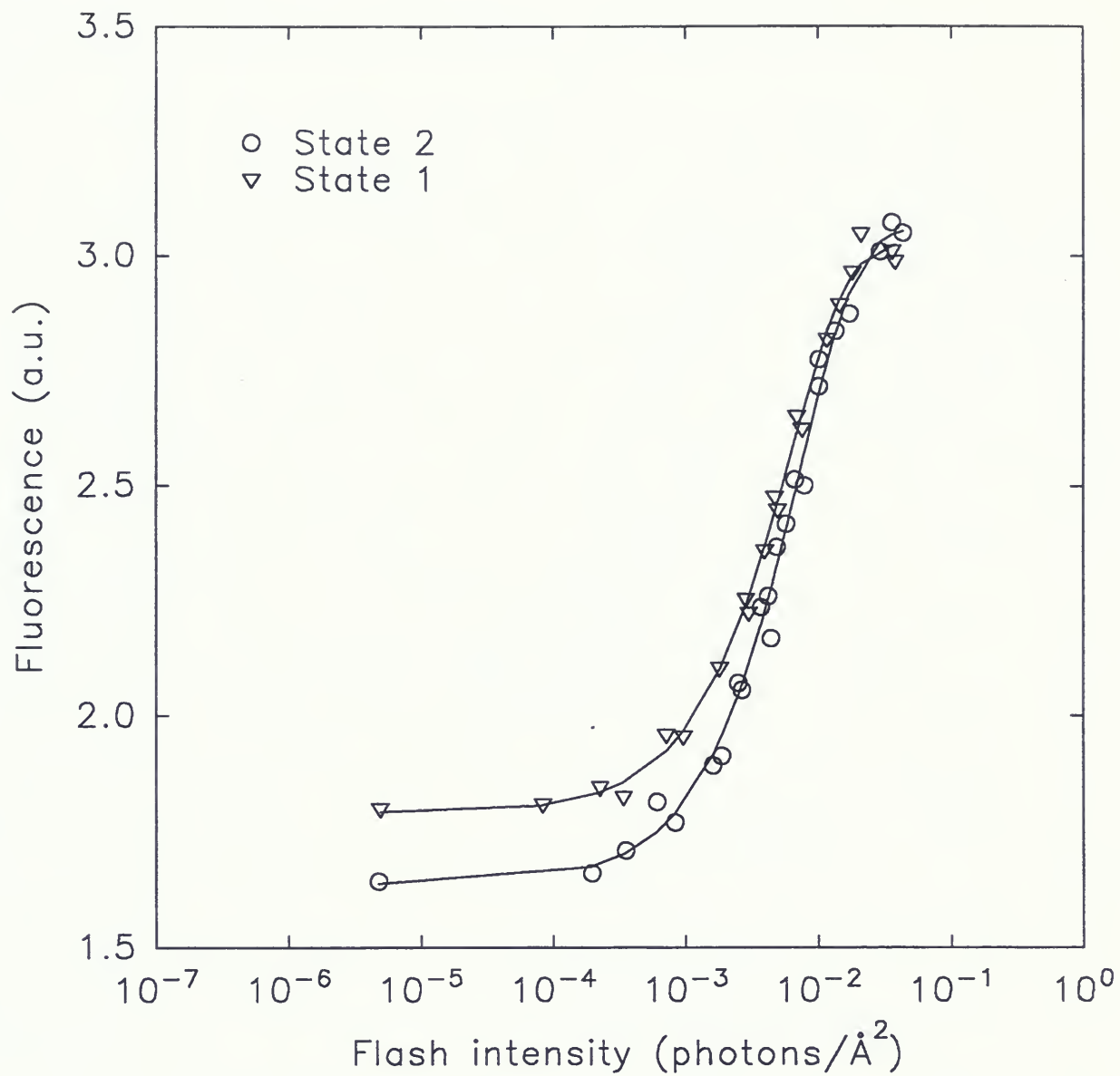


Figure 21. Sample PS2 flash saturation curve in both state 1 and state 2 for excitation wavelength 674nm (chlorophyll absorbed) for 7002 apcD- cells. Experimental protocol was the same as that described in figure 18.

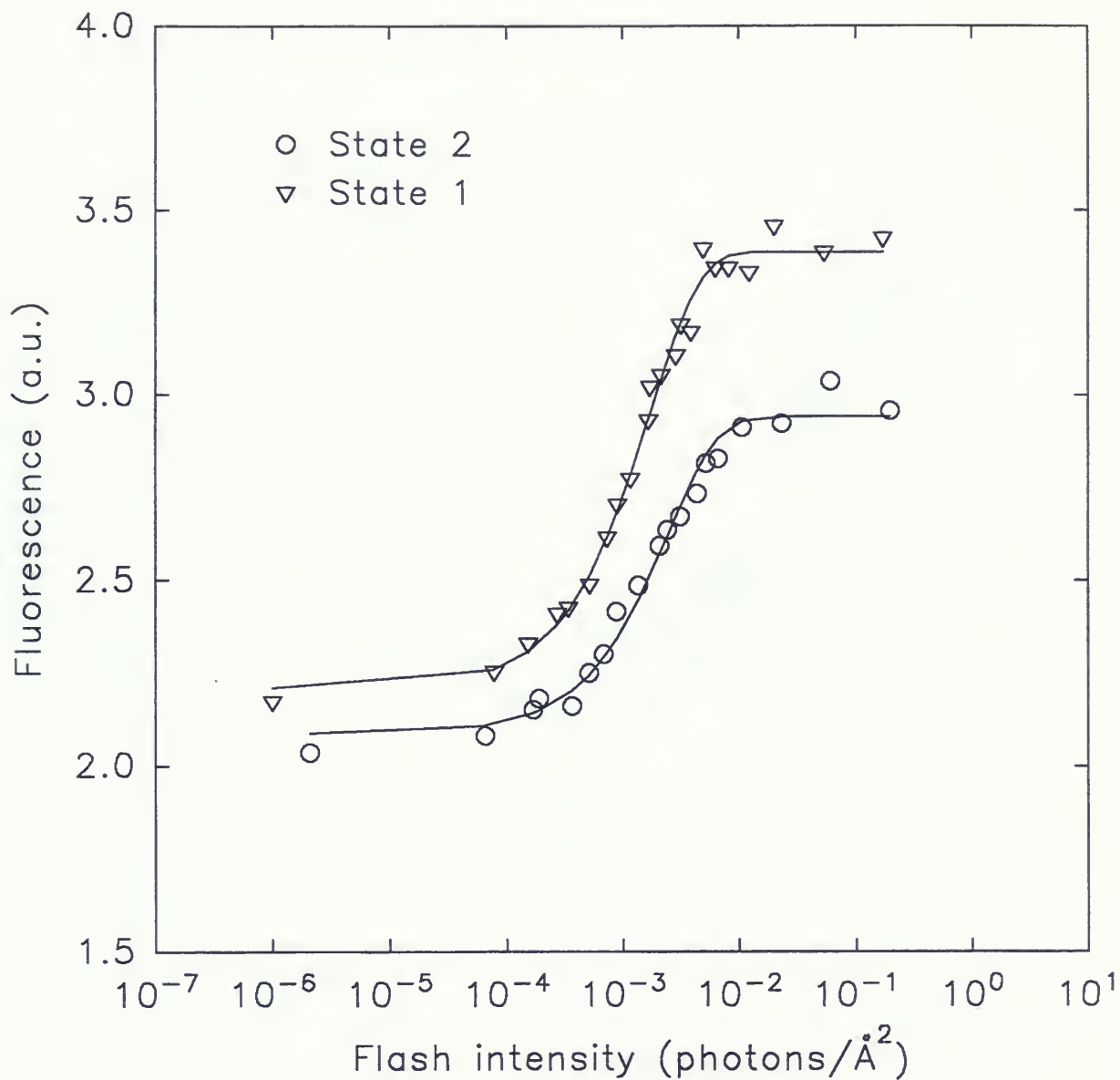


Figure 22. Sample PS2 flash saturation curve in both state 1 and state 2 for excitation wavelength 630nm (phycobilisome absorbed) for 7002 psal- cells. Experimental protocol was the same as that described in figure 18 with the exception that cells were dark adapted for at least 12 hours before measurements.

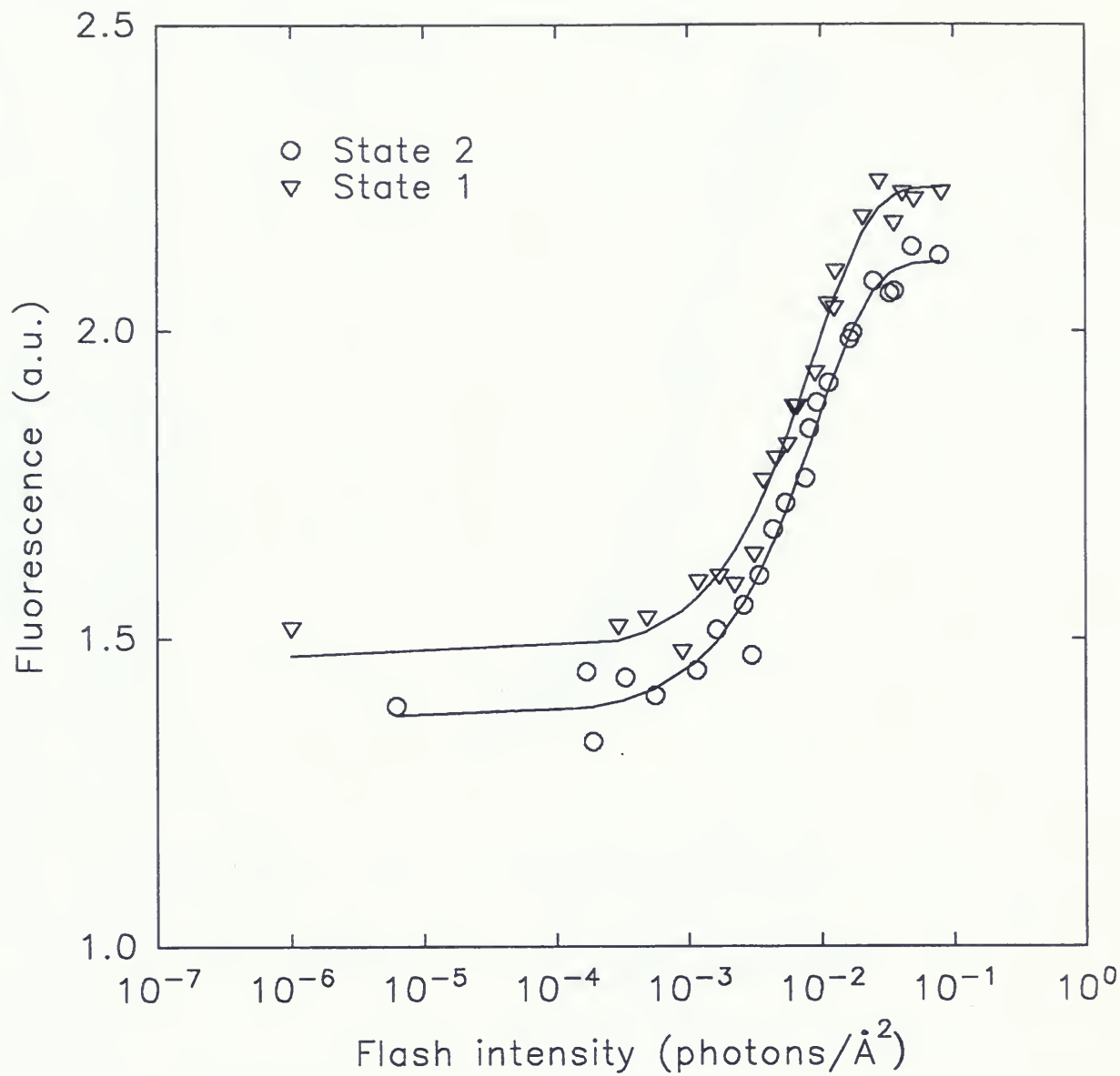


Figure 23. Sample PS2 flash saturation curve in both state 1 and state 2 for excitation wavelength 674nm (chlorophyll absorbed) for 7002 psaL⁻ cells. Experimental protocol was identical to that described in figure 22.

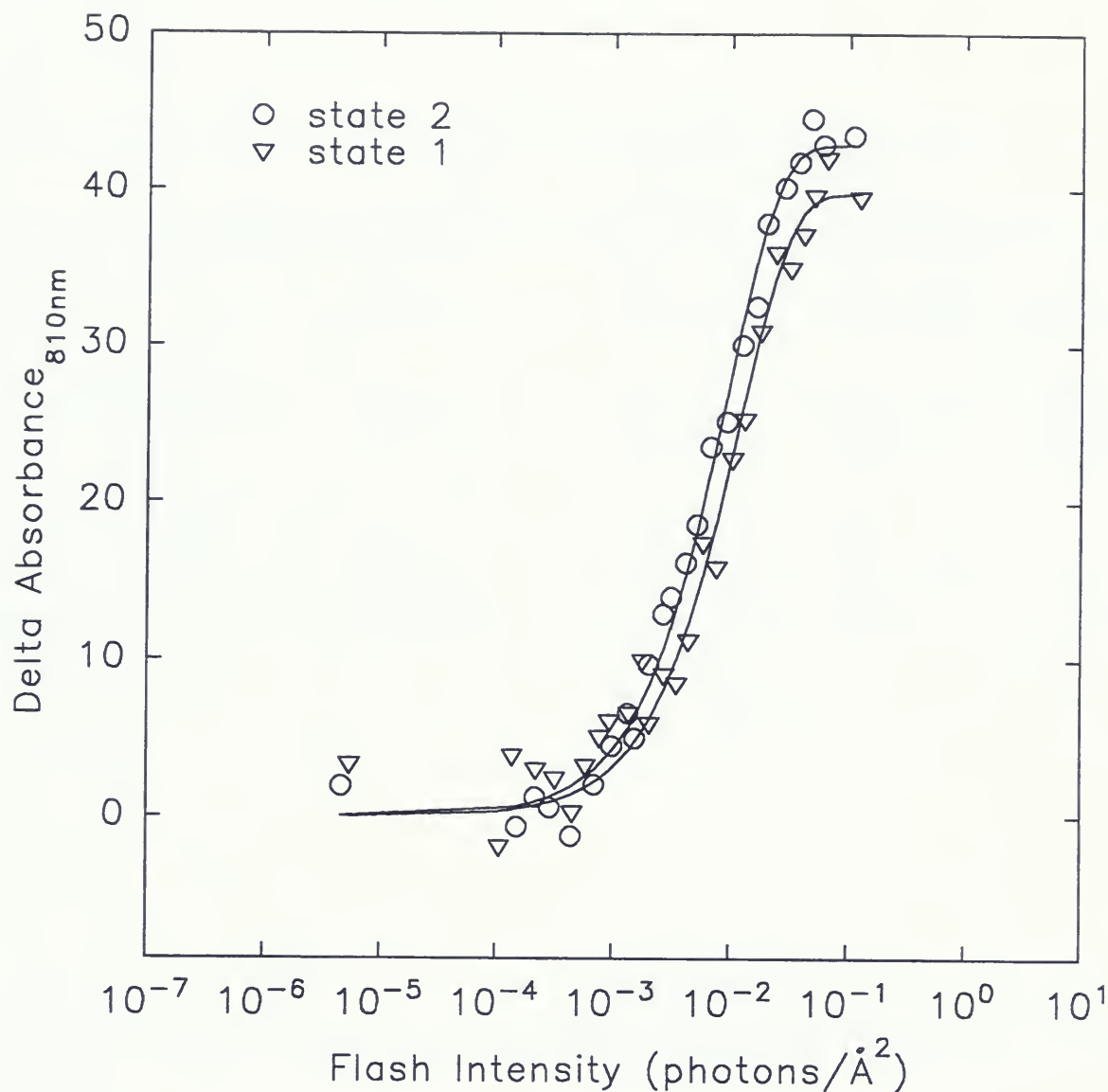


Figure 24. Sample PS1 flash saturation curve in both state 1 and state 2 for excitation wavelength 630nm (phycobilisome absorbed) for 7002 wild type cells. Cells were not circulated. State 2 was achieved by dark adaptation and state 1 by a timed light/dark regime as outlined in the materials and methods. Changes in P700 absorbance at 810nm at varying laser flash intensities were measured. The data was fit with a single hit Poisson distribution (plotted with the raw data) in order to determine the absorption cross-section in both states. In state 1 and 2 the PS1 cross-sections were $89 \pm 8 \text{ Å}$ and $106 \pm 3 \text{ Å}$ respectively (an increase of 19% in state 2).

Cell type	Excitation wavelength	PS 2 cross-section (\AA^2)		% increase
		State 2	State 1	
7002 wt	630nm	282 ± 12	407 ± 32	44%
	674nm	103 ± 5	121 ± 6	17%
7002 apc D ⁻	630nm	441 ± 34	475 ± 32	8%
	674 nm	134 ± 7	163 ± 7	22%
7002 psa L ⁻	630nm	378 ± 30	481 ± 39	27%
	674nm	116 ± 8	118 ± 3	2%

Table 2. Averaged PS2 absorption cross-section measurements in both state 1 and state 2 for excitation wavelengths 630nm (phycobilisome absorbed) and 674nm (chlorophyll absorbed) for 7002 wild type, 7002 apcD⁻ and 7002 psaL⁻ cells. Since cross-section measurements were taken on various days, daily mean cross-section measurements were averaged to give the final cross-sections above. Final standard deviations were achieved by expressing the daily standard deviation as a percent of that days mean cross-section size, then averaging the percent deviation from the various days and finally multiplying the final mean cross-section size by the averaged percent deviation.

Cell Type	Excitation wavelength	F_0		F_m	
		State 2	State 1	State 2	State 1
7002 wt	630nm	1.54	1.84	2.56	3.45
	674nm	1.48	1.79	2.37	3.26
7002 apcD-	630nm	1.78	1.88	3.16	3.21
	674nm	1.66	1.79	3.02	3.03
7002 psaL-	630nm	1.78	1.81	2.48	2.71
	674nm	1.72	1.86	2.56	2.84

Table 3. Averaged F_0 and F_m levels corresponding to absorption cross-section measurements shown in table 2.

PS2 Cross-Section Correction Using Connectivity Calibration Curves

Cross-section measurements in state 2 were done in the dark with a time delay of approximately 35seconds between exposures to the laser flash. Therefore, there was no elevation in F_o level due to residual closed traps from the previous exposure to a laser flash. However, in order to measure photosystem 2 cross-sections in state 1, cells were pre-illuminated with red light. The time between pre-illumination and measurement was only 3s, and as this light was absorbed by photosystem 1 as well as photosystem 2, it was likely that some or all of the observed increase in apparent F_o in state 1 was due to residual trap closure. Alternatively, the increase in apparent F_o was a real increase due to an increased cross-section. Further experiments estimated of how much of this increase in apparent F_o was due to trap closure.

If a similar transition to state 1 could be obtained, but with a smaller increase in the apparent F_o level, then at least the difference between this new apparent F_o increase and the previous (larger) increase was due to trap closure. Figure 25 shows that by using a filter which was red shifted by about 40nm and, therefore, preferentially absorbed by PS1 (referred to as a far red filter) compared to the red filter used previously, a similar level of increase in F_m , which is indicative of the degree of transition, was attained, but with a smaller increase in apparent F_o .

A detailed description of the calculations summarized here is found in Appendix B. From the PAM data using these two filters, it was determined that at least 42% of the increase in the apparent F_o between state 2 and state 1 was due to trap closure. This percentage assumes that the far red light did not close any PS2 reaction centers. If, however, it did close some reaction centers, then it is possible that 100% of the increase was due to trap closure. These two extremes describe the limitations which can be put on the effect of closed reaction centers on state 1 cross-sections.



What is the effect of an increase in apparent F_o on cross-section measurements? If there is free movement of excitons between PS2 antennas there will be an effect on the size of the measured cross-section if some traps are closed. To briefly reiterate this theory which is explained in the literature review: if there are two open PS2 centers in which excitons may move freely between the antennas, there will be an equal trapping of excitons by both reaction centers. If, however, one of the reaction centers is closed, then the other center will preferentially receive the exciton from the collective antenna. That is, both antennas will be absorbing energy for the one reaction center, and so its antenna will appear to be twice as large.

In order to measure the effect of some centers being closed, a preflash from a single turnover xenon flash lamp was used to close some centers before each laser flash (described in more detail in Materials and Methods). Figure 26 shows sample flash saturation curves at various levels of apparent F_o elevation in state 2. Figures 27 to 30 show the results of various levels of apparent F_o elevation on absorption cross-section sizes for wild type cells in state 1 and state 2 with phycobilisome and chlorophyll excitation. Due to day to day variation in the absolute cross-section sizes as well as the apparent F_o levels, data were normalized in the following manner. Apparent F_o increases were expressed as a fraction of the total variable fluorescence ($\Delta \text{apparent } F_o / (F_m - \text{non-elevated } F_o)$). Apparent F_o levels from different days which were within 0.05 of each other were grouped together. Absolute cross-section sizes were plotted against the relative increase in apparent F_o for a particular day, and the y-intercept of the linear regression through these data was assigned a relative cross-section size of 100. The rest of the cross-sections were normalized to this point.

For all conditions, an elevation in apparent F_o level resulted in an increase in cross-section, showing that there is connectivity between PS2 complexes. When the slopes of all four

calibration curves are overlapped, there is no significant difference in the amount of cross-section increase due to trap closure.

For each of the cell types, previously determined state 1 cross-section measurements were corrected for increases in cross-section due to apparent F_o elevation (changes in apparent F_o are found in table 3) using the connectivity correction curves. It is likely that there is some increase in the apparent F_o level from state 2 to state 1 due to cross-section increase. Therefore, the PS2 state 1 cross-sections are more likely to resemble the cross-sections with the minimum connectivity correction. These were used in the final analysis.

PsaL- State 2 F_o Correction

In addition to the correction for increased apparent F_o in state 1, a similar correction was first applied to the psaL- cells. Experiments discussed earlier (figure 16) show that addition of p-benzoquinone, which had a large effect on non-starved psaL- cells, also had an effect, although much smaller, on starved cells. That is, even when cells were starved, they still had a somewhat elevated apparent F_o level. The state 2 cross-section was first corrected for the elevation in apparent F_o , and then the state 1 cross-section was corrected.

Assuming that the fluorescence level after p-benzoquinone addition was the real F_o level, and the fluorescence level before addition was the apparent F_o level, the actual F_o level for the experiments was calculated. Using the apparent F_o values from table 3, the state 2 apparent F_o at 630nm of 1.78 was converted to 1.73 (7.0% of state 2 F_v) and the apparent F_o at 674nm of 1.72 was converted to 1.67 (6.0% of state 2 F_v).

A summary of the corrected cross-sections for all three cell types at both 630nm and 674nm excitation is found in table 4.



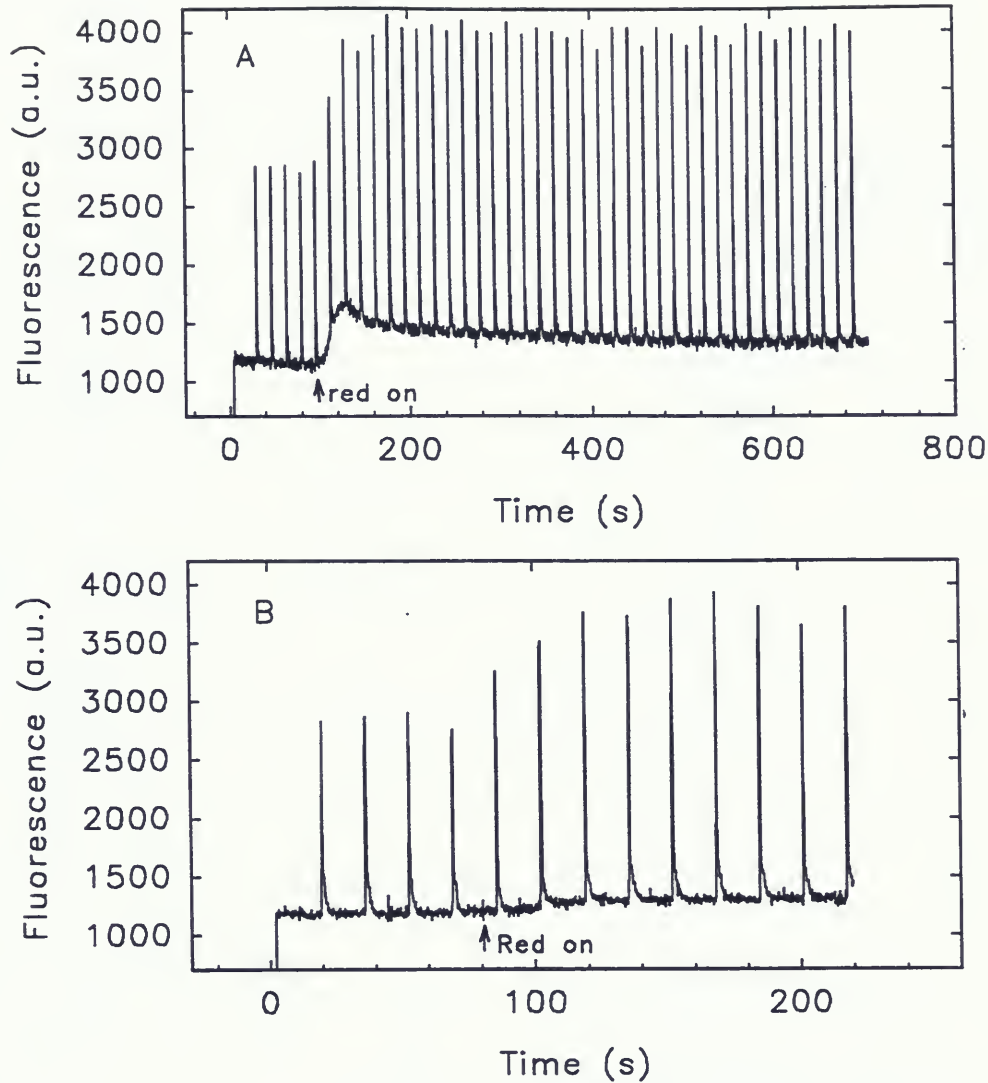


Figure 25. Room temperature fluorescence (on PAM) showing the different levels of apparent F_o increase of 7002 wild type cells when inducing state 1 with red and far red light. Fluorescence was measured using the circulating system (chl a concentration of $2.5\mu\text{g/ml}$) with the pulsed light from the PAM pulsed at 1.6KHz. In panel A state 1 is induced by illumination with a long pass red filter which has a half maximum transmittance at 662nm. In state 1 (measured at approximately 600 seconds), there was an elevation in apparent F_o of 7.2% (expressed as a percentage of state 1 F_v). In panel B state 1 is induced by illumination with a long pass far red filter which has a half maximum transmittance at 700nm. In state 1 there was an elevation in apparent F_o of 4.2%.

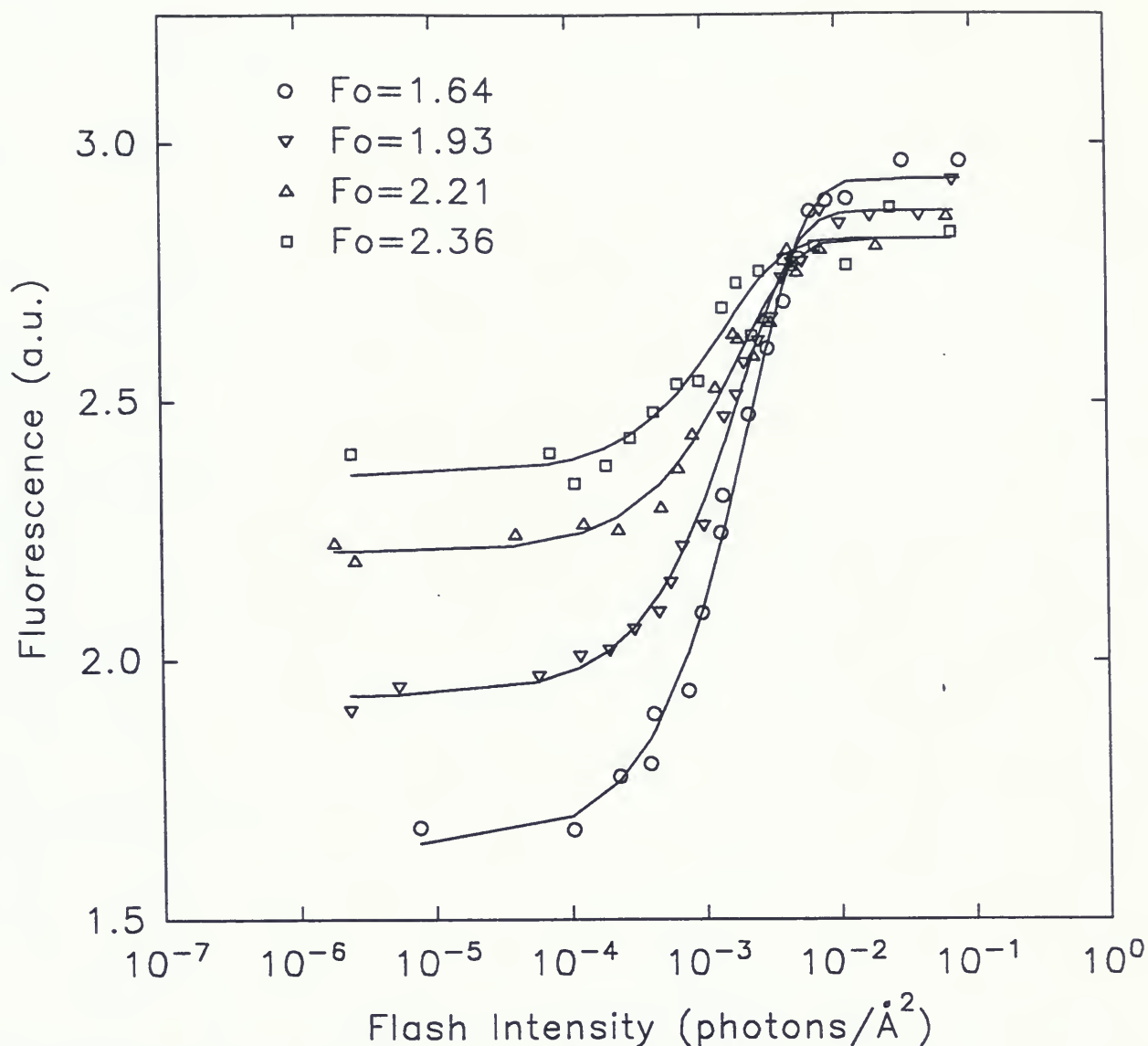


Figure 26. Sample PS2 absorption cross-sections in state 2 at 630nm excitation (phycobilisome absorbed) at various apparent F_o levels for 7002 wild type cells. Cells were diluted to a chlorophyll a concentration of $2.5\mu\text{g/ml}$ for experiments and circulated through the sample cuvette in the dark. Apparent F_o levels were increased above the F_o level of 1.64 by preflashing the sample with a single turnover xenon flash lamp $700\mu\text{s}$ before each laser pulse. As the intensity of the xenon flash lamp was increased, the apparent F_o level was elevated. As the apparent F_o was elevated, the cross-section size also increased. Apparent F_o levels of 1.64, 1.93, 2.21 and 2.36 gave cross-section sizes of 453\AA^2 , 511\AA^2 , 519\AA^2 and 660\AA^2 respectively.

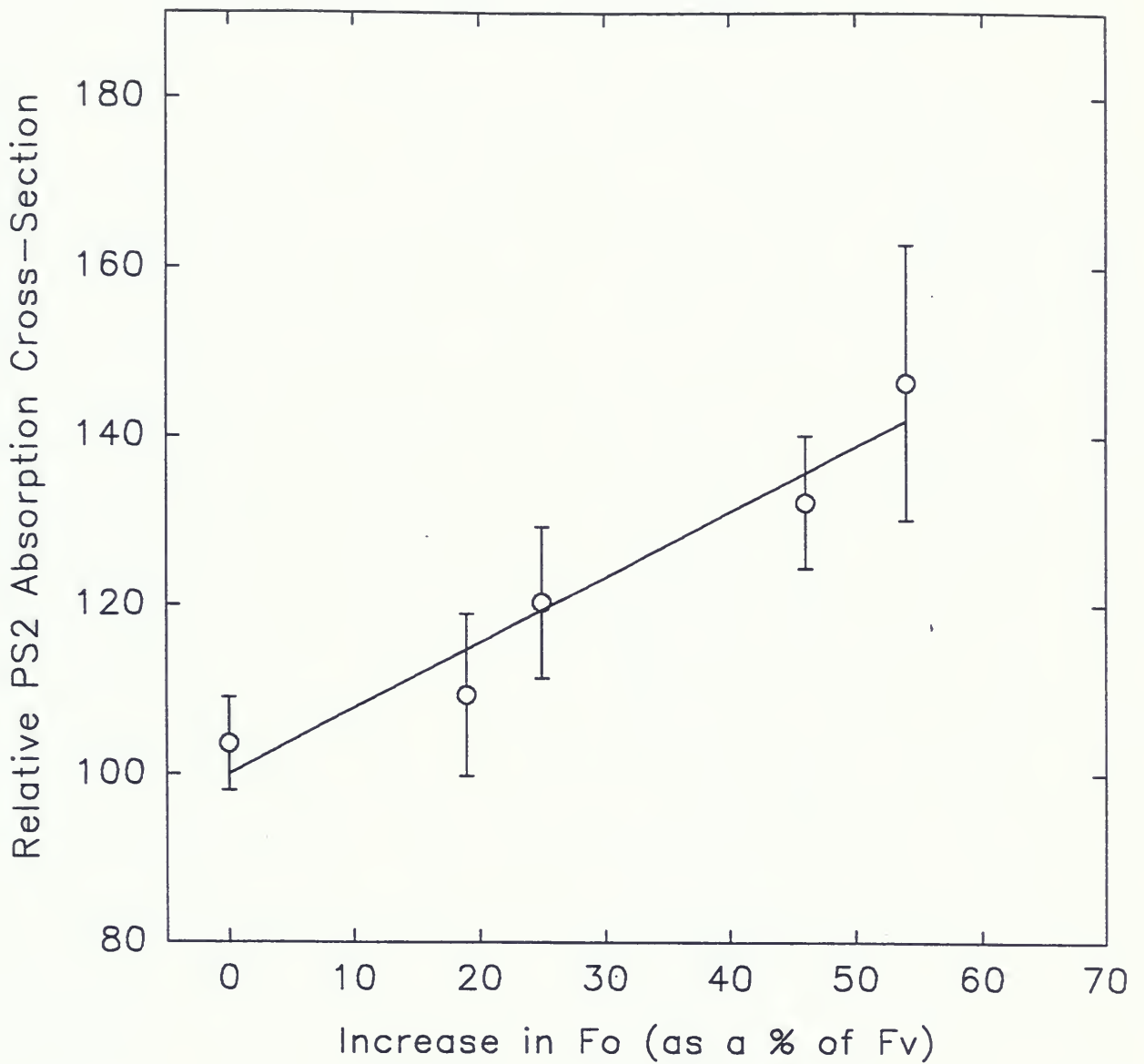


Figure 27. Calibration curve showing the dependence of cross-section size on the amount of increase of apparent F_o for 7002 wild type cells in state 1 with an excitation wavelength of 630nm (phycobilisome absorbed). Experimental conditions are outlined in figure 26. Normalization procedure is outlined in the accompanying text.

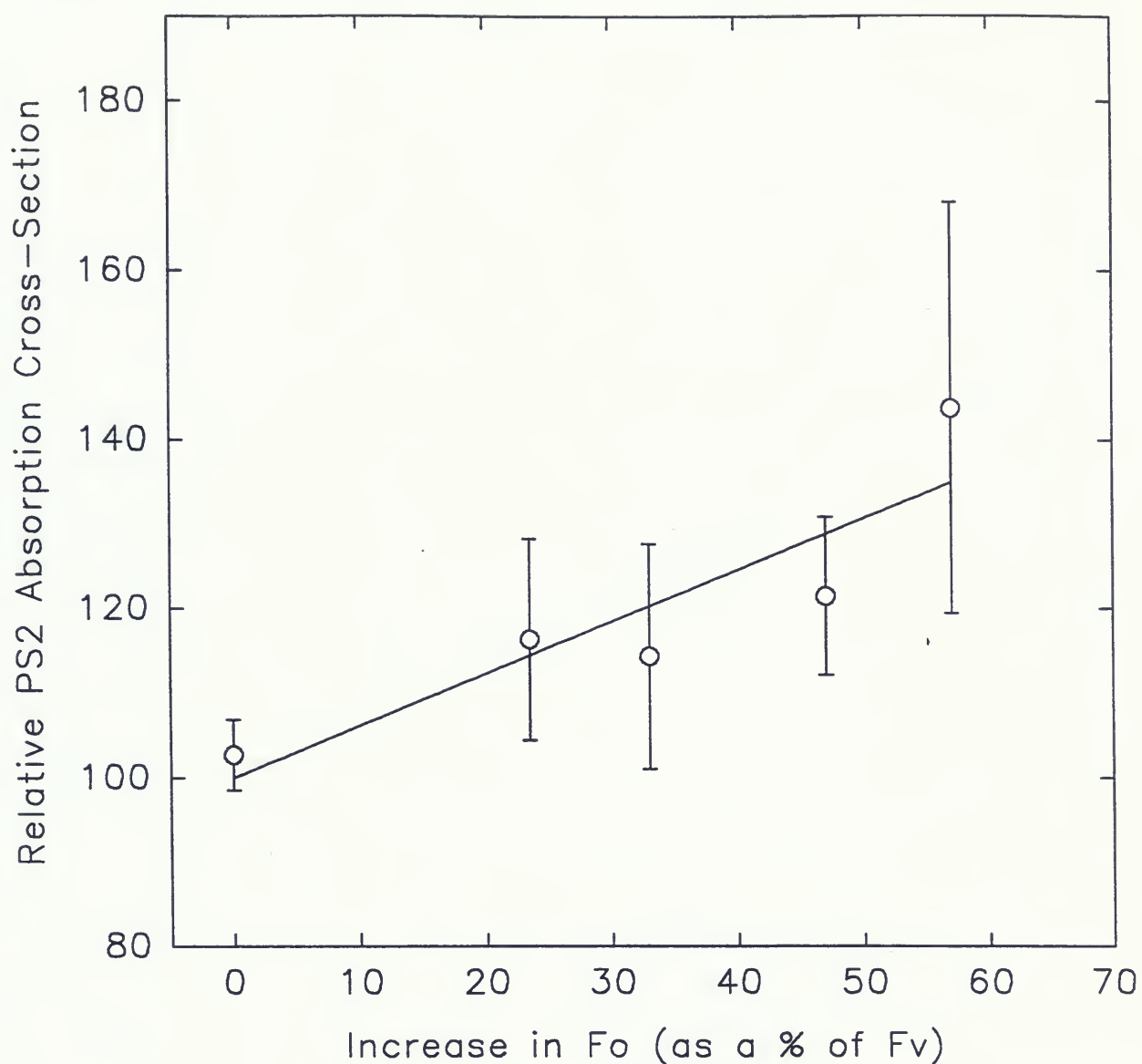


Figure 28. Calibration curve showing the dependence of cross-section size on the amount of increase in apparent Fo for 7002 wild type cells in state 2 with an excitation wavelength of 630nm (phycobilisome absorbed). Experimental conditions and normalization of data are outlined in figure 27.

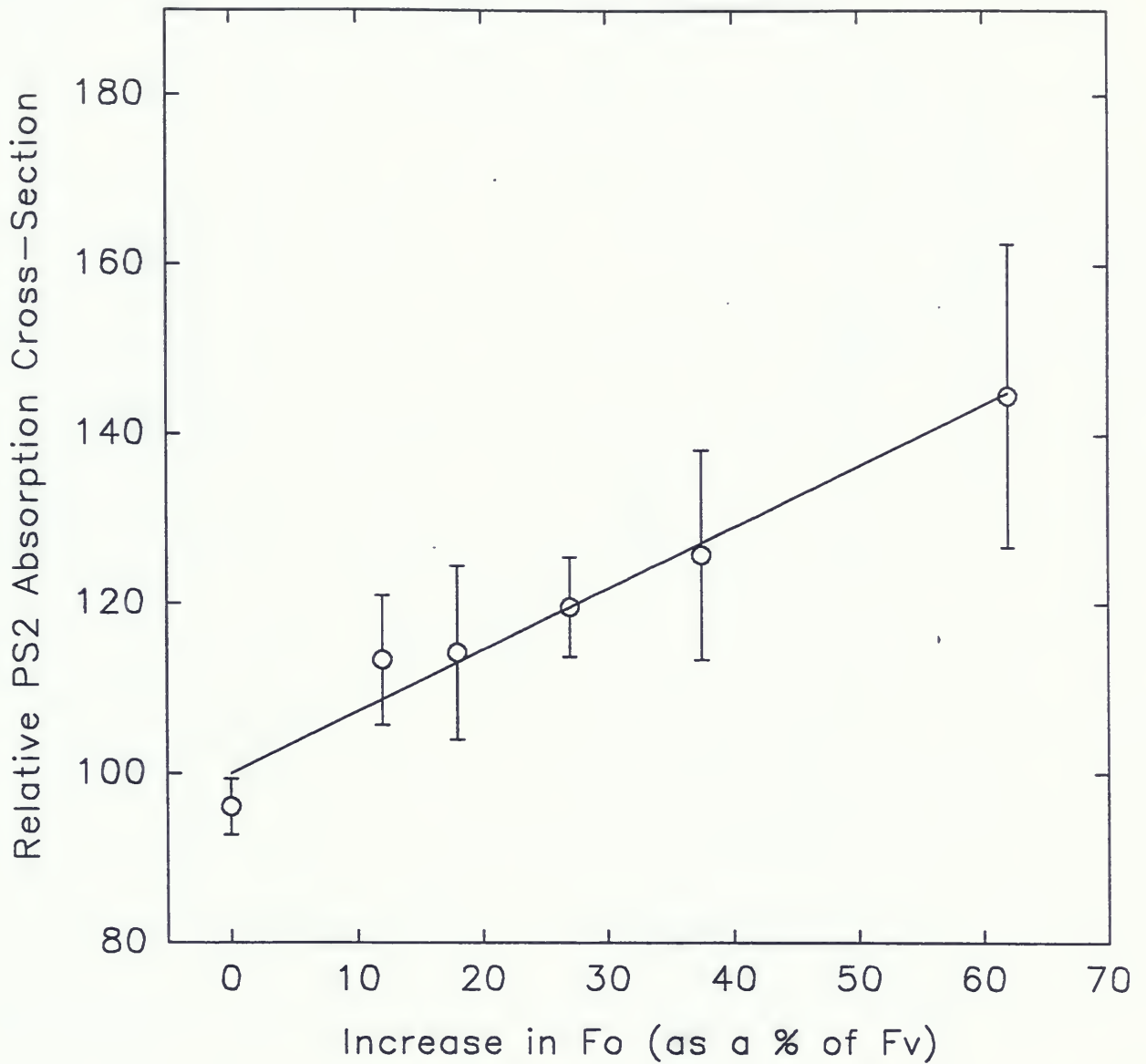


Figure 29. Calibration curve showing the dependence of cross-section size on the amount of increase in apparent F_o for 7002 wild type cells in state 1 with an excitation wavelength of 674nm (chlorophyll absorbed). Experimental conditions and normalization of data are outlined in figure 27.

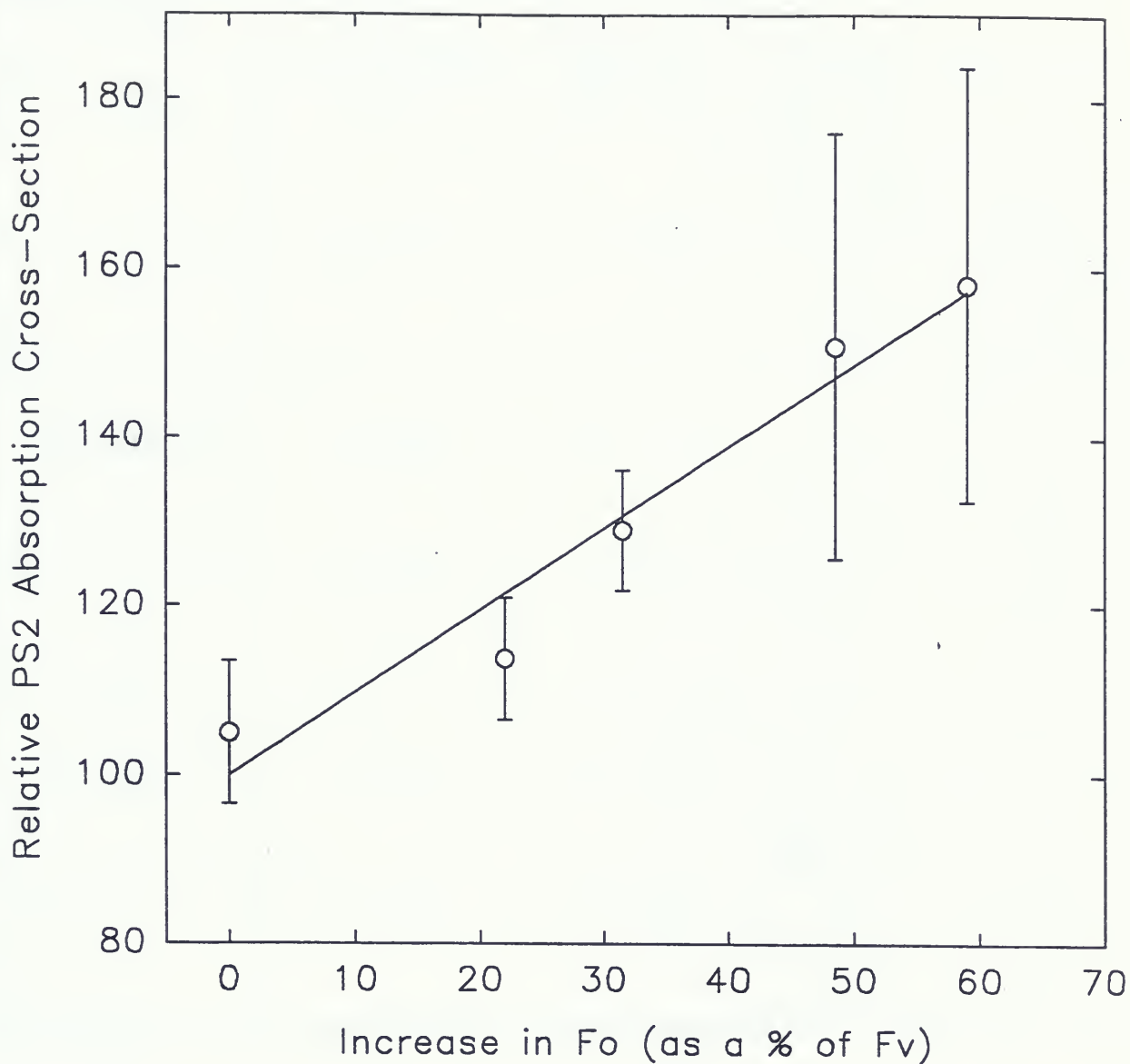


Figure 30. Calibration curve showing the dependence of cross-section size on the amount of increase in apparent F_o for 7002 wild type cells in state 2 with an excitation wavelength of 674nm (chlorophyll absorbed). Experimental conditions and normalization of data are outlined in figure 27.

Cell type	Excitation wavelength	PS 2 cross-section (Å ²)		% increase
		State 2	State 1	
7002 wt	630nm	282 ± 12	407 ± 32	44%
			384 ± 30	36%
			356 ± 28	26%
	674nm	103 ± 5	121 ± 6	17%
			114 ± 6	11%
			105 ± 5	2%
7002 apc D ⁻	630nm	441 ± 34	475 ± 32	7.7%
			463 ± 31	5%
			448 ± 30	1.6%
	674 nm	134 ± 7	163 ± 7	22%
			158 ± 7	18%
			151 ± 6	13%
7002 psa L ⁻	630nm	378 ± 30	481 ± 39	27%
			468 ± 38	24%
			450 ± 36	19%
	674nm	116 ± 8	118 ± 3	1.7%
			111 ± 3	-4.3%
			103 ± 3	-11%

Table 4. Summary of PS2 cross-section measurements before (normal type) and after (bold type) correction for connectivity. The two values for after the correction represent the minimum and maximum possible changes to the measured cross-section. The minimum change assumes that a portion of the increase in apparent F_0 is due to a real increase in F_0 because the absorption cross-section increases (the rest is due to closed reaction centers). The maximum change assumes that all of the increase in apparent F_0 is due to closed reaction centers. A complete outline of the calculations is included in the accompanying text.

Discussion

Redox State of the Electron Transport Chain

Experiments and a literature search intended to determine the source of apparent Fo elevation in the *psaL*- cells lead to some discoveries regarding the kinetics of the oxidation and reduction of the electron transport chain before, during and after illumination. In the PAM traces with the wild type, *psaL*- and *apcD*- cells, all cell types showed an increase in reduction during illumination followed by a fast oxidation, slower reduction, and finally a slow oxidation of Q_A after the light was turned off. These can be best understood in the context of the complex interaction between the photosynthetic and respiratory electron transport processes.

Experiments by various groups (Aoki and Katoh, 1982, Mi et al, 1992) have shown that PQ is an integral part of the respiratory electron transport chain in cyanobacteria. When cells are in the dark prior to illumination, there is a low level of reduction of PQ by the respiratory enzyme NAD(P)H dehydrogenase and an oxidation of either cytochrome b_6f or plastocyanin by an oxidase as shown in figure 31, panel A. In the model shown, both FNR and NAD(P)H dehydrogenase are depicted. However, it is likely that these two are actually the same enzyme (Scherer et al, 1988). The rate of reduction for cells which have been dark adapted is low because respiratory substrates, rather than NADPH produced directly by photosynthesis, are being used as electron donors (Mi et al, 1992a). The dark illumination prior to the experiment provided time in which excess NADPH produced by photosynthesis was likely consumed by respiration.

During illumination a number of processes are at work which contribute to the redox state of the electron transport chain (figure 31, panel B). Light which is absorbed by PS1 causes the oxidation of PQ. On the other hand, light which is absorbed by PS2 causes the reduction of

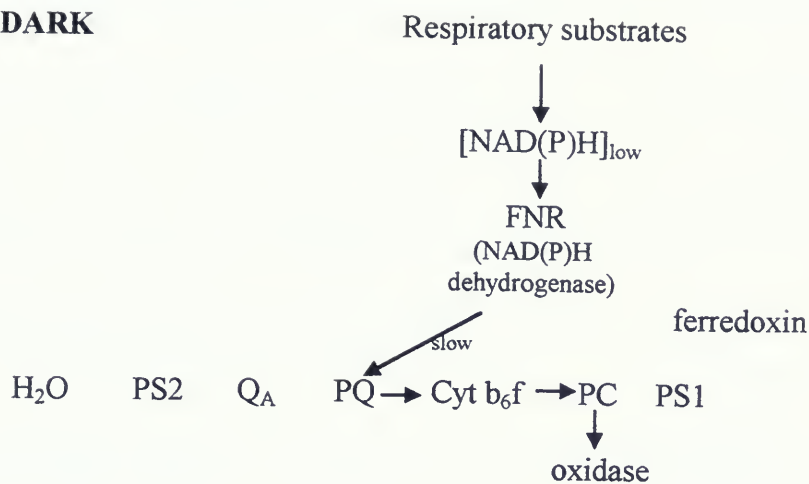
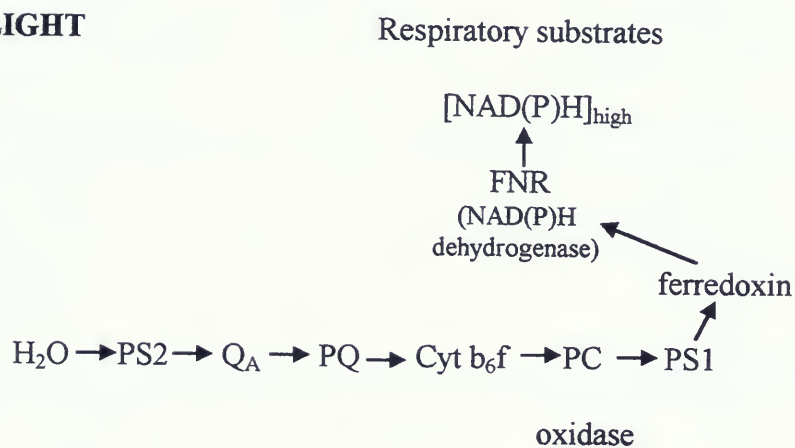
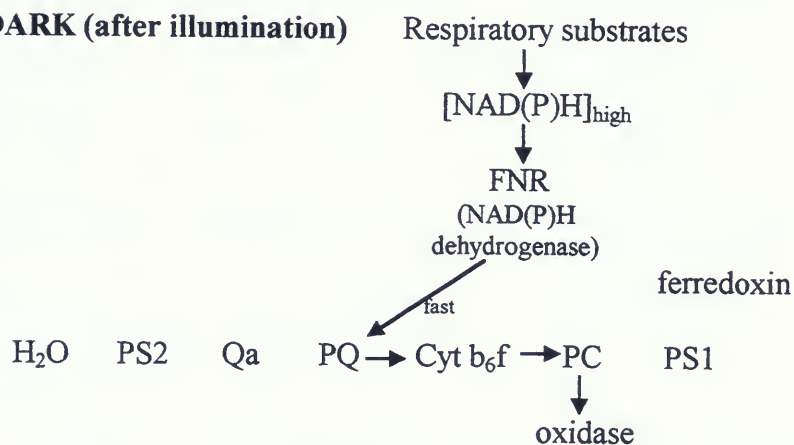
A. DARK**B. LIGHT****C. DARK (after illumination)**

Figure 31. Model for photosynthetic and respiratory electron flow in the dark, during illumination and after illumination.

Q_A and PQ. Respiration, which caused PQ reduction in the dark, has been shown to be light inactivated in cyanobacteria (Peschek, 1987). Therefore, the NAD(P)H dehydrogenase is not reducing PQ, nor is the oxidase functioning during illumination. The interaction between these kinetics gives rise to a final redox level of the electron transport chain. During this time of illumination, NADP⁺ is being reduced to NADPH.

When the light is turned off, the two processes which were contributing to the redox state of the electron transport chain, the reduction by PS2 activity and the oxidation by PS1 activity, cease to function. The large decrease in fluorescence just after the light is turned off, reveals that the electron transport chain had been relatively oxidized during illumination. This oxidation was masked by reduction of Q_A by PS2 activity. In addition to the cessation of these two processes, the activity of the oxidase and dehydrogenase (in reducing PQ) commences when the light is turned off.

During illumination, the NADPH concentration presumably increased, resulting in a high rate of dehydrogenase activity just after illumination. That is, the rate limiting step in the reduction of PQ by the dehydrogenase is the conversion from the respiratory substrate to NAD(P)H (Mi et al, 1992a). Therefore, during the time just after illumination when the concentration of NADPH is higher because of recent photosynthetic activity, PQ reduction will be higher (figure 31, panel C). As the concentration of NADPH decreases, the rate of PQ reduction gradually subsides to the level which can be carried out by oxidation of the respiratory substrates (figure 31, panel A).

Different rates and amplitudes of reduction and oxidation occurred after the red light was turned off for the different mutant cells. The *apcD*⁻ cells had a similar rate of initial oxidation, but a much slower and smaller reduction (figure 12). This suggests that either the NAD(P)H

dehydrogenase was unable to use the NADPH produced during illumination at a similar rate to the wild type or alternatively that not as much NADPH was produced during illumination. The latter explanation is more likely because not only was the amplitude smaller, but the duration of the reduction was shorter. If the same amount of NADPH was produced but was simply not used as quickly, we would expect to see a smaller amplitude which would last longer. The reason this difference was seen with the *apcD*- cells is likely because phycobilisome absorbed light is not transferred as readily to PS1 (because of the lack of connection between the two in this mutant), and this results in a decrease in PS1 activity. The final result is a decrease in the amount of NADPH produced.

The *psaL*-cells had an increase both in amplitude and duration of reduction after the red light illumination (figure 13). These kinetics appear to be the result of an increased production of NADPH during illumination for the same reasons stated above. That is, simply increasing the activity of the dehydrogenase without increasing the concentration of NADPH would account for the increase in amplitude but not the duration of reduction. However, since the rate of reduction of PQ by the dehydrogenase appears to be increased in the dark, it may be that both of these changes are occurring.

The model presented in the literature review suggests that FNR serves a dual function: it is the dehydrogenase responsible for PQ reduction, and it is responsible for the reduction of NADP⁺ to produce NADPH. One function occurs in the light, and one in the dark. Increasing the activity of FNR would lead to an increase in NADPH production in the light and an increase in NADPH dehydrogenase activity (and, therefore, PQ reduction) in the dark. The question remains as to what the link between the *psaL* mutation and increased FNR activity is. A recent review by Bald et al (1996) suggests that FNR binds to one of the PS1 complexes in the PS1

trimer and links PS1 to the phycobilisome rod. This tethers the trimer to the phycobilisome in a configuration such that the other two PS1 complexes are in direct contact with the phycobilisome core. Alternatively it could be proposed that the binding of the two PS1 complexes to the phycobilisome core positions the third complex such that it is able to bind to the rod via FNR. This controlled binding of FNR to the rod and PS1 complex could be responsible for controlling FNR activity. Under conditions where PS1 is no longer in trimers, the binding and, therefore, the activity of FNR may be altered. In the light, reduction of NADP⁺ by FNR would be increased and in the dark, reduction of PQ by FNR would increase.

PsaL Mutant Fo Level

The initial observation in the cross-section measurements that the apparent Fo level decreased under state 1 conditions lead to a series of experiments with the *psaL*- cells (data not shown). When an antenna cross-section increases, both of the fluorescence parameters, Fo and Fm, are expected to increase. Fo increases because the larger antenna will collect more energy and therefore, assuming the same inefficiency of energy trapping by the reaction center, will emit more fluorescence when all traps are open. The observation that the apparent Fo decreased in state 1 either meant that the PS2 cross-section was decreasing or that the apparent Fo level was elevated when in state 2 conditions. However, increases in the Fm level in state 1 suggested that the cross-section was not decreasing in state 1.

Experiments using various methods to oxidize the electron transport chain (far red illumination, benzoquinone addition, multiple turnover saturating flash) all showed that the apparent Fo level was elevated when cells were in the dark. A number of groups have used dark starvation, during which stored respiratory substrates are consumed, to decrease NAD(P)H dehydrogenase activity. This causes an oxidization of the PQ pool. As shown by the decreased

effect of benzoquinone on the apparent F_o level with the starved *psaL*- cells (figure 16), this starvation was able to decrease the reduction of PQ in the dark. Reversibility of the effects of starvation by the addition of an exogenous respiratory substrate showed that the decrease in PQ reduction was the result of starvation and not some other artifact due to extended dark adaptation. This showed that the apparent F_o level in *psaL*- cells was a result of reduction of PQ by oxidation of respiratory substrates. The reason for this increased PQ reduction was discussed above.

State Transitions

In figure 6 of the literature review, three models of the state transition were presented. At their most basic level, each one made predictions about where energy absorbed by the various pigments was transferred in state 1 and state 2. All models agree that in state 1 there is no spillover between chlorophyll antennas of PS2 and PS1, and that phycobilisome absorbed energy is transferred to PS2. Where each model differs is in its predictions for state 2. The nature of the transition to state 2 can be narrowed down to two main questions. First, regarding energy absorbed by the chlorophyll antenna of PS2: is some of this energy transferred to PS1 in state 2, and if so, is this by spillover? Second, regarding energy absorbed by the phycobilisomes: is energy from the phycobilisome transferred to PS1 in state 2, and if so, is this via the PS2 chlorophyll antenna (and therefore spillover between PS2 and PS1 chlorophyll antennas), or is it by direct transfer from the phycobilisome to PS1?

Chlorophyll Absorbed Light

Some of the first evidence for the state transition came from fluorescence measurements done at 77K. The results of the 77K fluorescence emission work with wild type cells are well supported by previous work (e.g. Murata, 1969, Salehian and Bruce, 1992). The observed

increase in the PS2:PS1 peak ratio in state 1 with 435nm excitation (chlorophyll absorbed) shows that there is an increase in the distribution of chlorophyll absorbed energy to PS2 relative to PS1 in state 1. Chlorophyll cross-section measurements (table 4) which showed an increase in the PS2 cross-section in state 1 (approximately 11%) confirmed that there was an increase in the distribution of chlorophyll absorbed energy to PS2 in state 1.

Similar 77K results were obtained with the *psaL*⁻ cells, suggesting that a change in chlorophyll absorbed energy distribution was occurring with these cells as well. The extent of the change in the PS2:PS1 ratio in the *psaL*⁻ cells was about half that in the wild type cells, indicating that the change was somewhat smaller. No significant difference in chlorophyll cross-section was observed between the state 1 and 2 in these cells. This does not support the 77K results. However, since the change in the PS2:PS1 ratio for the *psaL*⁻ cells was only slightly over half of the change observed in the wild type, the change in cross-section in the *psaL*⁻ cells would only be expected to be approximately half that observed in the wild type, about 6.5%. This small change is below the level of resolution with our equipment. It is not surprising therefore, that this was not observed.

77K results at 435nm excitation for *apcD*⁻ cells did not show an increase in the PS2:PS1 ratio in state 1. Rather, a slight decrease in fluorescence was observed. A similar, reversible trend was observed in the room temperature fluorescence emission. This evidence is contrasted with an increase in PS2 cross-section in state 1. It appears that there are two effects of red light illumination on the cells. The first is the quickly reversible (<3second) decrease in fluorescence yield that is observed with the 77K fluorescence and the room temperature fluorescence and the second is the increase in cross-section which should cause an increase in fluorescence yield. Recently, Delphin et al (1996) determined that in red algae, the majority of the change in PS2 Fm

under state 1 and state 2 conditions was the result of the non-photochemical quenching, qE, which is caused by the build up of a delta pH across the thylakoid membrane. They compared this to cyanobacteria where they saw no evidence for qE, only state transitions. However, in cyanobacteria, the delta pH may not be persistent (rather, it may be dissipated quickly by the ATPase) and therefore, it's effects not easily visualized. What complicates measurement of qE in cyanobacteria is the large change in Fm caused by the state transition. Small changes in Fm caused by qE could easily be hidden. In the *apcD*- cells, the largest contributor to the PS2 cross-section increase in state 1, the change in phycobilisome energy distribution, was blocked. Therefore, only a small increase in Fm due to the change in the chlorophyll cross-section would be expected. Under these conditions, it is less likely that qE would be masked by the state transition. If the decrease in fluorescence yield caused by qE was slightly larger than the increase in Fm which was caused by the small change in chlorophyll cross-section, then a decrease in Fm would be expected. This was observed. Assuming that there is qE in cyanobacteria, evidence that the delta pH is not long lived is provided by the fast (approximately 3s) return to the preillumination Fm level.

The cross-sections for the *apcD*- cells were determined using the circulating system and therefore measurements were made 3 seconds after illumination. It is likely therefore that the effects of the red light induced qE are relieved by the time cross-section measurements are made. This is evidenced by the lack of change in Fm between states in these measurements. Therefore, no effect of qE on the cross-section would be observed.

We can conclude from these experiments that there is a change in the distribution of chlorophyll absorbed energy between state 1 and state 2, with an increase in energy transfer to PS1 in state 2. Most groups who have measured 77K fluorescence have suggested a spillover

mechanism to explain these results. Indeed, it is probably the easiest to envision. The proposed mechanism of spillover is a movement of PS1 and PS2 such that they are in closer proximity in state 2 allowing energy transfer which was unable to occur in state 1. However, in trying to reconcile these results with other types of measurements, Mullineaux (1992) has suggested that another possible mechanism could account for these results. By way of analogy to higher plants which have a mobile chlorophyll antenna, he has suggested that a section of the PS2 chlorophyll antenna becomes dissociated from PS2 in state 2 and attaches to PS1. This would also account for the increased fluorescence from PS1 in state 1 at 77K. When only looking at the measurements of chlorophyll absorbed light, it is not possible to determine which of these two mechanisms is more likely to occur. However, by looking at the phycobilisome absorbed light experiments, a clearer picture is obtained.

Phycobilisome Absorbed Light

77K fluorescence emission data from wild type cells with phycobilisome excitation again confirms previously reported evidence. The increase in the PS2:PS1 ratio in state 1 shows that there is a change in the distribution of phycobilisome absorbed energy between the states. Relatively more energy is distributed to PS2 than to PS1 in state 1. An increase in the PS2 phycobilisome cross-section in state 1 confirms this increase in the amount of energy transferred to PS2. In order to determine whether this change in the PS2 phycobilisome cross-section was strictly the result of phycobilisome dissociation or whether there was increased energy transfer to PS1, direct measurements of PS1 cross-sections were made in both states. These measurements, which found that there was an increase in PS1 cross-section in state 2, show that the decrease in PS2 cross-section in state 2 is correlated with an increase in PS1 cross-section. The PS1 phycobilisome cross-section increases at the expense of the PS2 cross-section.

Both 77K fluorescence and cross-section measurements in the *psaL*⁻ cells confirm that this same mechanism is still intact in this mutant. The extent of the transition in this mutant is again significantly smaller, as is shown by both of these measurements.

77K fluorescence emission from the *apcD*⁻ cells showed that there was no increase in the PS2:PS1 peak under state 1 conditions. In addition, cross-section measurements show that there is no change in the phycobilisome association with PS2. These results were expected since it is thought that this mutant is deficient in energy transfer from the phycobilisome to PS1 and, therefore, the phycobilisome remains functionally associated with PS2 under all conditions (i.e. permanently in state 1).

The results with the *apcD*⁻ cells reveal some interesting evidences for how the phycobilisome light is redistributed in state 2 in the wild type. If the phycobilisome simply became detached from PS2 in state 2, it would be expected that there would be a decrease in the PS2:PS1 ratio in both the wild type and the *apcD*⁻ cells. That is, the dissociation of the phycobilisome from PS2 should not be dependent on loss of the allophycocyanin B (the *apcD* gene product). However, this change in fluorescence ratio is only seen in the wild type. Since allophycocyanin B is presumably only responsible for energy transfer from the phycobilisome to PS1, a different model may be suggested where PS2 remains bound to the phycobilisome in state 2. The only difference between the states is that a portion of the energy absorbed by the phycobilisome is directed to PS1 in state 2. This causes a decrease in the amount of energy transferred to PS2.

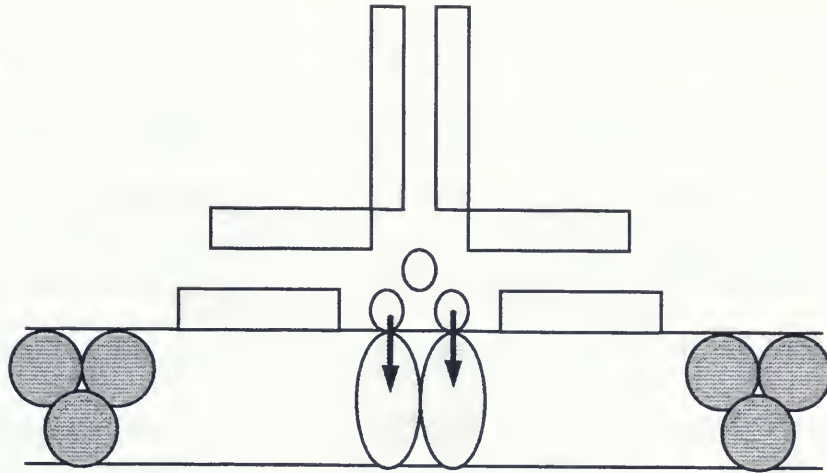
The *apcD*⁻ phycobilisome cross-section results have put some constraints on the model which describes how chlorophyll absorbed energy is transferred. As discussed earlier, the redistribution of energy between the chlorophyll antenna occurs either by spillover or by the

movement of part of the chlorophyll antenna from PS2 to PS1. If the energy transfer occurred by spillover, then energy which was absorbed by the phycobilisome attached to PS2 should also be able to transfer from the phycobilisome to the PS2 chlorophyll antenna and then by spillover to PS1. This would lead to a change in the phycobilisome cross-section between states that occurred irrespective of whether there was direct energy transfer from the phycobilisome to PS1. That is, if spillover occurred between PS2 and PS1, there would be two pathways of energy transfer from the phycobilisome to PS1: directly, through allophycocyanin B or indirectly via the PS2 chlorophyll antenna. In the *apcD*- cells I observed a change in chlorophyll cross-section but no change in phycobilisome cross-section. Therefore, we can conclude that the first pathway, from the phycobilisome to PS1 via the PS2 chlorophyll antenna, does not occur. This in turn shows that spillover does not occur between the chlorophyll antennas. Instead, a subset of chlorophylls from PS2 ceases to receive energy from the phycobilisomes, becoming functionally detached from PS2 and attached to PS1 in state 2. Assuming that in state 2 both PS1 and PS2 are bound to the phycobilisome, a large physical movement of chlorophyll is not necessary. Rather, an energetic uncoupling of some chlorophylls from PS2 with a coupling to PS1, which may be facilitated by a small movement, is proposed.

State Transition Model

The state transition model in figure 32 is based on the solutions to the two fundamental questions posed earlier. The answer to the chlorophyll question is that more chlorophyll absorbed energy is transferred to PS1 in state 2. However, this energy is not transferred by spillover but rather by the change in energy transfer from a subset of chlorophyll molecules from PS2 to PS1 in state 2. The answer to the phycobilisome question is that there is an increase in phycobilisome absorbed energy which is transferred to PS1 in state 1, and this is transferred via

State 1



State 2

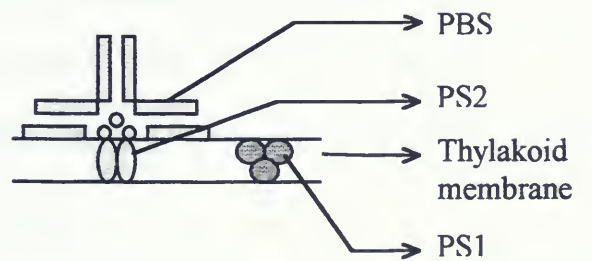
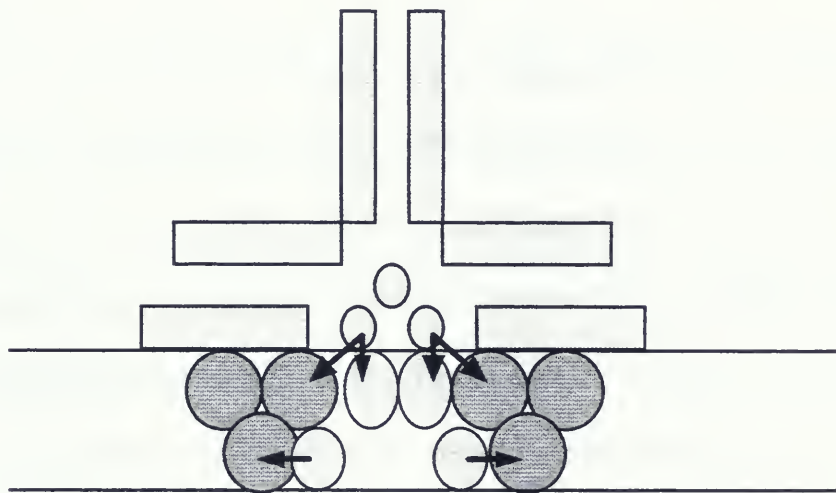


Figure 32. State transition model. Arrows indicate direction of energy transfer between pigment complexes.

allophycocyanin B directly to PS1. The model shows schematically this change in energy transfer between states. In state 1, the phycobilisome is connected to PS2, and there is no transfer of chlorophyll absorbed energy from PS2 to PS1. In state 2 there is energy transfer from the phycobilisomes to both PS2 and PS1 directly: to PS2 via the apcE terminal emitter of the phycobilisome and to PS1 via the apcD terminal emitter (allophycocyanin B). Energy transferred from the phycobilisome to PS2 is not transferred by spillover to PS1. There is an increased PS1 chlorophyll antenna size in state 2 which is the result of a subpopulation of PS2 chlorophyll (to which phycobilisome energy is not transmitted) which transfers energy to PS1.

Connectivity

Electron microscopy has shown that rows of phycobilisome/PS2 supercomplexes form on the thylakoid membrane (Morschel and Schatz, 1987), and that these rows are more prevalent in state 1 than in state 2 (Olive et al, 1986). Morschel and Schatz have constructed a model upon this observation in which there is greater connectivity between PS2 chlorophyll antenna and/or between the associated phycobilisomes in state 1 than in state 2. A recent review by Bald et al (1996) supported this model. However, no direct measurements of connectivity were made by either of these authors. In fact, a recent exploration into this phenomenon by picosecond fluorescence decay analysis in cyanobacteria suggests that very little or no connectivity exists between PS2 complexes (Mullineaux and Holzwarth, 1993). Showing a closer physical association without showing an increase in energetic coupling is insufficient evidence to prove that spatial movement is related to increased connectivity.

My research measuring absorption cross-sections at various levels of apparent F_0 elevation shows, contrary to the work by Mullineaux and Holzwarth, that increasing the apparent F_0 level by closing reaction centers does increase the PS2 cross-section. This shows that there is

connectivity between PS2 reaction centers. This is observed with chlorophyll or phycobilisome absorbed light showing that energy absorbed by either the chlorophyll antenna or the phycobilisomes may be transferred between PS2 centers.

There are a number of differences between the work done by Mullineaux and Holzwarth and my work which may have caused the discrepancy. First, to close reaction centers they illuminated a volume of 1.26ml of sample for a total time of 140ms with a white light, 80ms before measurement. This illumination time is sufficient for multiple PS2 turnovers. In my measurements I used a single turnover flash which was only 700 μ s before measurement. When using the multiple turnover light, it is not certain that reaction center closure is the only effect of illumination (outlined in the literature review). My experimental approach is better than these previous measurements because the assumption that multiple PS2 turnovers have no effect does not need to be made. A better way to close reaction centers in fluorescence lifetime experiments would be to use a focused laser beam on a fast flowing sample just prior to measurement, such that the illumination time is short enough to cause only single turnovers. We will soon be able to test this new approach in our lab. The second reason for the discrepancy is that in addition to this technical difference, my procedure eliminated the need to analyze complex changes in fluorescence lifetimes as measured by Mullineaux and Holzwarth.

In my experimental data there was no significant difference in the amount of connectivity using either phycobilisome or chlorophyll absorbed light or when cells were in state 1 or state 2. Therefore, an averaged increase in cross-section from these four conditions was used in the analysis. The average increase in the cross-section was 39% when the apparent F_0 level was elevated to 50% of the original F_v by the xenon pre-flash. Assuming that the elevation in apparent F_0 is directly correlated to the percentage of reaction centers which are closed, some

general conclusions can be drawn from these observations. First, since the cross-section did increase, as is predicted from the connectivity model, there is connectivity between PS2 centers in cyanobacteria. Second, since a doubling in cross-section with 50% of the centers closed was not observed, as is predicted if all the reaction centers are completely connected, the connectivity between centers is limited.

In order to determine with greater accuracy the extent to which PS2 centers are connected, a computer program was constructed which simulated the experimental results (changes in cross-section) with differing amounts of connectivity. This program generated a large sample of photosystems which were connected in certain integral numbers. For example, a sample of 1000 PS2's was generated in which there was only connectivity between pairs of photosystems. That is, there were 500 pairs of photosystems in which excess excitons absorbed by one photosystem could only be transferred to the other photosystem in the pair. There was no transfer between pairs. This generated a cross-section increase of 29% when 50% of the photosystems were closed with the preflash. This increase was smaller than the experimental increase, indicating that more than two centers were linked together. A second model in which photosystems were energetically linked in three's resulted in a cross-section increase of 60% with 50% of the centers closed.

The final model, which was intermediate between two and three centers linked, generated the appropriate cross-section increase (see appendix C for the program source code). Rather than saying that approximately 2.5 centers were linked, a more likely model was constructed based on previous work. The amount of connectivity between PS2 centers is likely influenced by the type of physical association that occurs between centers. As discussed previously, electron microscopy has shown that *in vivo*, PS2 centers occur as dimers and that these dimers are often

found aggregated in long rows. My present model is based upon these observations. In this model, there is complete connectivity between the two PS2 centers in a dimer but limited transfer between dimers in the row as can be seen in figure 33.

The assumptions inherent in this model are as follows:

A. Within a pair of completely connected PS2 centers:

1. That the rate of exciton movement between the two connected antenna is equal to that within each individual antenna.
2. That closed reaction centers are not good quenchers of excited states in the antenna.
3. That if two excitons were absorbed by the same reaction center, the second one would always first be transferred to the other photosystem in the pair if it was still open.

B. Between pairs of PS2 centers:

1. That if a pair of photosystems was collectively hit more than twice (i.e. both centers were closed), the excess excitons would be transferred to the pair of photosystems either directly behind or directly in front of itself in the row if there were open centers in either of these pairs.
2. That since in this model the transfer from one pair to another is less than 100% efficient, only a certain percentage of the excess excitons would be transferred to the neighbouring pairs.

By varying the efficiency of transfer between pairs of photosystems in the row, a model was generated which gave a cross-section increase of 39% when 50% of the centers were closed. In this model, only 16% of the excess excitons were transferred between pairs.

The model outlined in the review by Bald (1996) suggests that there will be greater connectivity between PS2 centers in state 1 than in state 2. My data, which measure connectivity directly, rather than by inference from electron microscopy, show that there is no significant

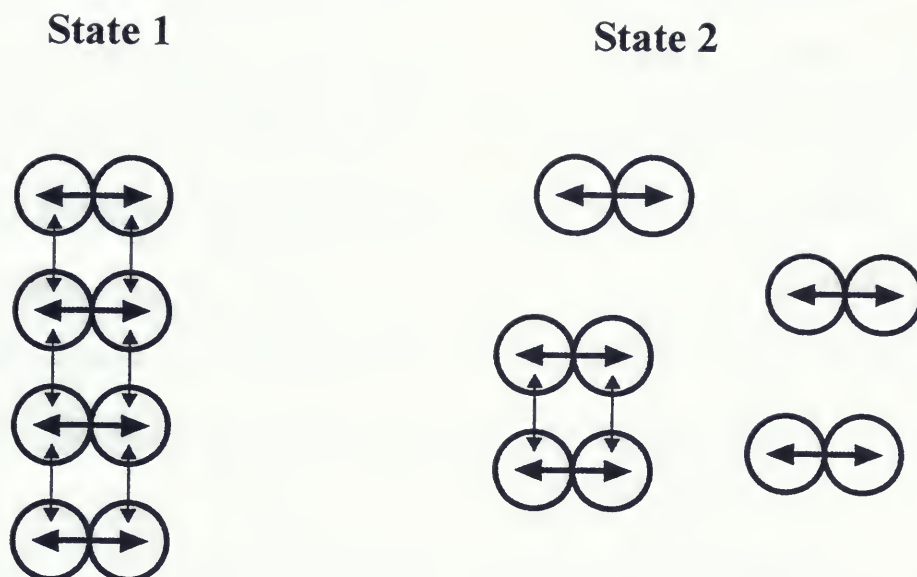


Figure 33. Model for connectivity between PS2 centers in cyanobacteria. Bold arrows represent high efficiency energy transfer and thin arrows low efficiency transfer between connected PS2 centers. Greater organization in rows in state 1 facilitates an increase in transfer between pairs of photosystems. Not shown in the diagram are phycobilisomes which would be attached in a ratio of one phycobilisome for every pair of PS2 centers. See accompanying text for a more complete explanation.

difference in the connection between PS2 complexes in either state. This could mean that there really is no difference in connectivity between states. Alternatively the difference in connectivity between states is very small, as would be predicted by my model. Since the difference between state 1 and 2 according to electron microscopy is whether the pairs of PS2 centers are in rows or not, only this part of the model would change between states. That is, in state 1, when the pairs are in rows, there is a small amount of energy transfer between pairs. In state 2, when the pairs are less likely to be in rows, there is a decrease in transfer between pairs, resulting in slightly less connectivity. This would only cause a small change in the magnitude of cross-section increase when centers are closed and would be below the resolution level of my experiments.

There was no observed difference in the amount of connectivity when either the phycobilisome or chlorophyll antenna cross-sections were measured. Assuming that two PS2 centers are associated with one phycobilisome complex, this result is easily explained by my model. Energy absorbed by the phycobilisome is transferred indiscriminately to either PS2 center in the pair when both centers are open. That is, the phycobilisome antenna is shared by two PS2 reaction centers. When one of these centers is closed, then all of the energy absorbed by the phycobilisome is directed to the remaining open center. As discussed earlier, when both reaction centers in a pair are closed, then there will be a small amount of energy transfer to neighbouring pairs in the row via the chlorophyll antenna.

Conclusions

The mechanism of the state transition was investigated, and a new model was constructed which incorporated ideas from a number of previous models. In state 1, phycobilisome energy is transferred to PS2, and there is no spillover of energy from the chlorophyll antennas of PS2 to PS1. In state 2, there is an increase in the amount of energy transferred to PS1 from the phycobilisome, resulting in a 35% decrease in the PS2 phycobilisome antenna cross-section. The transfer of energy to PS1 is direct rather than via the PS2 chlorophyll antenna. In state 2, PS2 may become dissociated from the phycobilisome. However, the data suggest that it is more likely that PS1 becomes associated with the phycobilisome while PS2 remains functionally linked. In state 2 there is also an increase in the energy transfer from the chlorophyll of PS2 to the antenna of PS1. This is due to a subset of chlorophylls which are not functionally attached to the phycobilisome but which transfer energy to PS1.

An investigation into the connectivity between PS2 centers showed that there was limited transfer of energy between neighbouring centers. The extent of transfer between centers was not significantly different in state 1 or 2 or with phycobilisome or chlorophyll absorbed light. A model was developed where there was very efficient energy transfer within pairs of PS2 centers but inefficient transfer between neighbouring pairs.

Work on the redox reactions of the electron transport chain supported published data which have shown a complex interaction of photosynthetic and respiratory electron transport. The data suggest that in addition to being unable to form PS1 trimers, the *psaL*⁻ cells also have an increased FNR activity which results in a higher level of reduction of PQ in the dark.

References

- Allen, J. and N. Holmes (1986) A general model for regulation of photosynthetic unit function by protein phosphorylation. *FEBS* 202:175-181
- Andersen, B., H. Scheller and B. Moller (1992) The PSI-E subunit of photosystem I binds ferredoxin:NADP⁺ oxidoreductase. *FEBS* 311(2):169-173
- Aoki, M. and S. Katoh (1982) Oxidation and reduction of plastoquinone by photosynthetic and respiratory electron transport in a cyanobacterium *Synechococcus* sp. *Biochimica et Biophysica Acta* 682:307-314
- Bald, D., J. Kruip and M. Rogner (1996) Supramolecular architecture of cyanobacterial thylakoid membranes: How is the phycobilisome connected with the photosystems? *Photosynthesis Research* 49:103-118
- Biggins, J., D. Bruce and P. Gibbs (1989) Regulation of excitation energy distribution by state transitions. *Photosynthesis* pp. 363-374
- Boekma, E., J. Dekker, M. van Heel, M. Rogner, W. Saenger, I. Witt and H. Witt (1987) Evidence for a trimeric organization of the photosystem I complex from the thermophilic cyanobacterium *Synechococcus* sp. *FEBS Letters* 217(2):283-286
- Bold, H. and J. La Claire. 1987. *The Plant Kingdom*. Prentice-Hall, Inc., Englewood Cliffs, New Jersey
- Bruce, D., S. Brimble and D. Bryant (1989) State transitions in a phycobilisome-less mutant of the cyanobacterium *Synechococcus* sp. PCC 7002. *Biochimica et Biophysica Acta* 974:66-73
- Bruce, D., J. Biggins, T. Steiner and M. Thewalt (1985) Mechanism of the light state transition in photosynthesis. IV. Picosecond fluorescence spectroscopy of *Anacystis nidulans* and *Porphyridium cruentum* in state 1 and state 2 at 77K. *Biochimica et Biophysica Acta* 806:237-246
- Bruce, D. and O. Salehian (1992) Laser-induced optoacoustic calorimetry of cyanobacteria. The efficiency of primary photosynthetic processes in state 1 and state 2. *Biochimica et Biophysica Acta* 1100:242-250
- Bryant, D., E. Rhiel, R. de Lorimier, J. Zhou, V. Stirewalt, G. Gasparich, J. Dubbs and W. Snyder (1990) Analysis of phycobilisome and photosystem I complexes of cyanobacteria. In: M. Baltscheffsky (ed) *Current Research in Photosynthesis*, Vol. II, 1-9. Kluwer Academic Publishers, Netherlands

- Capuano, V., A. Braux, N. Tandeau de Marsac and J. Houmard (1991) The "anchor polypeptide" of cyanobacterial phycobilisomes: molecular characterization of the *Synechococcus* sp. PCC 6301 *apcE* gene. *The Journal of Biological Chemistry* 266(11):7239-7247
- Chereskin, B., J. Clement-Metral and E. Gantt (1985) Characterization of a purified photosystem II-phycobilisome particle preparation from *Porphyridium cruentum*. *Plant Physiology* 77:626-629
- Chitnis, V. and P. Chitnis (1993) *PsaL* subunit is required for the formation of photosystem I trimers in the cyanobacterium *Synechocystis* sp. PCC 6803. *FEBS Letters* 336(2):330-334
- Chitnis, V., Q. Xu, L. Yu, J. Golbeck, H. Nakamoto, D. Xie and P. Chitnis (1993) Targeted inactivation of the gene *psaL* encoding a subunit of photosystem I of the cyanobacterium *Synechosystis* sp. PCC 6803. *The Journal of Biological Chemistry* 268(16):11678-11684
- Dekker, J., E. Boekma, H. Witt and M. Rogner (1988) Refined purification and further characterization of oxygen-evolving and Tris-treated photosystem II particles from the thermophilic cyanobacterium *Synechococcus* sp. *Biochimica et Biophysica Acta* 936:307-318
- Delphin, E., J. Duval, A. Etienne and D. Kirilovsky (1996) State transitions or delta pH-dependent quenching of photosystem II fluorescence in red algae. *Biochemistry* 35:9435-9445
- France, L., N. Geacintov, J. Breton and L. Valkunas (1992) The dependence of the degrees of sigmoidicities of fluorescence induction curves in spinach chloroplasts on the duration of actinic pulses in pump-probe experiments. *Biochimica et Biophysica Acta* 1101:105-119
- Ford, R. and A. Holzenburg (1988) Investigation of the structure of trimeric and monomeric photosystem I reaction centre complexes. *The EMBO Journal* 7(8):2287-2293
- Fork, D. (1989) Photosynthesis. In: K. Smith (ed) *The Science of photobiology*, pp 347-390. Plenum Press, New York
- Glazer, A., Y. Gindt, C. Chan and K. Sauer (1994) Selective disruption of energy flow from phycobilisomes to photosystem I. *Photosynthesis Research* 40:167-173
- Golbeck, J. (1994) Photosystem 1 in cyanobacteria. In: Bryant, D. (ed) *The Molecular Biology of Cyanobacteria*, pp 319-360. Kluwer Academic Publishers, Dordrecht
- Guedeney, G., S. Corneille, S. Cuine and G. Peltier (1996) Evidence for an association of *ndh B*, *ndh J* gene products and ferredoxin-NADP-reductase as components of a chloroplastic NAD(P)H dehydrogenase complex. *FEBS* 378:277-280
- Haehnel, W., A. Holzwarth and J. Wendler (1983) Picosecond fluoerscence kinetics and energy transfer in the antenna chlorophylls of green algae. *Photochemistry and Photobiology* 37(4):435-443

- Hladik, J. and D. Sofrova (1991) Does the trimeric form of the photosystem 1 reaction center of cyanobacteria *in vivo* exist? *Photosynthesis Research* 29:171-175
- Hodges, M. and I. Moya (1987) Modification of room-temperature picosecond chlorophyll fluorescence kinetics in photosystem-II-enriched particles by photochemistry. *Biochimica et Biophysica Acta* 892:42-47
- Keuper, H. and K. Sauer (1989) Effect of photosystem II reaction center closure on nanosecond fluorescence relaxation kinetics. *Photosynthesis Research* 20:85-103
- Kirilovsky, D. and I. Ohad (1986) Functional assembly in vitro of phycobilisomes with isolated photosystem II particles of eukaryotic chloroplasts. *The Journal of Biological Chemistry* 261(26):12317-12323
- Krause, G. (1991) Chlorophyll fluorescence and photosynthesis: the basics. *Annual Review of Plant Physiology and Molecular Biology* 42:313-49
- Kruip, J., D. Bald, E. Boekma and M. Rogner (1994) Evidence for the existence of trimeric and monomeric photosystem I complexes in thylakoid membranes from cyanobacteria. *Photosynthesis Research* 40:279-286
- Ley, A. and W. Butler (1980) Energy distribution in the photochemical apparatus of *Porphyridium cruentum* in state I and state II. *Biochimica et Biophysica Acta* 592:349-363
- Lundell, D., G. Yamanaka and A. Glazer (1981) A terminal energy acceptor of the phycobilisome: the 75,000-dalton polypeptide of *Synechococcus* 6301 phycobilisomes-a new biliprotein. *The Journal of Cell Biology* 91:315-319
- Mackinney, G. (1941) Absorption of light by chlorophyll solutions. *Journal of Biological Chemistry* 140:315-322
- Manodori, A. M. Alhadeff, A. Glazer and A. Melis (1984) Photochemical apparatus organization in *Synechococcus* 6301 (*Anacystis nidulans*). Effect of phycobilisome mutation. *Archives of Microbiology* 139:117-123
- Manodori, A. and A. Melis (1985) Phycobilisome-photosystem II association in *Synechococcus* 6301 (Cyanophyceae). *FEBS* 181(1):79-82
- Mauzerall, D. and N. Greenbaum (1989) The absolute size of a photosynthetic unit. *Biochimica et Biophysica Acta* 974:119-140
- Maxson, P., K. Sauer, J. Zhou, D. Bryant and A. Glazer (1989) Spectroscopic studies of cyanobacterial phycobilisomes lacking core polypeptides. *Biochimica et Biophysica Acta* 977:40-51

- Mi, H., T. Endo, U. Schreiber and K. Asada (1992a) Donation of electrons from cytosolic components to the intersystems chain in the cyanobacterium *Synechococcus* sp. PCC 7002 as determined by reduction of P700+. *Plant Cell Physiology* 33(8):1099-1105
- Mi, H., T. Endo, U. Schreiber, T. Ogawa and K. Asada (1992b) Electron donation from cyclic and respiratory flows to the photosynthetic intersystem chain is mediated by pyridine nucleotide dehydrogenase in the cyanobacterium *Synechocystis* PCC 6803. *Plant Cell Physiology* 33(8):1233-1237
- Mi, H., T. Endo, U. Schreiber, T. Ogawa and K. Asada (1994) NAD(P)H dehydrogenase-dependent cyclic electron flow around photosystem I in the cyanobacterium *Synechocystis* PCC 6803: a study of dark-starved cells and spheroplasts. *Plant Cell Physiology* 35(2):163-173
- Morschel, E. and G. Schatz (1987) Correlation of photosystem-II complexes with exoplasmic freeze-fracture particles of thylakoids of the cyanobacterium *Synechococcus* sp. *Planta* 172:145-154
- Moya, I., M. Hodges and J. Barbet (1986) Modification of room-temperature picosecond chlorophyll fluorescence kinetics in green algae by photosystem II trap closure. *FEBS* 198(2):256-262
- Mullineaux, C. (1992) Excitation energy transfer from phycobilisomes to photosystem I in a cyanobacterium. *Biochimica et Biophysica Acta* 1100:285-292
- Mullineaux, C. (1994) Excitation energy transfer from phycobilisomes to photosystem I in a cyanobacterium mutant lacking photosystem II. *Biochimica et Biophysica Acta* 1184:71-77
- Mullineaux, C. and J. Allen (1988) Fluorescence induction transients indicate dissociation of photosystem II from the phycobilisome during the state-2 transition in the cyanobacterium *Synechococcus* 6301. *Biochimica et Biophysica Acta* 934:96-107
- Mullineaux, C., E. Bittersmann, J. Allen and A. Holzwarth (1990) Picosecond time-resolved fluorescence emission indicate decreased energy transfer from the phycobilisome to photosystem II in light-state 2 in the cyanobacterium *Synechococcus* 6301. *Biochimica et Biophysica Acta* 1015:231-242
- Mullineaux, C., S. Griebenow and S. Braslavsky (1991) Photosynthetic energy storage in cyanobacterial cell adapted to light-states 1 and 2. A laser-induced optoacoustic study. *Biochimica et Biophysica Acta* 1060:315-318
- Mullineaux, C. and A. Holzwarth (1990) A proportion of photosystem II core complexes are decoupled from the phycobilisome in light-state 2 in the cyanobacterium *Synechococcus* 6301. *FEBS* 260(2):245-248

- Mullineaux, C. and A. Holzwarth (1993) Effect of photosystem II reaction center closure on fluorescence decay kinetics in a cyanobacterium. *Biochimica et Biophysica Acta* 1183:345-351
- Murata, N. (1969) Control of excitation transfer in photosynthesis. I. Light-induced change of chlorophyll a fluorescence in *Porphyridium cruentum*. *Biochimica et Biophysica Acta* 172:242-251
- Myers, J., J. Graham and R. Wang (1980) Light harvesting in *Anacystis nidulans* studied in pigment mutants. *Plant Physiology* 66:1144-1149
- Olive, J., I. M'Bina, C. Vernotte, C. Astier and F. Wollman (1986) Randomization of the EF particles in thylakoid membranes of *Synechocystis* 6714 upon transition from state I to state II. *FEBS* 208(2):308-312
- Owens, T., S. Webb, R. Alberte, L. Mets and G. Fleming (1988) Antenna structure and excitation dynamics in photosystem I. *Biophysical Journal* 53:733-745
- Peschek, G. (1987) Respiratory electron transport. In: Fay, P. and C. Baalen (ed.) *The Cyanobacteria*, pp 119-161. Elsevier Science Publishers B.V., New York
- Prescott, L., J. Harley and D. Klein. 1990. *Microbiology*. Wm.C.Brown Publishers, Dubuque, IA.
- Redlinger, T. and E. Gantt (1982) A Mr 95,000 polypeptide in *Porphyridium cruentum* phycobilisomes and thylakoids: possible function in linkage of phycobilisomes to thylakoids and energy transfer. *Proceedings of the National Academy of Science USA* 79:5542-5546
- Renger, G. and A. Schulze (1985) Quantitative analysis of fluorescence induction curves in isolated spinach chloroplasts. *Photobichemistry and Photobiophysics* 9:79-87
- Rogner, M., U. Muhlenhoff, E. Boekema and H. Witt (1990) Mono-, di- and trimeric PSI reaction center complexes isolated from the thermophilic cyanobacterium *Synechococcus* sp. Size, shape and activity. *Biochimica et Biophysica Acta* 1015:415-424
- Salehian, O. and D. Bruce (1992) Distribution of excitation energy in photosynthesis: quantification of fluorescence yields from intact cyanobacteria. *Journal of Luminescence* 51:91-98
- Scherer, S. (1990) Do photosynthetic and respiratory electron transport chains share redox proteins? *Trends in Biochemical Science* 15:458-462
- Scherer, S., I. Alpes, H. Sadowski and P. Boger (1988) Ferredoxin-NADP⁺ oxidoreductase is the respiratory NADPH dehydrogenase of the cyanobacterium *Anabaena variabilis*. *Archives of Biochemistry and Biophysics* 267(1):228-235

- Schluchter, W. and D. Bryant (1992) Molecular characterization of ferredoxin-NADP⁺ oxidoreductase in cyanobacteria: cloning and sequences of the *petH* gene of *Synechococcus* sp. PCC 7002 and studies on the gene product. *Biochemistry* 31:3092-3102
- Schluchter, W., G. Shen, J. Zhao and D. Bryant (1996) Characterization of *psaI* and *psaL* mutants of *Synechococcus* sp. strain PCC 7002: A new model for state transitions in cyanobacteria. *Photochemistry and Photobiology* 64(1):53-66
- Schreiber, U., W. Bilger and C. Neubauer (1994) Chlorophyll fluorescence as a non-intrusive indicator for rapid assessment of *in vivo* photosynthesis. in: *Ecophysiology of Photosynthesis*. Ecological Studies. Vol. 100 (E. Schulze and M. Caldwell, eds.) Springer Verlag, Berlin, pp. 49-70
- Schreiber, U. U. Schliwa and W. Bilger (1986) Continuous recording of photochemical and non-photochemical chlorophyll fluorescence quenching with a new type of modulation fluorimeter. *Photosynthesis Research* 10:51-62
- Strasser, R., A. Srivastava and Govindjee (1995) Polyphasic chlorophyll a fluorescence transient in plants and cyanobacteria. *Photochemistry and Photobiology* 61(1):32-42
- Tandeau de Marsac, N. and G. Cohen-Bazire (1977) Molecular composition of cyanobacterial phycobilisomes. *Proceedings of the National Academy of Science USA* 74(4):1635-1639
- Tsinoremas, N., J. Hubbard, M. Evans and J. Allen (1989) P-700 photooxidation in state 1 and state 2 in cyanobacteria upon flash illumination with phycobilin- and chlorophyll-absorbed light. *FEBS* 256:106-110
- Vernotte, C., C. Astier and J. Olive (1990) State 1-state 2 adaptation in the cyanobacteria *Synechocystis* PCC 6714 wild type and *Synechocystis* PCC 6803 wild type and phycocyanin-less mutant. *Photosynthesis Research* 26:203-212
- Vulkunas, L., N. Geacintov, L. France and J. Breton (1991) The dependence of the shapes of fluorescence induction curves in chloroplasts on the duration of illumination pulses. *Biophysical Journal* 59:397-408
- Yamazaki, I., M. Mimuro, T. Murao, T. Yamazaki, K. Yoshihara and Y. Fujita (1984) Excitation energy transfer in the light harvesting antenna system of the red alga *Porphyridium cruentum* and the blue-green alga *Anacystis nidulans*: Analysis of time resolved fluorescence spectra. *Photochemistry and Photobiology* 39(2):233-240
- Zhao J., J. Zhou and D. Bryant (1992) Energy transfer processes in phycobilisomes as deduced from analysis of mutants of *Synechococcus* sp. PCC 7002. In: Murata N. (ed) *Research in Photosynthesis*, Vol. 1 pp25-32. Kluwer Academic Publishers, Dordrecht

Zilinskas, B. and L. Greenwald (1986) Phycobilisome structure and function. *Photosynthesis Research* 10:7-35

Zubay, G., W. Parson and D. Vance. 1995. *Principles of Biochemistry*. Wm.C.Brown Publishers, Dubuque, Iowa.

Appendix A: Liquid A+ Growth Medium

Component	Amount/L of water
NaCl	18.0 g
KCl	0.6 g
NaNO ₃	1.0 g
KH ₂ PO ₄ stock	10 ml
MgSO ₄ .7H ₂ O	5.0 g
CaCl ₂ stock	20 ml
Na ₂ EDTA stock	20 ml
FeCl ₃ .6H ₂ O stock	1 ml
Pi metals stock	1 ml
Tris HCl pH 8.2	10 ml
Vitamin B12 stock	1 ml

Stock Solutions

Component	Concentration
Na ₂ EDTA stock	1.5 g/L
CaCl ₂ stock	18 g/L
KH ₂ PO ₄ stock	5 g/L
FeCl ₃ .6H ₂ O stock	3.89 g/L (in 0.1N HCl)
Vitamin B12 stock	0.008 g/L
Tris HCl pH 8.2	100g/L
Pi Metals stock	
H ₃ BO ₃	34.26 g/L
MnCl ₂ .4H ₂ O	4.32 g/L
ZnCl ₂	0.315 g/L
MoO ₃ (85%)	0.03 g/L
CuSO ₄ .5H ₂ O	0.003 g/L
CoCl ₂ .6H ₂ O	0.012 g/L

Note: To avoid degradation of Vitamin B12, it was added subsequent to autoclaving.

Appendix B: Connectivity Correction

As outlined in the results, cross-section measurements in state 2 were done in the dark with a time delay of approximately 35seconds between exposures to the laser flash. Therefore, there was no elevation in F_o level due to residual closed traps from the previous exposure to a laser flash. However, in order to measure photosystem 2 cross-sections in state 1, cells were pre-illuminated with red light. The time between pre-illumination and measurement was only 3s and as this light was absorbed by photosystem 1 as well as photosystem 2 it was likely that some or all of the observed increase in apparent F_o in state 1 was due to residual trap closure. Alternatively, the increase in apparent F_o was a real increase due to an increased cross-section. To obtain an estimate of how much of this increase in apparent F_o was due to trap closure, further experiments were carried out.

If a similar transition to state 1 could be obtained, but with a smaller increase in the apparent F_o level, then at least the difference between this new apparent F_o increase and the old (larger) increase was due to trap closure. Figure 25 shows that by using a filter which was red shifted by about 40nm and therefore preferentially absorbed by PS1 (referred to as a far red filter) compared to the red filter used previously it was possible to obtain a similar level of increase in F_m which is indicative of the degree of transition but with a smaller increase in apparent F_o .

From the PAM data using these two filters it was determined that at least 42% of the increase in apparent F_o between state 2 and state 1 was due to trap closure as is shown in the following calculations:

The increase in apparent F_o as a proportion of state 1 $F_v = (\text{State 1 apparent } F_o - \text{State 2 } F_o) / \text{State 1 } F_v$

With the far red filter: state 1 apparent $F_o = 1297$

$$\text{state 2 } F_o = 1191$$

$$\text{state 1 } F_m = 3796$$

$$\text{state 1 } F_v = 3796 - 1297$$

Therefore, the apparent F_o increase is 4.2%.

For the red filter: state 1 apparent $F_o = 1334$ (measured between 610-620 seconds)

$$\text{state 2 } F_o = 1143 \text{ (measured between 80-100 seconds)}$$

$$\text{state 1 } F_m = 3997$$

$$\text{state 1 } F_v = 2663$$

Therefore, the apparent F_o increase is 7.2%.

Increase due to trap closure = apparent F_o increase with red filter - apparent F_o increase with far red filter

Therefore, the increase due to trap closure is 3.0%.

Therefore, it is assumed that at least 42% (3.0/7.2) of the increase in apparent F_o in state 1 is due to trap closure. On the other extreme, it is possible that all of the increase in apparent F_o is due to trap closure. In this case 100% of the increase in apparent F_o can be attributed to this.

What is the effect of an increase in apparent F_o on cross-section measurements? If there is free movement of excitons between PS2 antenna there will be an effect on the size of the measured cross-section if some traps are closed. To briefly reiterate this theory which is explained in the literature review: if there are two open PS2 centers in which excitons may move freely between the antenna, there will be an equal trapping of excitons by both reaction centers. If however, one of the reaction centers is closed, then the other center will preferentially receive the exciton from the collective antenna. That is, both antenna will be absorbing energy for the one reaction center and so its antenna will appear to be twice as large.

In order to measure the effect of some centers being closed, a preflash from a single turnover xenon flash lamp was used to close some centers before each laser flash (described in more detail in the materials and methods). Figure 26 shows an example flash saturation curves at various levels of apparent F_o elevation. Figures 27 to 30 show the results of various levels of apparent F_o elevation on absorption cross-section sizes for wild type cells in state 1 and state 2 at 630nm and 674nm excitation. For all conditions, an elevation in apparent F_o level resulted in an increase in cross-section. When the slopes of all of the calibration curves are overlapped, there is no significant difference in the amount of increase with increasing apparent F_o .

For each of the cell types, cross-section measurements in state 1 were corrected for apparent F_o elevation as is shown in the following example (the level of apparent F_o elevation in state 1 for each can be found in table 3).

For the wild type cells (at 630nm excitation) the apparent F_o level increased from 1.54 to 1.84, which, given as a proportion of the state 1 F_v , is 18.6%. According to the calculations from the PAM data, at least 42% of this 18.6% increase in F_v (i.e. 7.8%) is due to trap closure and at the most 100% of the 18.6% increase is due to trap closure. Using the state 1 (630nm) connectivity calibration curve, the amount of increase of cross-section due to trap closure was determined.

0% increase in F_o due to connectivity: relative cross-section = 98.03

7.8% increase: relative cross-section = 103.98

18.6% increase: relative cross-section = 112.22

Using these relative cross-sections to convert the absolute state 1 cross-section of 407 \AA^2 for wild type cells at 630nm excitation:

0% increase = 407 \AA^2

$$7.8\% \text{ increase} = 384 \text{ \AA}^2$$

$$18.6\% \text{ increase} = 356 \text{ \AA}^2$$

Therefore, an observed 44% increase in cross-section from 283 in state 2 to 407 in state 1, which not only includes a real increase in absorbance cross-section due to the state transition, but also an increase due to connectivity, can be constrained to an increase of at least 26% (356 \AA^2) and at the most 36% (384 \AA^2).

Appendix C: Computer Simulated Connectivity

The source code for the simulation program is shown below. By varying the efficiency of energy transfer between pairs of photosystems in a row (fraction to remove), the cross-section can be increased or decreased to simulate the experimental data.

This program was a joint effort between Sergej Vasil'ev and myself; Sergej providing the programming expertise and both of us providing the rationale for the model.

```
#include <stdlib.h>
#include <stdio.h>
#include <conio.h>
#include <math.h>

int excited_ps[10000];
int excitations_in_pair[5000];
int overexcited_pair[5000];
float fraction_to_remove=.86;
int pump_int=561;
int num_ps=1000;
int num_averages=10;

int num_overexcited_pairs;
unsigned long int F_yield;
int both_open_neighb_closed2;
int both_open_neighb_closed1;
int both_open_neighb_closed0;
int one_closed_neighb_closed2;
int one_closed_neighb_closed1;
int one_closed_neighb_closed0;
int num_overexc;
int num_overex_pairs;
int exc_previous;
int exc_next;
float xs_both_open_neighb_closed2;
float xs_both_open_neighb_closed1;
float xs_both_open_neighb_closed0;
float xs_one_closed_neighb_closed2;
float xs_one_closed_neighb_closed1;
float xs_one_closed_neighb_closed0;
```



```

float pump[101];
float cross_section[101];
float flu1[101];
float flu2[101];
float flu3[101];
float flu4[101];
float flu5[101];
float flu6[101];
FILE *fp;

void reset(void);
void equilibrate_pairs(void);
void mark_overexcited_pairs(void);
void number_overexcitations_to_remove(void);
void generate_saturation_curves(void);
void remove_overexcitations(void);
void count_fractions(void);

void main(void)
{
    fp=fopen("out.txt","wt");
    int i,j;
    randomize();
    fprintf(fp," X-sections RANDYmization proceeding >> \r\n");
    fprintf(fp,"Hitting %i Photosystems with %i Photons >>\r\n\n",num_ps,pump_int);
    fprintf(fp,"-----\r\n");

    for(j=0;j<num_averages;j++)
    {
        for(i=0;i<pump_int;i++)excited_ps[random(num_ps)]++;
        equilibrate_pairs();
        mark_overexcited_pairs();
        number_overexcitations_to_remove();
        remove_overexcitations();
        //fprintf(fp,"overex=%i\r\n",num_overexc);
        //for(i=0,j=0;i<num_ps;j++,i+=2)fprintf(fp,"%i. %i %i %i %i \r\n" ,i,
excited_ps[i],excited_ps[i+1],excitations_in_pair[j],overexcited_pair[j]);
        //fprintf(fp,"\r\n");
        equilibrate_pairs();
        count_fractions();
        for(i=0;i<num_ps;i++)if(excited_ps[i])F_yield++;
        //for(i=0,j=0;i<num_ps;j++,i+=2)fprintf(fp,"%i. %i %i %i %i \r\n" ,i,
excited_ps[i],excited_ps[i+1],excitations_in_pair[j],overexcited_pair[j]);
        //fprintf(fp,"\r\n");
        reset();
    }
}

```



```

    }
    generate_saturation_curves();

    fprintf(fp, "both_open_neighb_closed2, %i, %f\r\n",
both_open_neighb_closed2,xs_both_open_neighb_closed2);
    fprintf(fp, "both_open_neighb_closed1, %i, %f\r\n",
both_open_neighb_closed1,xs_both_open_neighb_closed1);
    fprintf(fp, "both_open_neighb_closed0, %i, %f\r\n",
both_open_neighb_closed0,xs_both_open_neighb_closed0);
    fprintf(fp, "one_closed_neighb_closed2, %i, %f\r\n",
one_closed_neighb_closed2,xs_one_closed_neighb_closed2);
    fprintf(fp, "one_closed_neighb_closed1, %i, %f\r\n",
one_closed_neighb_closed1,xs_one_closed_neighb_closed1);
    fprintf(fp, "one_closed_neighb_closed0, %i, %f\r\n",
one_closed_neighb_closed0,xs_one_closed_neighb_closed0);
    fprintf(fp, "F_yield, %u\r\n", F_yield);
    fprintf(fp, "-----\r\n");
    fprintf(fp, "saturation curve\r\n");
    for(i=0;i<100;i++)fprintf(fp,"%f, %f\r\n", pump[i],cross_section[i]);
    fclose(fp);
}

```

```

void reset()
{
    int i;
    for(i=0;i<num_ps;i++)excited_ps[i]=0;
        for(i=0;i<num_ps/2;i++)
        {
            excitations_in_pair[i]=0;
            overexcited_pair[i]=0;
        }
        // F_yield=0;
        num_overexc=0;
        num_overex_pairs=0;
        num_overexcited_pairs=0;
}

```

```

void equilibrate_pairs()
{
    int i;

```



```

for(i=0;i<num_ps;i+=2)
{
    if (excited_ps[i]>1){excited_ps[i]-- ;excited_ps[i+1]++;}
    if (excited_ps[i+1]>1){excited_ps[i]++;excited_ps[i+1]--;}
}

```

```

void mark_overexcited_pairs()
{
    int i,j;
    for(i=0,j=0;i<num_ps;i+=2,j++)
    {
        excitations_in_pair[j]+=(excited_ps[i]+excited_ps[i+1]);
        if(excitations_in_pair[j]>2)overexcited_pair[j]=1;
    }
}

```

```

void number_overexcitations_to_remove()
{
    int i;
    for(i=0;i<num_ps/2;i++)
    {
        num_overexcited_pairs+=overexcited_pair[i];
        if(overexcited_pair[i])num_overexc+=excitations_in_pair[i];
    }
    num_overexc-=2*num_overexcited_pairs;
    num_overexc*=fraction_to_remove;
}

```

```

void generate_saturation_curves()
{
    int i;
    xs_both_open_neighb_closed2=1+(1-fraction_to_remove)*2;
    xs_both_open_neighb_closed1=1+(1-fraction_to_remove)*1;
    xs_both_open_neighb_closed0=1;
    xs_one_closed_neighb_closed2=2+(1-fraction_to_remove)*4;
    xs_one_closed_neighb_closed1=2+(1-fraction_to_remove)*2;
    xs_one_closed_neighb_closed0=2;
    for(i=0,pump[i]=0.03;i<100;i++)
    {
        pump[i+1]=pump[i]*1.1;
        flul[i]=1.74*(1-exp(-pump[i]*0.0781578*xs_both_open_neighb_closed0))+1;
    }
}

```



```

        flu2[i]=1.74*(1-exp(-pump[i]*0.0781578*xs_both_open_neighb_closed1))+1;
        flu3[i]=1.74*(1-exp(-pump[i]*0.0781578*xs_both_open_neighb_closed2))+1;
        flu4[i]=1.74*(1-exp(-pump[i]*0.0781578*xs_one_closed_neighb_closed0))+1;
        flu5[i]=1.74*(1-exp(-pump[i]*0.0781578*xs_one_closed_neighb_closed1))+1;
        flu6[i]=1.74*(1-exp(-pump[i]*0.0781578*xs_one_closed_neighb_closed2))+1;
        cross_section[i]=
            (both_open_neighb_closed0*flu1[i]+
            both_open_neighb_closed1*flu2[i]+
            both_open_neighb_closed2*flu3[i])*2+
            one_closed_neighb_closed0*flu4[i]+
            one_closed_neighb_closed1*flu5[i]+
            one_closed_neighb_closed2*flu6[i];
    }
}

void remove_overexcitations()
{
    int count=0, num, i, k;
    while(count<=num_overexc)
    {
        num=random(num_ps/2);
        if(overexcited_pair[num])
        {
            excited_ps[num*2]--;
            excitations_in_pair[num]=0;

excitations_in_pair[num]+=(excited_ps[num*2]+excited_ps[num*2+1]);

            if(excitations_in_pair[num]>2)overexcited_pair[num]=1;
            else overexcited_pair[num]=0;

                        if
(excited_ps[num*2]>1&&excited_ps[num*2+1]==0){excited_ps[num*2]--
;excited_ps[num*2+1]++;}

                        if
(excited_ps[num*2+1]>1&&excited_ps[num*2]==0){excited_ps[num*2]++;excited_ps[num*2+
1]--;}

                        count++;

        }

        num_overex_pairs=0;
        for(i=0;i<num_ps;i++)
            if(overexcited_pair[i])num_overex_pairs++;
            if(!num_overex_pairs)break;
    }

    //      for(i=0,j=0;i<num_ps;j++,i+=2)fprintf(fp,"%i.  %i %i %i %i \r\n" ,i,
excited_ps[i],excited_ps[i+1],excitations_in_pair[j],overexcited_pair[j]);

```



```

for(k=0;k<4;k++)
{
    for(i=1;i<num_ps/2-1;i++)
    {
        exc_previous=0;
        exc_next=0;
        if(overexcited_pair[i])
        {
            exc_previous+=excitations_in_pair[i-1];
            exc_next+=excitations_in_pair[i+1];

            if(exc_previous<2||exc_next<2)
                if(exc_previous<=exc_next)
                {
                    excitations_in_pair[i-1]++;excited_ps[(i-1)*2]++;
                    excitations_in_pair[i]--;excited_ps[i*2]--;
                }
                else
                {
                    excitations_in_pair[i+1]++;
                    excited_ps[(i+1)*2]++;
                    excitations_in_pair[i]--;
                    excited_ps[i*2]--;
                }
        }
    }
    for(i=1;i<num_ps/2-1;i++)
    if(excitations_in_pair[i]<=2)overexcited_pair[i]=0;
}

```

```

void count_fractions()
{
    int i;

    for(i=1;i<num_ps/2-1;i++)
    {
        exc_previous=0;
        exc_next=0;
        exc_previous+=excitations_in_pair[i-1];
        exc_next+=excitations_in_pair[i+1];
        switch(excitations_in_pair[i])
        {
            case 0:

```



```

if(exc_previous>1&&exc_next>1)both_open_neighb_closed2++;

if(exc_previous<2&&exc_next<2)both_open_neighb_closed0++;

if((exc_previous>1&&exc_next<2)||((exc_previous<2&&exc_next>1))
    both_open_neighb_closed1++;
    break;
    case 1:

if(exc_previous>1&&exc_next>1)one_closed_neighb_closed2++;

if(exc_previous<2&&exc_next<2)one_closed_neighb_closed0++;

if((exc_previous>1&&exc_next<2)||((exc_previous<2&&exc_next>1))
    one_closed_neighb_closed1++;
    break;
    }
}

}

```